NOTICE

The quality of this microform is heavily dependent upon the quality of the original thesis submitted for microfilming. Every effort has been made to ensure the highest quality of reproduction possible.

If pages are missing, contact the university which granted the degree.

Some pages may have indistinct print especially if the original pages were typed with a poor typewriter ribbon or if the university sent us an inferior photocopy.

Reproduction in full or in part of this microform is governed by the Canadian Copyright Act, R.S.C. 1970, c. C-30, and subsequent amendments.

AVIS

La qualité de cette microforme dépend grandement de la qualité de la thèse soumise au microfilmage. Nous avons tout fait pour assurer une qualité supérieure de reproduction.

S'il manque des pages, veuillez communiquer avec l'université qui a conféré le grade.

La qualité d'impression de certaines pages peut laisser à désirer, surtout si les pages originales ont été dactylographiées à l'aide d'un ruban usé ou si l'université nous a fait parvenir une photocopie de qualité inférieure.

La reproduction, même partielle, de cette microforme est soumise à la Loi canadienne sur le droit d'auteur, SRC 1970, c. C-30, et ses amendements subséquents.

THE UNIVERSITY OF ALBERTA

THE HIGHER ORDER TERMS OF THE ASYMPTOTIC RAY THEORY

BY

ZHENG BAO-SHAN

A THESIS

SUBMITTED TO THE FACULTY OF GRADUATE STUDIES AND RESEARCH

IN PARTIAL FULFILMENT OF THE REQUIREMENTS FOR THE DEGREE

OF DOCTOR OF PHILOSOPHY

IN

GEOPHYSICS

DEPARTMENT OF PHYSICS

EDMONTON, ALBERTA

SPRING 1989

ISBN 0-315-52927-X

THE UNIVERSITY OF ALBERTA

RELEASE FORM

NAME OF AUTHOR ZHENG BAO-SHAN

TITLE OF THESIS THE HIGHER ORDER TERMS OF THE ASYMPTOTIC RAY THEORY

DEGREE FOR WHICH THESIS WAS PRESENTED DOCTOR OF PHILOSOPHY

YEAR THIS DEGREE GRANTED SPRING 1989

(SIGNED) Baoshan Zheng

PERMANENT ADDRESS:

c/o DEPARTMENT OF PHYSICS

UNIVERSITY OF ALBERTA

EDMONTON, ALBERTA, CANADA

T6G 2J1

DATED April 25, 1989

THE UNIVERSITY OF ALBERTA

FACULTY OF GRADUATE STUDIES AND RESEARCH

The undersigned certify that they have read, and recommend to the Faculty of Graduate Studies and Research for acceptance, a thesis entitled THE HIGHER ORDER TERMS OF THE ASYMPTOTIC RAY THEORY submitted by ZHENG BAO-SHAN in partial fulfilment of the requirements for the degree of DOCTOR OF PHILOSOPHY in GEOPHYSICS.

.....
Supervisor

.....

.....

.....

.....
External Examiner

Date April 10, 1989

Abstract

Asymptotic Ray Theory (ART), a technique in which the amplitude of the total body wave field is expanded into an infinite ray series, has become a powerful tool in the numerical solution of both the direct and inverse problem in seismic oil exploration and crustal seismology. However, thus far only the zero order term has been used in practice. In order to meet the current demands of seismic oil exploration and crustal seismology, the need to study the higher order terms in the ray series has become ever more pressing.

A systematic and detailed treatment of the higher order approximations to ART, and a rigorous mathematical analysis of the first order approximation to some typical problems in particular are discussed. In addition to the presentation of the basic theoretical formulae, numerical examples are given in order to demonstrate the importance of the first order terms in the ray series. It is our experience that they should be used whenever ART is applied to inhomogeneous media, because the first order amplitudes become larger as the inhomogeneity of media increases. In the thesis we present the first order correction to the zero order approximation for PS and PP waves reflected from the free surface. The dependence of the first order correction on the depth of the explosive point source is demonstrated in several numerical examples. Our synthetic seismograms show,

in particular, that the amplitude of the first order term in the ray series is sensitive to the depth of the source, and to the ratio of P and S wave velocities in the medium below the free surface. The first order approximation of ART for transmitted and reflected waves due to a spherical wave incident on a boundary between two elastic media has also been investigated with the help of synthetic seismograms. The numerical examples suggest that the first order correction should be included for the transmitted and reflected PS waves because of the high amplitudes of their additional components at normal incidence that can be as great as 10% of the total amplitude of the converted PP waves.

ACKNOWLEDGEMENTS

I wish to express my sincere thanks to Professor F. Hron for his guidance and advice throughout the course of this work.

I am also grateful to Dr. P. F. Daley for his helpful discussions.

Over all, this scientific work could not have been completed without the loving support of my wife, Yu-zhen, and our daughters, Yue and Yao.

During the course of this study, I received financial support from my supervisor Dr. F. Hron research funds (NSERC, AMOCO), and the University of Alberta (teaching assistantship) as well as the Canadian Society of Exploration Geophysicists (CSEG scholarship).

Table of Contents

List of Tables

List of Figures

Figure Page

Figure Page

Figure Page

Figure Page

Figure Page

Figure Page

1. Introduction

Problems in elastic wave propagation, sometimes called forward problems, are of paramount importance in various branches of seismology. This usually means that the wave field at any given position is of interest and computed when the sources and the structures of models are known. By comparing synthetic seismograms for different models with recorded seismograms, it is possible to investigate the real structures and sources. Unfortunately, analytical solutions to the wave equations governing wave phenomena, in terms of physical quantity $\Phi(r,t)$ where r is a position vector, and t is time, are known for only a few relatively simple medium types, which generally do not closely resemble real structures.

Consequently, two different approaches for computing synthetic seismograms for a given model, approximate and highly accurate numerical methods which are based on the direct numerical solution of the elastodynamic equations, have been achieved and developed. For instance, the finite difference method is a numerical implementation of the most general accurate numerical solution (Alterman and Loewenthal, 1972; Boore, 1972; Alford et al., 1974; Kelly et al., 1976). The Alekseev-Mikhailenko Method (Mikhailenko, 1973; Alekseev and Mikhailenko, 1976, 1977, 1978, 1979, 1980) which combines the use of finite differences with the finite integral transforms is another example of a highly

accurate numerical method. Derived in a similar manner as geometrical optics (Kline, 1951), Asymptotic Ray Theory (Babich and Alekseev, 1958; Karal and Keller, 1959; Alekseev et al, 1961; Cerveny, 1972; Hron and Kanasewich, 1971; Cerveny and Hron, 1980; Hron, 1984), is an example of an approximate method.

Recently Asymptotic Ray Theory (ART) has gained wide acceptance for use in seismic modeling because it is fast, efficient, and adaptable enough to be applied to a variety of geological structures, including three-dimensional models with arbitrary curved interfaces and both vertical and lateral inhomogeneities.

The basic theory of ART assumes that the solution of the basic elastodynamic wave equation (sometimes known as the Navier-Stokes equation) characterized by Lame coefficients $\lambda=\lambda(\mathbf{r})$, $\mu=\mu(\mathbf{r})$ and the density $\rho=\rho(\mathbf{r})$ as

$$(1.1) \qquad \rho\frac{\partial^2\mathbf{u}}{\partial t^2} = (\lambda+\mu)\nabla\theta + \mu\nabla^2\mathbf{u} + \theta\nabla\lambda + 2(\nabla\mu\cdot\nabla)\mathbf{u} + \nabla\mu\times(\nabla\times\mathbf{u})$$

in the form of a ray series as follows:

$$(1.2) \qquad \mathbf{u}(\mathbf{r},t) = \sum_k \mathbf{W}^{(k)}(\mathbf{r})\, F_k(t-\tau(\mathbf{r}))$$

where $\theta\equiv\nabla\cdot\mathbf{u}$, and $\mathbf{W}^{(k)}(\mathbf{r})$ are amplitude terms represented by complex vectors independent of time, t, and $F_k(\zeta)$ are generally complex functions of a real variable ζ, $F_k(\zeta) = f_k(\zeta) + i\, g_k(\zeta)$, satisfying the relation $F_k'(\zeta) = F_{k-1}(\zeta)$, and where τ is an arrival time at the location with position

vector $\mathbf{r}$ in a given coordinate system which may be generally curvilineal.

It is understood that only one part, either the real or the imaginary part of the complex valued vector $\mathbf{W}(\mathbf{r},t)$ in (1.2), represents the actual displacement associated with a given ray path. Complex variables are used in order to simplify the algebra, and to utilize the powerful theory of complex functions.

Understandably the displacement $\mathbf{W}(\mathbf{r},t)$ in (1.2) representing a given ray path must, according to the principal of superposition, also satisfy the basic elastodynamic equation (1.1).

Writing the Cartesian components of the amplitude term $\mathbf{W}^{(k)}$ as $W_j^{(k)}$, i.e.

$$\mathbf{W}^{(k)} = \sum_j W_j^{(k)} \hat{\mathbf{e}}_j , \qquad j = 1, 2, 3,$$

and defining $\mathbf{W}^{(-2)} \equiv \mathbf{W}^{(-1)} \equiv \mathbf{0}$, and inserting (1.2) to (1.1), a recurrence system of equations can be obtained as follows:

$$\mathbf{N}(\mathbf{W}^{(k)}) = \mathbf{M}(\mathbf{W}^{(k-1)}) - \mathbf{L}(\mathbf{W}^{(k-2)}), \quad k = 0, 1, \ldots\ldots \tag{1.3}$$

The vector operators $\mathbf{N}$, $\mathbf{M}$, and $\mathbf{L}$ are given by the following formulae:

$$\mathbf{N}(\mathbf{u}) \equiv (\lambda+\mu)(\mathbf{u}\cdot\nabla\tau)\nabla\tau + [\mu(\nabla\tau)^2-\rho]\mathbf{u}$$

$$\begin{aligned}\mathbf{M}(\mathbf{u}) \equiv\ & (\lambda+\mu)[\theta\nabla\tau+\nabla(\mathbf{u}\cdot\nabla\tau)] + \mu[2(\nabla\tau)^2 d\mathbf{u}/d\tau + (\nabla^2\tau)\mathbf{u}] \\ & + \nabla\lambda(\nabla\tau\cdot\mathbf{u}) + \nabla\tau(\nabla\mu\cdot\mathbf{u}) + (\nabla\tau\cdot\nabla\mu)\mathbf{u}\end{aligned} \tag{1.4}$$

$$L(\mathbf{u}) \equiv (\lambda+\mu)\nabla\theta + \mu\nabla^2\mathbf{u} + \theta\nabla\lambda + 2(\nabla\mu\cdot\nabla)\mathbf{u} + \nabla\mu\times(\nabla\times\mathbf{u})$$

It is of note that the ART solution allows for the inclusion of as many terms (k = 0, 1, 2, ...) as are required for the problems at hand.

For the most part, the zero order term (k=0) is sufficient to supply an accurate description of ordinary body waves. However, attention should be paid to some of the more sensitive areas of solution where the zero order term produces unaccountable inaccuracies when compared to a highly accurate numerical solution. For example, two special effects have been found by Drs. Hron and Mikhailenko in 1981 when they used the Alekseev-Mikhailenko Method (AMM) to deal with the following special model, named model #1 in this thesis (see Fig. 1.1). In computations of synthetic seismograms for model #1, the following source pulse was used:

$$f(t) = \exp[-(2\pi\nu t/\gamma)^2] \sin(2\pi\nu t) \tag{1.5}$$

where ν, the predominant frequency of the pulse, was chosen as 1 Hz. The damping factor γ was set equal to 4.0.

The vertical components of the displacement vector computed using the Alekseev-Mikhailenko Method for model #1 is shown in Figure 1.2. For the sake of simplicity, units of time and distance were expressed in terms of periods and wavelengths. A wavelength is defined as the ratio of the compressional wave velocity in the halfspace to the

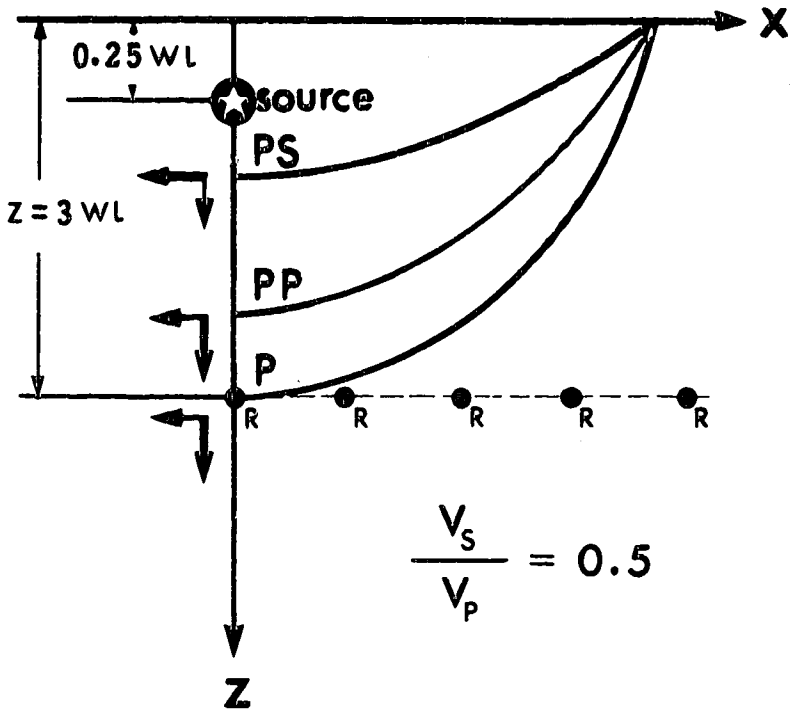

Figure 1.1 Model #1. A point source was buried a small distance (0.25 WL) from the free surface in homogeneous elastic half-space. To minimize the contribution of the Rayleigh wave the receivers were placed at depth z=3 WL below the free surface.

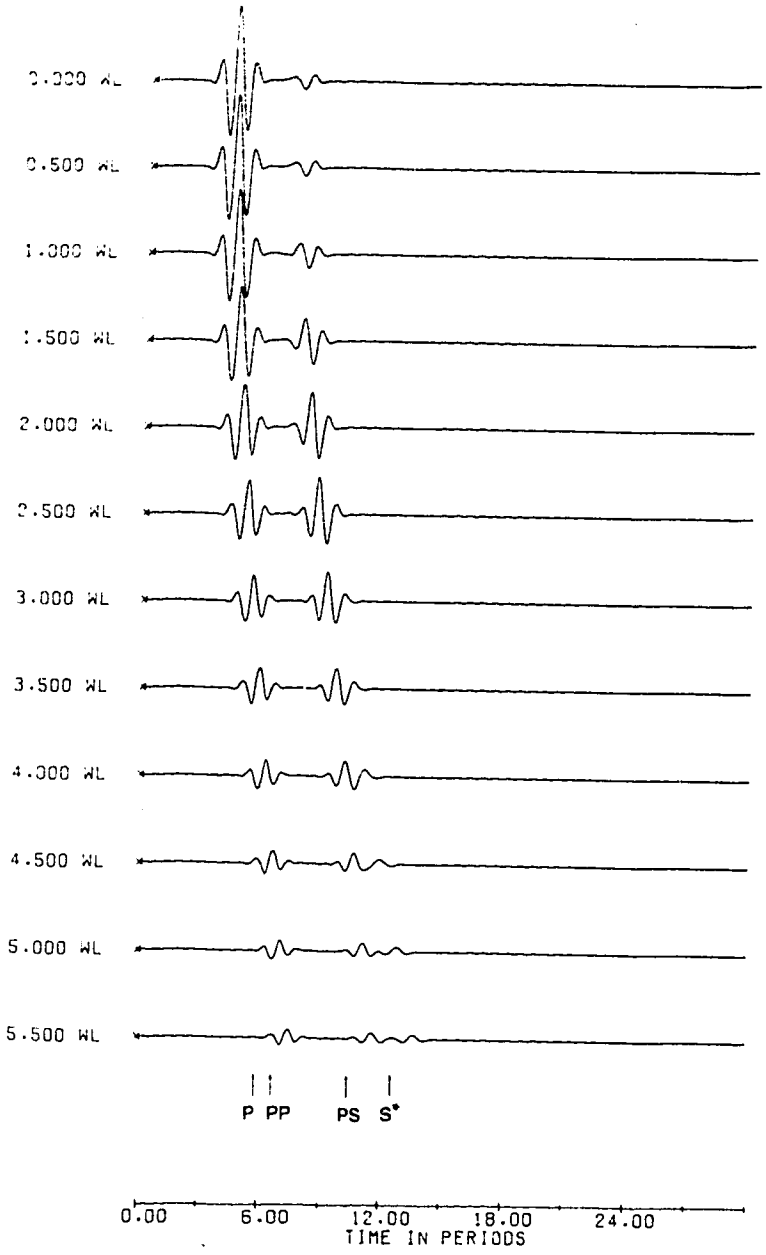

Figure 1.2 Solutions computed by AMM for Model #1 (with author's permission). Vertical components of the displacement vector were computed for the depth z = 3 WL at all epicentral distances. The P source was buried at the depth h = 0.25 WL. The ratio of S to P velocities was taken to be $\beta/a = 0.5$.

predominant frequency of the source pulse. As we can see from Fig. 1.2, two effects have been found as follows:

(1) There is a nonzero vertical component of the converted PS wave reflected at normal incidence from the free surface.

(2) At large epicentral distance we can see the S* and PS waves are already well separated from one another.

Our next question addresses the behaviour of the zero order solution of the Asymptotic Ray Theory for the same model. The zero order approximation solution of ART for model #1 is shown in Figure 1.3 .

The most noticeable difference between the two methods (other than the existance of the Rayleigh wave and the nongeometrical S* arrival in the AMM seismograms) was the obvious inability of the zero order ART approximation to explain the presence of a vertical component of the PS reflected arrival from the free surface at vertical incidence. This difference can be seen clearly by comparision of the zero order ART solution (Fig. 1.3) with the original results of AMM (Fig. 1.2). Thus, it is becoming increasingly important to include effects of the higher order terms in the computation of synthetic seismograms.

This thesis will be devoted to derive mathematical formulae suitable for calculations of the higher order effects of ART, and to investigate the nature of them. Special attention will be paid to investigating the effects of the first order term of ART. The solution including the

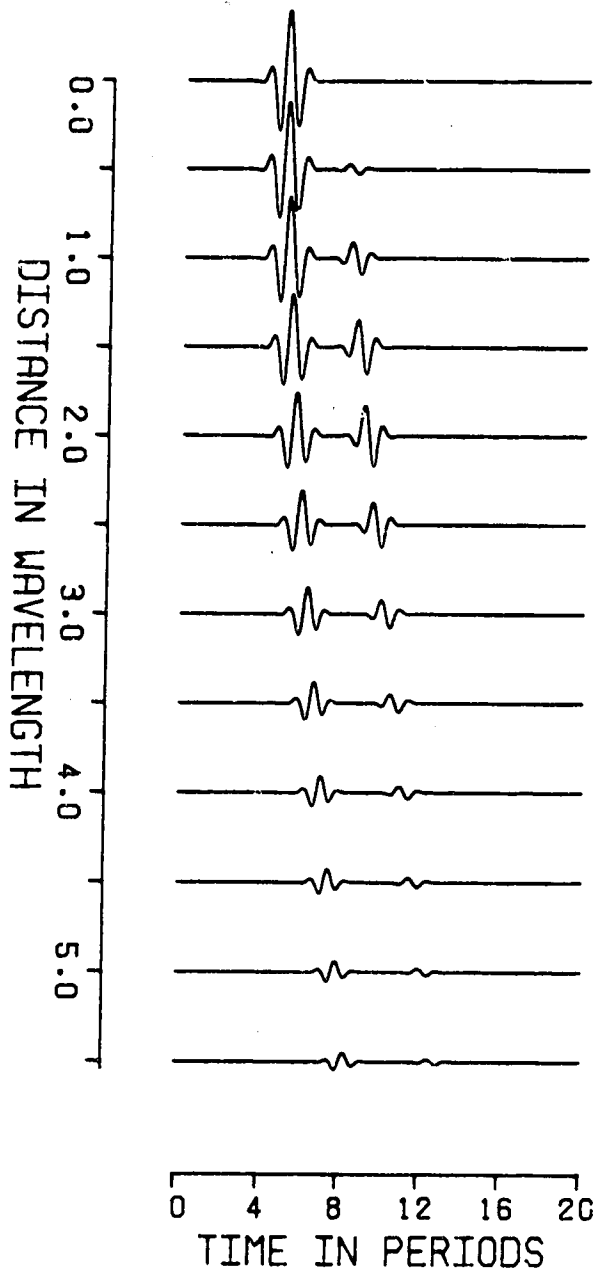

Figure 1.3 The zero order solutions computed by ART for Model #1. Vertical components of the displacement vector were computed for the depth z=3 WL at all epicentral distances. The P source was buried at the depth h=0.25 WL. The ratio of S to P velocities was taken to be β/a = 0.5 .

first order effects will be often compared with the zero order approximation solution, and with results obtained from the Alekseev-Mikhailenko Method. Various computational topics related to it will be described in detail in the next chapters. They will be supplemented by many numerical examples.

2. Higher Order Terms of ART in a Continuous Elastic Medium

In this chapter we shall investigate expressions for the higher order terms as functions of the lower order terms in a continuous elastic medium. Since the formulae for the zeroth order terms for many different models have been presented in many authors' works, we shall use them without derivation. However, appropriate references to the more detailed literature will always be given.

2.1 The Zeroth Order Approximation in The Ray Series

In the zeroth order approximation the ray displacement vector $W(r,t)$ in (1.2) is represented only by the leading term in the ray expansion:

$$(2.1) \qquad W(r,t) = W^{(0)}(r)\, f_0(t-\tau(r))$$

Noticing that $M(W^{(-1)}(r)) = L(W^{(-2)}(r)) = 0$, the recurrent relations (1.3) become:

$$(2.2) \qquad N(W^{(0)}) = (\lambda+\mu)(\nabla\tau\cdot W^{(0)})\nabla\tau + [(\nabla\tau)^2\mu-\rho]W^{(0)} = 0$$

Using a matrix formulation (2.2) may be rewritten as

$$(2.3) \qquad [(\lambda+\mu)B_iB_j + \delta_{ij}(\mu(\nabla\tau)^2-\rho)]W^{(0)} = 0$$

where

$$B_{i(j)} = \partial\tau/\partial x_{i(j)}, \qquad i(j) = 1, 2, 3;$$

are frequently called the slowness vector (slowness is equal

to the inverse of the speed of wave propagation). Assuming $W^{(0)} \neq 0$ in (2.3) a zero value of the determinant of the above system is then required, i.e.

$$(2.4) \qquad [\mu(\nabla\tau)^2-\rho]^2[(\lambda+2\mu)(\nabla\tau)^2-\rho] = 0$$

which leads to the following eikonal equations for the P-wave and S-wave:

$$(2.5) \qquad \begin{aligned} |\nabla\tau| &= 1/\alpha = [\rho/(\lambda+2\mu)]^{1/2}, \\ |\nabla\tau| &= 1/\beta = (\rho/\mu)^{1/2}. \end{aligned}$$

The corresponding orientation of the displacement vectors $W^{(0)}$ in the zeroth order approximation can be easily found, remembering that β in (2.5) represents the phase speed of transverse (shear) elastic S waves, whereas α in (2.5) stands for the phase speed of longitudinal (compressional) P waves.

Writing the leading term in the ray series expansion for the P wave displacement vector as

$$(2.6) \qquad W^{(0)} = P^{(0)}$$

and applying the vector product $(\nabla\tau\times)$ to (2.2) yields:

$$(2.7) \qquad \nabla\tau\times[(\lambda+\mu)(\nabla\tau\cdot P^{(0)})\nabla\tau + ((\nabla\tau)^2\mu-\rho)P^{(0)}] = 0,$$

so that we must have:

$$(2.8) \qquad P^{(0)}\times\nabla\tau = 0,$$

which means the zero order approximation for the amplitude

of the P wave, $\mathbf{P}^{(0)}$, must be oriented along the ray.

In the same way, writing the leading term in the ray series expansion for the S wave displacement vector as

$$\mathbf{W}^{(0)} = \mathbf{S}^{(0)} \tag{2.9}$$

and applying the scalar product $(\nabla\tau\cdot)$ to (2.2) yields:

$$\nabla\tau\cdot[(\lambda+\mu)(\nabla\tau\cdot\mathbf{S}^{(0)})\nabla\tau + ((\nabla\tau)^2\mu-\rho)\mathbf{S}^{(0)}] = 0, \tag{2.10}$$

so that

$$\nabla\tau\cdot\mathbf{S}^{(0)} = 0 \tag{2.11}$$

which means the zero order approximation for the S wave amplitude, $\mathbf{S}^{(0)}$, must be oriented perpendicularly to the ray.

The zero order approximation expressions of the displacement vector for various differential models can be found in Hron and Daley's work (1984). Basically, it is assumed that seismic energy travels through an elastic medium along well-defined paths termed rays. The geometry of these paths is governed by Snell's law. This definition, however, gives no information on energy properties (amplitudes). For this, it is necessary to turn to the law of conservation of energy. This states that the energy flux across the wave front must be equal at all times as long as the elastic parameters of the medium are continuous. Thus, if a value for the displacement is known at some reference point on the ray, (r_0), it is a simple matter to compute

displacement at any other point, (r), along the ray by comparing surface areas of the wave fronts, velocities and densities at these two points plus the effect of energy partitioning at interfaces. For example,

(1) In the case of homogeneous media, the seismic ray is a straight line, and the amplitudes for P and S waves are given respectively by:

$$(2.12a)\quad P^{(0)}(r) = P^{(0)}(r_0) \,/\, L(r)$$

$$(2.12b)\quad S^{(0)}(r) = S^{(0)}(r_0) \,/\, L(r)$$

where r_0 and r express the reference point position and the receiver point position, respectively, and the geometrical spreading, $L(r)$, is given as the following:

$$(2.13)\quad L(r) = r \,/\, r_0$$

(2) In the case of a vertically inhomogeneous medium with constant speed gradient g, i.e. $V(z)=V_0+gz$, the seismic rays are plane curves. If we assume that we know the time-distance curve $t=t(r)$ of the wave under consideration, the amplitude coefficients of P and S waves reached at time t are given respectively by:

$$(2.14a)\quad P^{(0)}(t) = P^{(0)}(t_0)\left[\frac{\rho(t_0)\alpha(t_0)}{\rho(t)\alpha(t)}\right]^{1/2}\frac{1}{L(t)}$$

$$(2.14b)\quad S^{(0)}(t) = S^{(0)}(t_0)\left[\frac{\rho(t_0)\beta(t_0)}{\rho(t)\beta(t)}\right]^{1/2}\frac{1}{L(t)}$$

where α and β are speeds of P and S waves, respectively. The

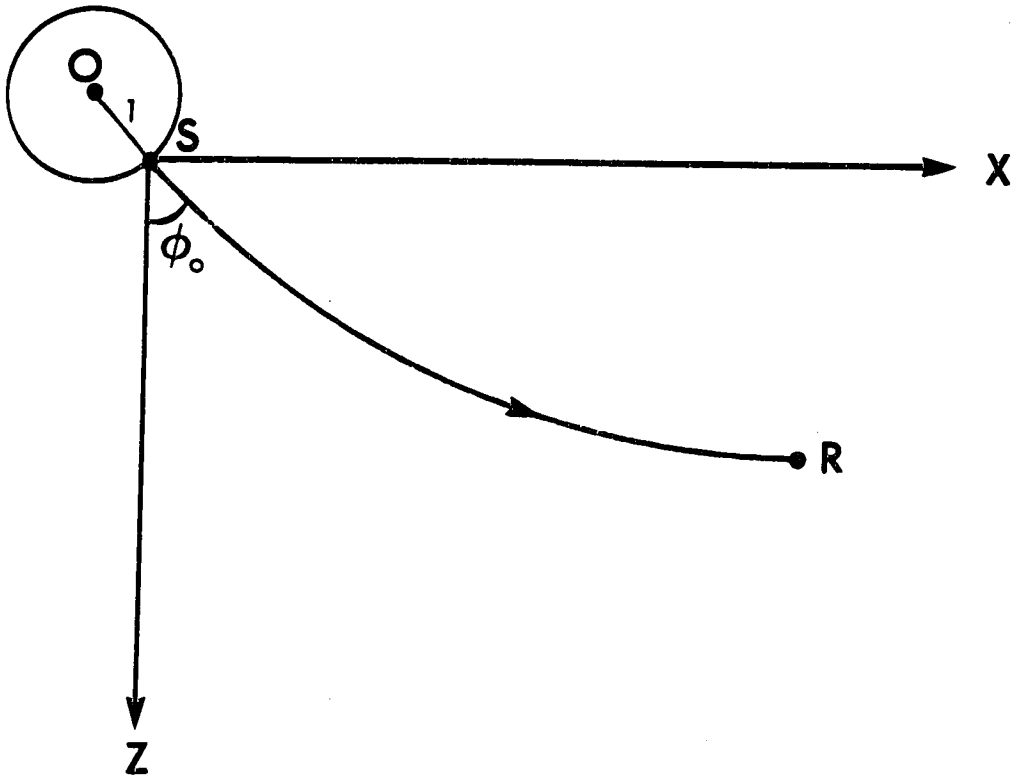

Figure 2.1 An elementary segment between two points S and R on the ray situated on two different wavefronts t_o and t in a vertically inhomogeneous medium. Due to the usual practice of making the region in the vicinity of the source homogeneous, the geometrical spreading L(t) is given in (2.15).

geometrical spreading L(t) between the receiver at R, on the ray reached at time t (t=0 corresponds to the explosive source O) and the point, S, on the unit distance from the source reached at time $t_0=1/V_0$ (see Fig. 2.1) is given by:

$$(2.15) \quad L(t) = 1 + \frac{V(t)}{g} \, sh[g(t-1/V_0)]$$

where V(t) is the phase speed at the receiver point on the ray reached at time t, which is equal to

$$(2.16) \quad V(t) = V_0 \frac{(1+a) \, \exp[g(t-1/V_0)]}{1 + a \, \exp[2g(t-1/V_0)]},$$

where $a = \tan^2(\phi_0/2)$ with ϕ_0 being the take off angle, and V_0 the phase speed at a unit distance from the source.

2.2 Additional Components of Higher Order Terms

Let us write the ray series for the P wave displacement as

$$(2.17) \quad W_t(r,t) = \sum_k W_t^{(k)}(r) \, F_{(k)}(t-\tau(r))$$

The recurrence relations (1.3) then can be rewritten as

$$(2.18) \quad N(W_t^{(k)}) = M(W_t^{(k-1)}) - L(W_t^{(k-2)}), \qquad k = 0, 1, \ldots$$

which makes it possible to derive formulae for all the amplitude terms of P waves.

Since no assumption has been made about the vector $W_t^{(k)}$ besides the requirement that it is carried by a P

wavefront, we have to assume that we may write $W_t^{(k)}$ as the sum of the vector components $\mathbf{P}^{(k)}$ and $\mathbf{p}^{(k)}$.

$$(2.19)\quad W_t^{(k)} = \mathbf{P}^{(k)} + \mathbf{p}^{(k)} = P^{(k)}\hat{e}_= + p^{(k)}\hat{e}_+, \qquad k = 0, 1, \ldots\ldots$$

where $\hat{e}_=$ and $\hat{e}_+$ are the unit vectors along the ray and in the normal plane of the ray, respectively. In (2.19) the component normal to the wave front surface, $P^{(k)}$, is termed the principal component while the component tangent to the wave front surface, $p^{(k)}$, is called the additional component. Analogous definitions exist for S waves.

We may write the recurrent relations (1.3) for S waves as

$$(2.20)\quad N(W_s^{(k)}) = M(W_s^{(k-1)}) - L(W_s^{(k-2)}), \qquad k = 0, 1, \ldots$$

and we must assume that

$$(2.21)\quad W_s^{(k)} = \mathbf{S}^{(k)} + \mathbf{s}^{(k)} = S^{(k)}\hat{e}_+ + s^{(k)}\hat{e}_=, \qquad k = 0, 1, \ldots\ldots$$

where $S^{(k)}$ and $s^{(k)}$ are called the principal and the additional components, respectively.

Using the above concepts of principal and additional components, we can rewrite the results obtained from section 2.1 as follows:

$$(2.8')\quad \mathbf{P}^{(0)}(\mathbf{r}) = P^{(0)}\hat{e}_= + 0\ \hat{e}_+$$

$$(2.11')\quad \mathbf{S}^{(0)}(\mathbf{r}) = S^{(0)}\hat{e}_+ + 0\ \hat{e}_=$$

which means that in the zero order approximation the additional components of P or S waves always equal to zero for any kind of media.

However, the higher order additional components $p^{(k)}$ and $s^{(k)}$ should be different from the zeroth order additional components even through the medium is an elastic isotropic homogeneous one. Let us first derive general expressions for $p^{(k)}$ and $s^{(k)}$, respectively.

In the case of P rays, applying the scalar product operation $(\hat{e}_+ \cdot)$ to (2.18) yields:

$$N_+(W_t^{(k)}) = M_+(W_t^{(k-1)}) - L_+(W_t^{(k-2)}), \qquad k = 0, 1, \ldots\ldots \tag{2.22}$$

where
$$N_+(W_t^{(k)}) \equiv \hat{e}_+ \cdot \mathbf{N}(W_t^{(k)})$$
$$M_+(W_t^{(k-1)}) \equiv \hat{e}_+ \cdot \mathbf{M}(W_t^{(k-1)})$$
$$L_+(W_t^{(k-2)}) \equiv \hat{e}_+ \cdot \mathbf{L}(W_t^{(k-2)})$$

Substituting (2.19) into (2.22) and using (1.4), we may obtain, after some vector operations:

$$N_+(W_t^{(k)}) = \rho(\beta^2-\alpha^2)p^{(k)} / \alpha^2 \tag{2.23}$$

$$M_+(W_t^{(k-1)}) = (\lambda+\mu)[\nabla(\frac{p^{(k-1)}}{\alpha})]_+ + 2\mu P^{(k-1)}\frac{1}{\alpha\, r_1} + \frac{2\mu}{\alpha^2}\frac{dp^{(k-1)}}{d\tau} + \mu\nabla^2\tau\; p^{(k-1)} + \frac{p^{(k-1)}}{\alpha}[\nabla\mu]_= + \frac{p^{(k-1)}}{\alpha}[\nabla\lambda]_+ \tag{2.24}$$

where r_1 is the radius of curvature of the ray segment. Then we can write

$$(2.25)\qquad p^{(k)} = \frac{\alpha^2}{\rho(\beta^2-\alpha^2)}[M_+(W_t^{(k-1)}) - L_+(W_t^{(k-2)})]$$

Taking k=1 in (2.25), noticing that $L_+(W_t^{(-1)}) = 0$ and using (2.24), we may obtain the following general formula for the first order additional component of P waves:

$$(2.26)\qquad p^{(1)} = \frac{\alpha^2}{\rho(\beta^2-\alpha^2)} M_+(W_t^{(0)})$$

$$= \frac{\alpha^2}{\rho(\beta^2-\alpha^2)} \{(\lambda+\mu)[\nabla(\frac{p^{(0)}}{\alpha})]_+ +$$

$$+ 2\mu p^{(0)}\frac{1}{\alpha\, r_1} + \frac{p^{(0)}}{\alpha}[\nabla\lambda]_+\}$$

It may be easily seen that for an elastic isotropic homogeneous medium, (2.26) becomes $p^{(1)} = 0$, since the values of $[\nabla P^{(0)}]_+ = \nabla P^{(0)}\cdot\hat{e}_+$, $[\nabla\lambda]$ and $[1/r_1]$ are all equal to zero in this instance.

In the case of S waves, applying the scalar product operation $(\hat{e}_=\cdot)$ to (2.20) yields:

$$(2.27)\qquad N_=(W_s^{(k)}) = M_=(W_s^{(k-1)}) - L_=(W_s^{(k-2)}),\quad k = 0,1,\ldots$$

where
$$N_=(W_s^{(k)}) \equiv \hat{e}_=\cdot\mathbf{N}(W_s^{(k)})$$
$$M_=(W_s^{(k-1)}) \equiv \hat{e}_=\cdot\mathbf{M}(W_s^{(k-1)})$$
$$L_=(W_s^{(k-2)}) \equiv \hat{e}_=\cdot\mathbf{L}(W_s^{(k-2)})$$

Substituting (2.21) into (2.27) and using (1.4), we have, after some vectorial operations:

$$(2.28)\qquad N_{=}(W_{s}^{(k)}) = \rho(\alpha^2-\beta^2)s^{(k)} / \beta^2$$

$$(2.29)\qquad M_{=}(W_{s}^{(k-1)}) = \frac{(\lambda+\mu)}{\beta}[\nabla\cdot W_{s}^{(k-1)}] + \frac{2\mu}{\beta^2}\frac{ds^{(k-1)}}{d\tau_{s}} +$$
$$+ (\lambda+\mu)[\nabla(\frac{s^{(k-1)}}{\beta})]_{=} - \frac{2\mu\, S_{n}^{(k-1)}}{\beta\, r_{1}} +$$
$$+ \frac{[\nabla\lambda]_{=}}{\beta}s^{(k-1)} + \mu s^{(k-1)}\nabla^2\tau_{s} +$$
$$+ \frac{2[\nabla\mu]_{=}}{\beta}s^{(k-1)} + \frac{[\nabla\mu]_{+}}{\beta}S_{n}^{(k-1)}$$

where as before r_1 is the radius of curvature of the ray segment. We can then write

$$(2.30)\qquad s^{(k)} = \frac{\beta^2}{\rho(\alpha^2-\beta^2)}\,[M_{=}(W_{s}^{(k-1)}) - L_{=}(W_{s}^{(k-2)})]$$

Taking k=1 in (2.30), noticing that $L_{=}(W_{s}^{(-1)}) = 0$ and using (2.29) we obtain the following general formula for the first order additional component of S waves:

$$(2.31)\qquad s^{(1)} = \frac{\beta^2}{\rho(\alpha^2-\beta^2)}\,M_{=}(W_{s}^{(0)})$$

$$= \frac{\beta^2}{\rho(\alpha^2-\beta^2)}\,\{\frac{(\lambda+\mu)}{\beta}\nabla\cdot(S^{(0)}\hat{e}_{+}) - \frac{2\mu\, S_{n}^{(0)}}{\beta\, r_{1}} +$$
$$+ \frac{[\nabla\mu]_{+}}{\beta}\,S_{n}^{(0)}\}$$

For an elastic homogeneous medium Eq. (2.31) becomes:

$$s^{(1)}(r) = \beta\, S^{(0)}(r)\, \nabla\cdot\hat{e}_{+} \tag{2.32}$$

Equation (2.32) shows that the first order additional component of S waves, $s^{(1)}$ is generally not equal to zero even though the elastic medium is isotropic and homogeneous.

When a point source is placed in elastic isotropic homogeneous medium, the pure P or S rays are all symmetrical and radiological. As a result the evaluation of $\nabla\cdot\hat{e}_{+}$ and $\nabla\cdot\hat{e}_{=}$ can be easily carried out in a spherical coordinate system as follows:

$$\begin{aligned} \nabla\cdot\hat{e}_{+} &= \cot(\theta)/r \\ \nabla\cdot\hat{e}_{=} &= 2/r \end{aligned} \tag{2.33}$$

where θ is the angle between the Z direction and the given ray, and r the ray length.

Finally the following expressions for the first order additional components of P or S waves in an elastic isotropic homogeneous medium may be summarized as follows:

$$\begin{aligned} p^{(1)}(r) &= 0 \\ s^{(1)}(r) &= \beta\, S^{(0)}(r)\, \cot(\theta)\, /\, r \end{aligned} \tag{2.34}$$

2.3 Principal Components of Higher Order Terms

We have shown how to determine the formulae for the additional components of the higher order terms in the last section. In this section it is therefore very useful to be able to find formulae for the principal components of the higher order terms, $P^{(k)}$ and $S^{(k)}$.

Let us first concentrate on the case of P waves. Assuming $W_t^{(k)} = P^{(k)}\hat{e}_= + p^{(k)}\hat{e}_+$ and applying the scalar product operation $(\hat{e}_= \cdot)$ to (2.18) yields:

$$N_=(W_t^{(k)}) = M_=(W_t^{(k-1)}) - L_=(W_t^{(k-2)}), \qquad k = 0, 1, \ldots \tag{2.35}$$

where:

$$N_=(W_t^{(k)}) = 0, \qquad k = 0, 1, 2, \ldots\ldots \tag{2.36}$$

Then (2.35) can be rewritten as:

$$M_=(P^{(k-1)}\hat{e}_=) = - M_=(p^{(k-1)}\hat{e}_+) + L_=(W_t^{(k-2)}), \qquad k = 0,1,\ldots\ldots \tag{2.37}$$

where:

$$M_=(P^{(k-1)}\hat{e}_=) = P^{(k-1)}[\alpha\rho\ \nabla\cdot\hat{e}_= + \hat{e}_=\cdot\nabla(\alpha\rho)] + \frac{dP^{(k-1)}}{ds}\,2\alpha\rho \tag{2.38}$$

$$M_=(p^{(k-1)}\hat{e}_+) = p^{(k-1)}[\frac{-2\mu}{\alpha r_1} + \frac{\hat{e}_+\cdot\nabla\mu}{\alpha}] + \tag{2.39}$$

$$+ \frac{(\lambda+\mu)}{\alpha} p^{(k-1)} \nabla\cdot\hat{e}_+ \ .$$

Here r_1 is the radius of curvature of the ray segment.

Thus (2.37) should be rewritten in the following recurrent form:

$$(2.40) \quad \frac{dP^{(k-1)}}{ds} 2\alpha\rho = - P^{(k-1)}[\alpha\rho\ \nabla\cdot\hat{e}_= + \hat{e}_=\cdot\nabla(\alpha\rho)] - M_=(p^{(k-1)}\hat{e}_+) + L_=(W_t^{(k-2)})$$

$$k = 0,\ 1,\ 2,\ .....$$

The principal component of the first order terms can be derived from (2.40) by setting k=2 in:

$$(2.41) \quad \frac{dP^{(1)}}{ds} 2\alpha\rho = - P^{(1)}[\alpha\rho\ \nabla\cdot\hat{e}_= + \hat{e}_=\cdot\nabla(\alpha\rho)] - M_=(p^{(1)}\hat{e}_+) + L_=(P^{(0)}\hat{e}_=)$$

where

$$(2.42) \quad L_=(P^{(0)}) = \frac{d^2P^{(0)}}{ds^2}(\lambda+2\mu) + \frac{dP^{(0)}}{ds}[(\lambda+\mu)\nabla\cdot\hat{e}_= + \hat{e}_=\cdot(\nabla\lambda+2\nabla\mu)] + \hat{e}_=\cdot[\nabla\mu\times(\nabla\times P^{(0)})] + P^{(0)}[(\lambda+\mu)\frac{d(\nabla\cdot\hat{e}_=)}{ds} + (\hat{e}_=\cdot\nabla\lambda)\nabla\cdot\hat{e}_= - \frac{\mu}{r_1^2}]$$

In the case of elastic isotropic homogeneous media, (2.41) becomes:

$$(2.43) \quad \frac{dP^{(1)}(r)}{dr} = - P^{(1)}(r)\frac{\nabla\cdot\hat{e}_=}{2} + \frac{d^2P^{(0)}(r)}{dr^2}\frac{\alpha}{2} +$$

$$+ \frac{dP^{(0)}(r)}{dr} \frac{(\lambda+\mu)}{2\alpha\rho} \nabla\cdot\hat{e}_z + P^{(0)}(r) \frac{(\lambda+\mu)}{2\alpha\rho} \frac{d(\nabla\cdot\hat{e}_z)}{dr}$$

From the above equation it can be seen that for a pure P wave produced by a point source and propagating in elastic isotropic homogeneous medium, with $\nabla\cdot\hat{e}_z$ given by (2.33), and the zero order term determined by (2.12a), (2.43) can be further simplified to yield:

$$(2.44) \quad \frac{dP^{(1)}(r)}{dr} = - P^{(1)}(r) \frac{1}{r} - \frac{\lambda}{\alpha\rho r^2} P^{(0)}(r)$$

which has the following general solution:

$$(2.45) \quad P^{(1)}(r) = \frac{\lambda}{\alpha\rho r} P^{(0)}(r) + \frac{C_0}{r}$$

where C_0 is a constant determined by the initial conditions.

Defining the ratio of S to P wave speeds to be

$$(2.46) \quad \Omega \equiv \frac{\beta}{\alpha}$$

which implies $(\lambda/\alpha\rho) = (1-2\Omega^2)\alpha$, (2.46) may be rewritten as:

$$(2.45') \quad P^{(1)}(r) = (1 - 2\Omega^2)\ \alpha \frac{1}{r} P^{(0)}(r) + \frac{C_0}{r}$$

To determine the constant C_0, we compare (2.45') with the following classical formula under the condition that $\mu=0$ (Alekseev, Babich and Gel'chinskiy, 1958):

$$(2.47) \quad P^{(1)}/P^{(0)} = \alpha/r$$

As a result, C_0 in both (2.45) and (2.45') must be equal to zero, and the principal component of the first order term of a pure P wave in homogeneous medium has the final expression:

$$(2.48) \qquad P^{(1)}(r) = \frac{\lambda}{\alpha\rho r} P^{(0)}(r)$$

Secondly, we shall consider the principal component of higher order terms for S waves. Applying the scalar product operation $(\hat{e}_+ \cdot)$ to (2.20) yields:

$$(2.49) \qquad N_+(W_s^{(k)}) = M_+(W_s^{(k-1)}) - L_+(W_s^{(k-2)}), \quad k = 0,1,...$$

Substituting (2.21) into (1.4), we can obtain, after some vectorial operations:

$$(2.50) \qquad N_+(W_s^{(k)}) = 0, \qquad k = 0, 1, 2,.....$$

Then (2.49) becomes:

$$(2.51) \qquad M_+(S^{(k-1)}\hat{e}_+) = - M_+(s^{(k-1)}\hat{e}_=) + L_+(W_s^{(k-2)})$$
$$k = 0, 1, 2,.....$$

where:

$$(2.52) \qquad M_+(S^{(k-1)}\hat{e}_+) = \frac{dS^{(k-1)}}{dr} \frac{2\mu}{\beta} + S^{(k-1)}\hat{e}_= \cdot \nabla(\frac{\mu}{\beta}) +$$
$$+ S^{(k-1)} \frac{\mu}{\beta} \nabla \cdot \hat{e}_=,$$
$$k = 0, 1, ...$$

and

$$(2.53)\quad M_+(s^{(k-1)}\hat{e}_=) = (\lambda+\mu)s^{(k-1)}\hat{e}_+\cdot\nabla(\frac{1}{\beta}) + \frac{1}{\beta}\, s^{(k-1)}\hat{e}_+\cdot\nabla\lambda + \frac{2\mu}{\beta r_1}\, s^{(k-1)}, \qquad k = 0, 1, \ldots$$

Thus (2.51) can be rewritten in the following recurrent form:

$$(2.54)\quad \frac{dS^{(k-1)}}{dr}\,\frac{2\mu}{\beta} = -\, S^{(k-1)}[\hat{e}_=\cdot\nabla(\frac{\mu}{\beta}) + \frac{\mu}{\beta}\,\nabla\cdot\hat{e}_=] + - M_+(s^{(k-1)}\hat{e}_=) + L_+(W_s^{(k-2)}), \qquad k = 0, 1, 2, \ldots\ldots$$

After setting k=2 in (2.54) we have:

$$(2.55)\quad \frac{dS^{(1)}}{dr}\,\frac{2\mu}{\beta} = -\, S^{(1)}[\hat{e}_=\cdot\nabla(\frac{\mu}{\beta}) + \frac{\mu}{\beta}\,\nabla\cdot\hat{e}_=] + - M_+(s^{(1)}\hat{e}_=) + L_+(S^{(0)}\hat{e}_+),$$

where:

$$(2.56)\quad L_+(S^{(0)}\hat{e}_+) = 2\,\nabla\mu\cdot\hat{e}_=\frac{dS^{(0)}}{dr} + S^{(0)}[(\nabla\cdot\hat{e}_+)(\hat{e}_+\cdot\nabla\lambda) + + (\lambda+\mu)\hat{e}_+\cdot\nabla(\nabla\cdot\hat{e}_+) - \frac{\mu}{r_1^{\,2}} - \mu T^2] + + \mu\,\frac{d^2S^{(0)}}{dr^2} + \hat{e}_+\cdot\nabla\mu\times(\nabla\times S^{(0)}).$$

Here T is the rotation of the ray segment.

For the case of an elastic isotropic homogeneous medium, (2.55) can be further simplified to yield:

$$(2.57)\quad \frac{dS^{(1)}(r)}{dr} = -S^{(1)}(r)\frac{\nabla\cdot\hat{e}_{=}}{2} + \frac{d^2S^{(0)}(r)}{dr^2}\frac{\beta}{2} + \\ + S^{(0)}(r)\frac{(\lambda+\mu)\beta}{2\mu}\hat{e}_{+}\cdot\nabla(\nabla\cdot\hat{e}_{+})$$

For a pure S wave produced by a point source and propagating in elastic isotropic homogeneous medium, with $\nabla\cdot\hat{e}_{=}$ and $\nabla\cdot\hat{e}_{+}$ given by (2.33), and the zero order term $S^{(0)}(r)$ determined by (2.12b), (2.57) can be simplified as follows:

$$(2.58)\quad \frac{dS^{(1)}(r)}{dr} = -S^{(1)}(r)\frac{1}{r} + \beta S^{(0)}(r)\frac{1}{r^2}$$

which has the following general solution:

$$(2.59)\quad S^{(1)}(r) = -\beta\frac{S^{(0)}(r)}{r} + \frac{C_0}{r}$$

In Chapter 4, higher order effects of ART in some complex models will be considered in details. In that case the expressions for the first order terms of reflected or transmitted P and S waves will have more complex forms, even though they are all generated from the general formulae derived in this chapter.

In the next two sections, the first order effects of ART in vertically inhomogeneous elastic media will be investigated based on the general formulae (2.31) and (2.55) for the first order P waves. To do so, some fundamental formulae, describing the kinematic and dynamic

characteristics of a seismic ray in vertically inhomogeneous elastic media, are going to be given in the next section.

2.4 Fundamental Formulae in Vertically Inhomogeneous Elastic Media

One medium type which lends itself easily to calculations discussed in the previous sections is a vertically inhomogeneous medium. If we specify that the P wave speed is given by

$$\alpha(z) = \alpha_0 + gz \tag{2.60}$$

where α_0 is the initial speed at the point source, and g the velocity gradient. Both of them will be assumed constant. The vertical coordinate Z is chosen such that its orientation is positive downwards into the medium.

For this type of medium we shall use the relations for the other elastic parameters in terms of the P wave speed as given by Gardner et al. (1974), viz.,

$$\begin{aligned} \beta(z) &= \alpha(z) \,/\, \sqrt{3} \\ \rho(z) &= \alpha^{1/4}(z)\, \sqrt{3} \\ \lambda(z) &= \mu(z) = \alpha^{9/4}(z) \,/\, \sqrt{3} \end{aligned} \tag{2.61}$$

The use of compact analytic expressions for the elastic parameters allows easy differentiation which simplifies matters when the vector operators **N**, **M**, and **L** in ART are evaluated.

Formulae suitable for computations of the higher order terms for these types of media will be derived in this and the next sections. In this section some fundamental formulae shall be derived first.

Rays emanating from a point source are circular arcs in a common plane in vertically inhomogeneous media (Nettleton, 1940). Based on Snell's law, the ray parameter, p, is constant along the whole ray so that

$$(2.62) \qquad p = \frac{\sin\phi_o}{\alpha_o} = \frac{\sin\phi(s)}{\alpha(z)} \, .$$

It can be conveniently introduced into the computations of the travel time t, and of the range $R=(x^2+y^2)^{1/2}$, which is the imaged length of the ray segment in the horizontal plane. Thus

$$(2.63) \qquad dR = \tan\phi(s)\, dz = \frac{p\alpha(z)\, dz}{[1 - p^2\alpha^2(z)]^{1/2}}$$

$$(2.64) \qquad dt = \frac{dz}{\alpha(z)\cos\phi(s)} = \frac{dz}{\alpha(z)[1 - p^2\alpha^2(z)]^{1/2}}$$

Here $\phi(s)$ represents the acute angle made by the ray with the vertical direction, and $\alpha(z)$ the wave speed along the ray. Thus using (2.60) and integrating (2.63) yields:

$$(2.65) \qquad R = \int_o^z \frac{p(\alpha_o + gz)\, dz}{[1 - p^2(\alpha_o+gz)^2]^{1/2}}$$

$$= \frac{1}{p\, g} \{(1-p^2\alpha_o^2)^{1/2} - [1-p^2(\alpha_o+pz)^2]^{1/2}\}$$

Noticing $p\alpha_o = \sin\phi_o$ the above equation becomes:

$$R = \frac{\alpha_o}{g \tan\phi_o} - \left[\left(\frac{\alpha_o}{g \sin\phi_o}\right)^2 - \left(\frac{\alpha_o}{g} + z\right)^2\right]^{1/2}$$

or

$$(2.66) \quad (R - R_1)^2 + (Z - z_1)^2 = r_1^2$$

where:

$$R_1 = \frac{\alpha_o}{g \tan\phi_o} = \frac{(1 - p^2\alpha_o^2)^{1/2}}{p\, g}$$

$$(2.67) \quad z_1 = -\frac{\alpha_o}{g}$$

$$r_1 = \frac{\alpha_o}{g \sin\phi_o} = \frac{1}{p\, g}$$

Equations (2.66) and (2.67) describe a circular family of rays with the same source point and different ray parameters. Each circular ray path has different centre (R_1, z_1) and different radius of curvature r_1.

To obtain a convenient equation describing wavefront surfaces produced by a point source in vertically inhomogeneous media, we apply (2.60) and integrate (2.64) as follows:

$$(2.68) \quad t = \int_o^z \frac{dz}{(\alpha_o+gz)[1-p^2(\alpha_o+gz)^2]^{1/2}}$$

$$= \frac{1}{g} \ln \frac{1 + gz/\alpha_o + [(1+gz/\alpha_o)^2 - \sin^2\phi(s)]^{1/2}}{1 + \cos\phi(s)}$$

Taking the exponential of the above expression yields:

$$(2.69)\quad e^{gt}[1+\cos\phi(s)] = 1+gz/\alpha_o+[(1+gz/\alpha_o)^2-\sin^2\phi(s)]^{1/2}$$

which can be rewritten as

$$(2.70)\quad \cos\phi(s) = \frac{1 + gz/\alpha_o - ch(gt)}{sh(gt)} .$$

Thus, due to the relationship of $\cos^2\phi(s)+\sin^2\phi(s)=1$ we have:

$$(2.71)\quad \sin\phi(s) = \frac{[2(1+gz/\alpha_o)ch(gt) - (1+gz/\alpha_o)^2 - 1]^{1/2}}{sh(gt)} .$$

Noticing $p\alpha(z)=\sin\phi(s)$ (2.65) becomes:

$$(2.72)\quad R = \frac{[\alpha^2(z)-\sin^2\phi(s)\alpha_o^2]^{1/2} - \alpha(z)\cos\phi(s)}{g\ \sin\phi(s)} .$$

Substituting (2.70) and (2.71) into (2.72) yields:

$$(2.73)\quad R^2 = \frac{\alpha_o^2[2(1+gz/\alpha_o)ch(gt) - (1+gz/\alpha_o)^2 - 1]}{g^2}$$

$$= -\{Z - \frac{\alpha_o}{g}[ch(gt)-1]\}^2 + [\frac{\alpha_o}{g} sh(gt)]^2$$

which can be rewritten as $R^2=X^2+Y^2$ in the following manner:

$$(2.74)\quad X^2 + Y^2 + (Z - z_2)^2 = r_2^2$$

where:

$$z_2 = \frac{\alpha_0[ch(gt) - 1]}{g}$$

(2.75)

$$r_2 = \frac{\alpha_0\, sh(gt)}{g}$$

Equation (2.74) shows that the desired wavefront surfaces are a family of spherical surfaces with the centre $(0,0,z_2(t))$ and a radius of curvature $r_2(t)$.

Due to the fact that in an isotropic medium the ray segment is always perpendicular to the wavefront surface, it is convenient to use the wavefront surface equation (2.74) to find expressions for $\nabla\cdot\hat{e}_=$ and $\nabla\cdot\hat{e}_+$, where $\hat{e}_=$ and $\hat{e}_+$ are the unit vectors along the ray and in the plane normal to the ray, respectively (see Figure 2.2).

The form of the wavefront surface equation (2.74) indicates that we choose the following spherical coordinate system (r_2,θ,χ) to work in:

$$\begin{aligned} X &= r_2 \sin\theta \cos\chi \\ Y &= r_2 \sin\theta \sin\chi \\ Z &= r_2 \cos\theta + z_2 \end{aligned} \qquad (2.76)$$

in which the scale factors are:

$$H_1 = 1$$

$$H_2 = r_2$$

$$H_3 = r_2 \sin\theta$$

and

$$\begin{aligned} \hat{e}_= &= \hat{e}_1 = (1,\ 0,\ 0) \\ \hat{e}_+ &= \hat{e}_2 = (0,\ 1,\ 0) \end{aligned} \qquad (2.77)$$

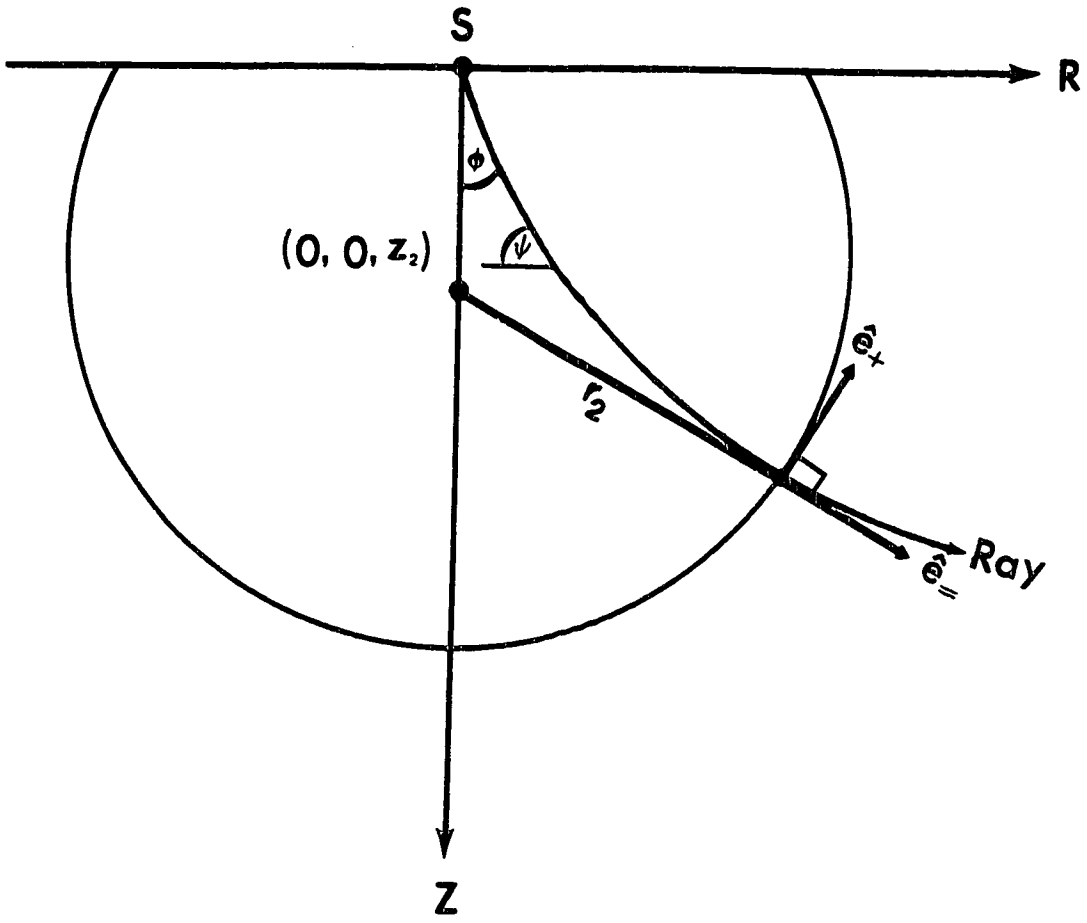

Figure 2.2 Relationships among the ray segment, $\hat{e}_=$, $\hat{e}_+$, and the wavefront surface in vertically inhomogeneous media.

Thus we are able to calculate

$$(2.78\text{-}1)\quad \nabla\cdot\hat{e}_{=} = \frac{1}{r_2^2 \sin\theta}\frac{\partial(r_2^2 \sin\theta)}{\partial r_2} = \frac{2}{r_2}$$

$$(2.78\text{-}2)\quad \nabla\cdot\hat{e}_{+} = \frac{1}{r_2^2 \sin\theta}\frac{\partial(r_2 \sin\theta)}{\partial \theta} = \frac{\operatorname{cotan}\theta}{r_2}$$

with

$$(2.79)\quad \operatorname{cotan}\theta = \frac{Z - z_2}{[X^2 + Y^2]^{1/2}}$$

where r_2 and z_2 are given in (2.75).

An interesting fact which should be pointed out here is that we are able to get the expressions of $\nabla\cdot\hat{e}_{=}$ and $\nabla\cdot\hat{e}_{+}$ in homogeneous media from (2.78) and (2.79), which will be the same as those given in (2.33), by taking the velocity gradient g=0 in (2.75). In the case of g=0, (2.75) becomes:

$$(2.80)\quad \begin{aligned} r_2(g=0) &= \frac{[\mathrm{sh}(gt)\alpha_0]'}{g'}\Big|(g=0) = \alpha_0 t = r \\ z_2(g=0) &= \frac{[\mathrm{ch}(gt)-1]'\alpha_0}{g'}\Big|(g=0) = 0 \end{aligned}$$

where $r = (X^2 + Y^2 + Z^2)^{1/2}$

Substituting (2.80) into (2.78) yields:

$$(2.81)\quad \nabla\cdot\hat{e}_{=} = \frac{2}{r}$$

$$\nabla\cdot\hat{\mathbf{e}}_{\star} = \frac{\text{cotan}\theta}{r}$$

with

$$(2.82)\qquad \text{cotan}\theta = \frac{Z - z_2(g=0)}{[X^2 + Y^2]^{1/2}} = \frac{Z}{[X^2 + Y^2]^{1/2}} .$$

Here θ is the acute angle between the ray segment and the direction, and r the length of the ray segment in homogeneous media. Thus we once again see the same result as shown in (2.33).

It should be emphasized here that Eqs. (2.78-1), (2.78-2) and (2.79) will often be used when we derive the expressions of the higher order terms for vertically inhomogeneous media in the next section.

The values of the useful expressions $\nabla\times\mathbf{P}^{(0)}$ and $\nabla\times\mathbf{S}^{(0)}$ may also be easily found using the above spherical coordinate system and also will be often used in the next section. In the above coordinate system we have $\mathbf{P}^{(0)}=(P^{(0)}(r_2),0,0)$, $\mathbf{S}^{(0)}=(0,S^{(0)}(r_2),0)$, and the following quantities:

$$[\nabla\times\mathbf{P}^{(0)}]_1 = 0$$

$$[\nabla\times\mathbf{P}^{(0)}]_2 = 0$$

$$[\nabla\times\mathbf{P}^{(0)}]_3 = 0$$

or

$$(2.83)\qquad \nabla\times\mathbf{P}^{(0)} = 0,$$

which means that the zero order term of the **P** wave

physically describes a non-rotational wave.

In the similar matter we have:

$$[\nabla\times\mathbf{S}^{(0)}]_1 = 0$$

$$[\nabla\times\mathbf{S}^{(0)}]_2 = 0$$

$$[\nabla\times\mathbf{S}^{(0)}]_3 = S^{(0)}/r_2 + dS^{(0)}/dr_2$$

or

$$\nabla\times\mathbf{S}^{(0)} = \left[\frac{S^{(0)}}{r_2} + \frac{dS^{(0)}}{dr_2}\right]\hat{b} \tag{2.84}$$

where $\hat{b} = \hat{e}_2 \times \hat{e}_1$. The above expression indicates that the zero order term of the S wave describing some rotational characteristics of a wave field is totally different from the zero order term of the P wave.

2.5 First Order Terms in Vertically Inhomogeneous Elastic Media

Based on the results produced in the last two sections, the first order terms in a vertically inhomogeneous elastic medium will be discussed in detail for the following two cases.

(1) First, we shall concentrate on the case of a pure P wave propagating in vertically inhomogeneous media. Recalling the general formula of the additional component of the first order terms for P waves, (2.26), and taking into consideration the common relations of the elastic parameters (2.61) for a vertically inhomogeneous medium, we have:

$$(2.85)\qquad p^{(1)}(s) = -\frac{1}{8}\,P^{(0)}(s)[\nabla\alpha]_{+} - \frac{\alpha(z)}{r_1}\,P^{(0)}(s)\ .$$

Noticing

$$(2.86)\qquad [\nabla\alpha]_{+} = -\,g\,\sin\phi(s)$$

and

$$(2.67)\qquad r_1 = \frac{\alpha_0}{g\,\sin\phi_0} = \frac{\alpha(z)}{g\,\sin\phi(s)}$$

we finally have the additional component of the first order term in this case as follows:

$$(2.87)\qquad p^{(1)}(s) = -\frac{7}{8}\,g\,\sin\phi(s)\,P^{(0)}\ .$$

To obtain the expression of the principal component of the first order term $P^{(1)}$, we recall its general formula (2.41) which after taking (2.61) into consideration yields:

$$(2.88)\qquad \frac{dP^{(1)}}{dr} = -\,P^{(1)}\left[\frac{\nabla\cdot\hat{e}_{=}}{2} + \frac{5g\,\cos\phi}{8\alpha}\right] - \frac{M_{=}(p^{(1)}\hat{e}_{+})}{2\alpha\rho} + \frac{L_{=}(P^{(0)}\hat{e}_{=})}{2\alpha\rho}\ .$$

In (2.88) $M_{=}(p^{(1)}\hat{e}_{+})$ is going to be obtained from its general formula (2.39) using the simplifications (2.60), (2.61) and (2.67) to yield:

$$(2.89)\qquad \frac{-M_{=}(p^{(1)}\hat{e}_{+})}{2\alpha\rho} = \left[\frac{17g\,\sin\phi}{24\alpha} - \frac{1}{3}\,\nabla\cdot\hat{e}_{+}\right]p^{(1)}$$

$$= P^{(0)}\left[\frac{7}{24}\, g \sin\phi\, \nabla\cdot\hat{e}_+ - \frac{119 g^2 \sin^2\phi}{192\alpha}\right]$$

At the same time, $L_=(P^{(0)}\hat{e}_=)$ is obtained from (2.42) using the simplifications (2.60), (2.61), (2.67), (2.75) and (2.83) as follows:

$$(2.90)\quad \frac{L_=(P^{(0)}\hat{e}_=)}{2\alpha\rho} = \frac{d^2P^{(0)}}{dr^2}\,\frac{\alpha}{2} + \frac{dP^{(0)}}{dr}\left[\frac{\alpha\nabla\cdot\hat{e}_=}{3} + \frac{9g\cos\phi}{8}\right] + P^{(0)}\left[\frac{3g\cos\phi\,\nabla\cdot\hat{e}_=}{8} - \frac{g^2\sin^2\phi}{6\alpha} - \frac{2g^2}{3\alpha_0}\,\frac{ch(gt)}{sh^2(gt)}\right].$$

Substituting (2.89) and (2.90) into (2.88) yields:

$$(2.91)\quad \frac{dP^{(1)}}{dr} = F_1P^{(1)} + F_2P^{(0)} + F_3\,\frac{dP^{(0)}}{dr} + F_4\,\frac{d^2P^{(0)}}{dr^2}$$

where:

$$(2.92)\quad \begin{aligned} F_1 &= -\frac{1}{2}\,\nabla\cdot\hat{e}_= - \frac{5}{8}\,\frac{g\cos\phi(s)}{\alpha(z)} \\ F_2 &= \frac{7}{24}\, g\sin\phi(s)\,\nabla\cdot\hat{e}_+ + \frac{3}{8}\, g\cos\phi(s)\,\nabla\cdot\hat{e}_= + \\ &\quad - \frac{151}{192}\,\frac{g^2\sin^2\phi(s)}{\alpha(z)} - \frac{2}{3}\,\frac{g^2\, ch[gt(s)]}{\alpha_0\, sh^2[gt(s)]} \\ F_3 &= \frac{1}{3}\,\alpha(z)\,\nabla\cdot\hat{e}_= + \frac{9}{8}\, g\cos\phi(s) \\ F_4 &= \frac{1}{2}\,\alpha(z)\ . \end{aligned}$$

The quantities $\nabla\cdot\hat{e}_=$ and $\nabla\cdot\hat{e}_+$ have been given by (2.78-1) and

(2.78-2), respectively.

If the kinematic properties of a pure P wave propagating in a vertically inhomogeneous medium have been successfully computed by a ray tracing technique, the above functions F_1, F_2, F_3 and F_4 will be known. Equation (2.91) can then be solved by choosing the following boundary condition:

$$(2.93) \qquad P^{(1)}(1) = \frac{\alpha_{(1)}}{3} P^{(0)}(1)$$

where $\alpha_{(1)}$ is the speed of the P wave at the intersection point of the unit sphere with the ray. The reason for choosing (2.91) as the boundary condition is due to traditional assumption that the region about the source, within a unit sphere, is homogeneous even in a generally inhomogeneous medium. Taking r=1 in the relevant formula (2.45) results in the above equation (2.93).

In Chapter 3, some applications of (2.91) in the investigation on the first order effects for vertically inhomogeneous media shall be shown.

An interesting fact should be mentioned here. If g = 0 is taken in (2.92) by using (2.33) instead of $\nabla\cdot\hat{e}_-$ and $\nabla\cdot\hat{e}_+$, according to the case of a pure P wave propagating in homogeneous media, (2.92) becomes:

$$F_1 = -\frac{1}{r}$$

$$F_2 = -\frac{2\alpha_0}{3r^2}$$

(2.94)

$$F_3 = \frac{2\alpha_0}{3r}$$

$$F_4 = \frac{\alpha_0}{2} ,$$

then substituting (2.94) into (2.91) yields:

$$(2.95) \quad \frac{dP^{(1)}(r)}{dr} = -\frac{1}{r} P^{(1)}(r) - \frac{\alpha_0}{3r^2} P^{(0)}(r)$$

$$= -\frac{1}{r} P^{(1)}(r) - \frac{\lambda}{\alpha_0 \rho r^2} P^{(0)}(r) .$$

This is the same as equation (2.44), which describes the principal component of the first order terms of a pure P wave propagating in homogeneous media.

(2) Second, we concentrate on the case of a pure S wave propagating in vertically inhomogeneous media. The general formulae of the additional component of the first order terms for S waves, (2.31), can be simplified in this case using (2.61):

$$(2.96) \quad s^{(1)}(s) = S^{(0)}(s)[\beta(z)(\nabla\cdot\hat{e}_r - \frac{1}{r_1}) - \frac{3\sqrt{3}}{8} g \sin\phi(s)]$$

where r_1 is given by

$$(2.67) \quad r_1 = \frac{\alpha(z)}{g \sin\phi(s)} .$$

Finally we have:

$$(2.97)\qquad s^{(1)}(s) = S^{(0)}(s)\left[\beta(z)\nabla\cdot\hat{e}_{+} - \frac{17\sqrt{3}}{24}\, g\, \sin\phi(s)\right]$$

To find the expression for the principal component of the first order term of a pure S wave propagating in vertically inhomogeneous media, we recall the general expression (2.55) for $S^{(1)}$ which is as follows:

$$(2.98)\qquad \frac{dS^{(1)}}{dr} = -S^{(1)}\left[\frac{\nabla\cdot\hat{e}_{=}}{2} + \frac{5\, g\, \cos\phi(s)}{8\alpha}\right] - \frac{\beta(z)M_{+}(s^{(1)}\hat{e}_{=})}{2\mu} + \frac{\beta(z)L_{+}(S^{(0)}\hat{e}_{+})}{2\mu}$$

Here $M_{+}(s^{(1)}\hat{e}_{=})$ will be obtained from its general formula (2.52) by using simplifications (2.60), (2.61), (2.67) and (2.97) as follows:

$$(2.99)\qquad \frac{-\beta M_{+}(s^{(1)}\hat{e}_{=})}{2\mu} = -\frac{7}{8}\,\frac{1}{\alpha}\, g\, \sin\phi\; s^{(1)}(s) = \left[\frac{119\sqrt{3}}{192\alpha}\, g^{2}\sin^{2}\phi - \frac{7\sqrt{3}}{24}\, g\sin\phi\nabla\cdot\hat{e}_{+}\right]S^{(0)}.$$

The quantity $L_{+}(S^{(0)}\hat{e}_{+})$ will be obtained from its general formula (2.56) by using the simplifications (2.60), (2.61), (2.67) and (2.84) as follows:

$$(2.100)\quad \frac{\beta L_{+}(S^{(0)}\hat{e}_{+})}{2\mu} = \frac{d^2S^{(0)}}{ds^2}\frac{\beta}{2} + \frac{dS^{(0)}}{ds}\frac{3\sqrt{3}}{8}\left(2 - \frac{\alpha}{\alpha_0 ch(gt)}\right)\cdot$$

$$\cdot g\cos\phi + S^{(0)}\left[\frac{3\sqrt{3}}{8r_2} g\cos\phi - \frac{3\sqrt{3}}{8} g\sin\phi(\nabla\cdot\hat{e}_{+}) +\right.$$

$$\left. + \beta\hat{e}_{+}\cdot\nabla(\nabla\cdot\hat{e}_{+}) - \frac{1}{6\beta} g^2\sin^2\phi\right] .$$

Substituting (2.99) and (2.100) into (2.98) yields:

$$(2.101)\quad \frac{dS^{(1)}}{dr} = F_1 S^{(1)} + F_2 S^{(0)} + F_3 \frac{dS^{(0)}}{dr} + F_4 \frac{d^2S^{(0)}}{dr^2}$$

with

$$F_1 = -\frac{\nabla\cdot\hat{e}_{=}}{2} - \frac{5\sqrt{3}}{24}\frac{1}{\beta(z)} g\cos\phi(s)$$

$$F_2 = \frac{29}{64}\frac{1}{\beta(z)} g^2\sin^2\phi(s) - \frac{2\sqrt{3}}{3} g\sin\phi(s)\,\nabla\cdot\hat{e}_{+} +$$

$$(2.102) \qquad + \frac{3\sqrt{3}}{8}\frac{1}{r_2} g\cos\phi(s) + \beta(z)\,\hat{e}_{+}\cdot\nabla(\nabla\cdot\hat{e}_{+})$$

$$F_3 = \frac{3\sqrt{3}}{8}\left(2 - \frac{\alpha}{\alpha_0\, ch(gt)}\right) g\cos\phi(s)$$

$$F_4 = \frac{\beta(z)}{2}$$

where $\nabla\cdot\hat{e}_{=}$, $\nabla\cdot\hat{e}_{+}$ and r_2 have been given by (2.78-1), (2.78-2) and (2.75), respectively.

If the kinematic properties of a pure S wave propagating in a vertically inhomogeneous medium have been successfully computed by a ray tracing technique, the above

functions F_1, F_2, F_3 and F_4 are easily determined. Choosing a suitable boundary or initial condition in this instance for equation (2.101) shall be more difficult.

An interesting fact that should be pointed out here is if setting g=0 in (2.102) and using (2.33) instead of $\nabla\cdot\hat{e}_{\cdot\cdot}$, the above problem becomes a pure S wave propagating in homogeneous media, and (2.102) reduces to:

$$
\begin{aligned}
F_1 &= -\frac{1}{r} \\
F_2 &= 0 \\
F_3 &= 0 \\
F_4 &= \frac{\beta_0}{2}
\end{aligned}
\tag{2.103}
$$

Substituting (2.103) into (2.101) yields:

$$
\frac{dS^{(1)}(r)}{dr} = -\frac{1}{r} S^{(1)}(r) + \beta_0 \frac{S^{(0)}(r)}{r^2} , \tag{2.104}
$$

which is the same as equation (2.58), which describes the principal component of the first order term of a pure S wave propagating in homogeneous media.

3. Relationships between Inhomogeneity of a Medium and The Higher Order Effects of ART

When investigating higher order terms in ART, a very interesting question presents itself: **What are the relationships between the higher order effects and the inhomogeneity of media?** In this chapter we shall use the mathematical results obtained in Chapter 2 to study the first order effect for two models, called model #2 and model #3 in this thesis.

Model #2, shown in Figure 3.1, is a set of five perfectly elastic isotropic halfspaces of differing constant vertical velocity gradients as follows:

$$
\begin{aligned}
&\text{A:}\quad V_1(z) = 2.0 \ \text{(km/s)} \\
&\text{B:}\quad V_2(z) = 2.0 + 0.02\,z \ \text{(km/s)} \\
&\text{C:}\quad V_3(z) = 2.0 + 0.2\,z \ \text{(km/s)} \\
&\text{D:}\quad V_4(z) = 2.0 + 0.3\,z \ \text{(km/s)} \\
&\text{E:}\quad V_5(z) = 2.0 + 0.5\,z \ \text{(km/s)}
\end{aligned}
\tag{3.1}
$$

In all models the constant velocity ratio $\alpha/\beta=\sqrt{3}$ was assumed. Five seismic rays a, b, c, d and e are also shown in Figure 3.1. Note that ray a, which corresponds to the constant velocity model, is a straight line segment with zero curvature. This is required by Fermat's principal. For comparative purpose, all rays have the same source-receiver configuration, consisting of the same starting point S (x=0km, z=0km), where the unit sphere around a point source

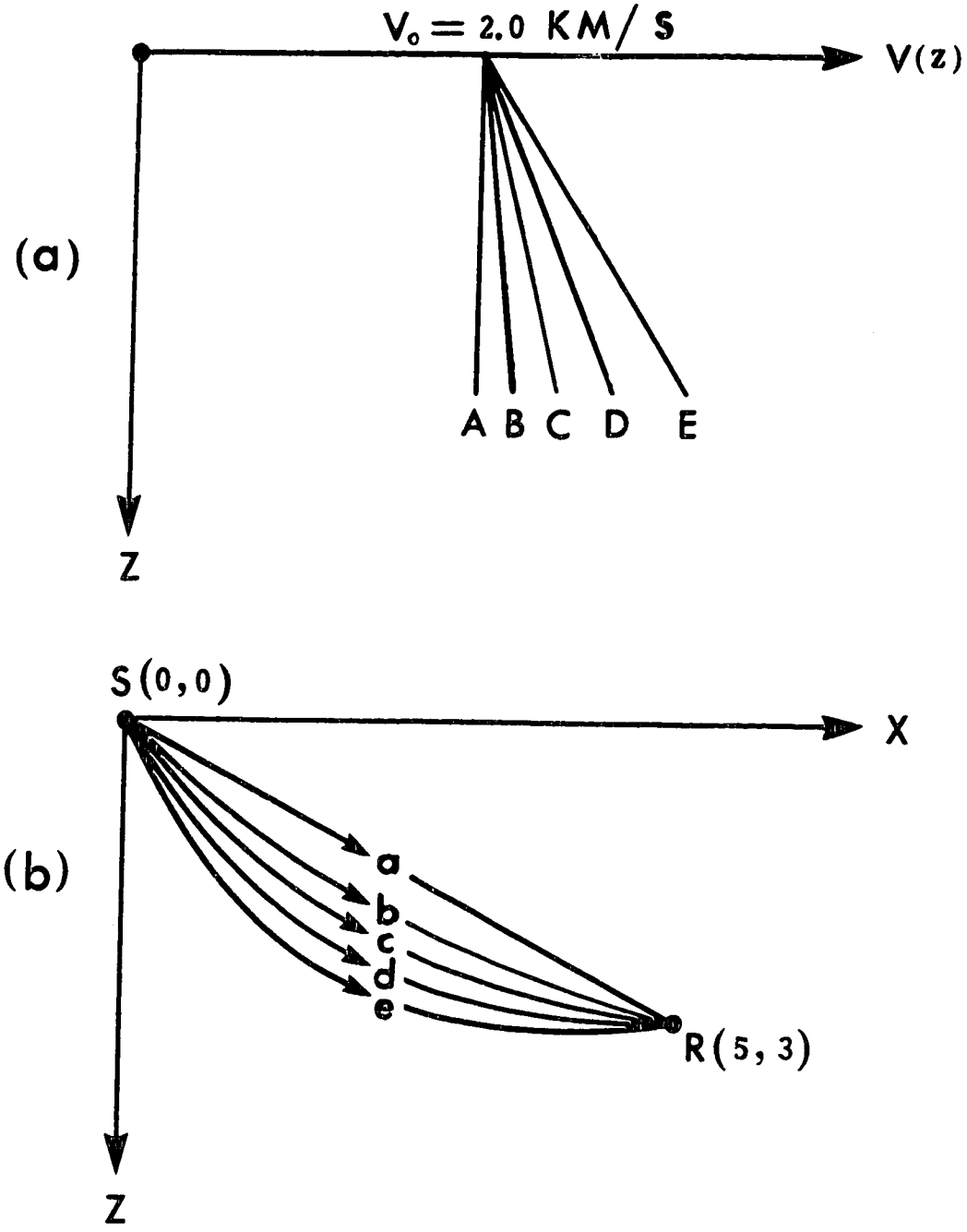

Figure 3.1 Model #2. (a) Schematic velocity-depth structures for longitudinal waves in the five models represented by the vertically inhomogeneous half spaces of five different velocity gradients "g". (b) Ray paths of the direct longitudinal rays from S to R. The individual ray paths are drawn to scale and labelled according to the text.

intersected with the rays, and the same receiver location buried at R (x=5km, z=3km). If we could obtain dynamic properties such as the amplitude coefficients of $P^{(0)}(r)$, $p^{(1)}(r)$ and $P^{(1)}(r)$ along the total length of rays with different velocity gradients, it will be possible to extrapolate some relationships between the inhomogeneity of media and the higher order effects.

To study dynamic properties of the above five rays in Model #2 we have to determine their kinematic properties first, i.e. we have to consider first the so-called two point seismic-ray tracing problem. The two point seismic-ray tracing problem has been discussed in detail in Zheng (1985). To avoid unnecessary duplication, only the final equations obtained in that work will be given here to aid in the solution of our present problem.

3.1 Two Point Ray Tracing in Inhomogeneous Continuous Elastic Media

Two point seismic ray tracing equations in a three dimensional inhomogeneous elastic continuous medium have been given in the form of the first order differential system:

$$
\begin{aligned}
Y_1' &= Y_8 Y_2, \\
Y_2' &= Y_8 V[\partial U/\partial x - G(Y) Y_2], \\
Y_3' &= Y_8 Y_4, \\
Y_4' &= Y_8 V[\partial U/\partial y - G(Y) Y_4], \qquad 0 \le \xi \le 1
\end{aligned} \tag{3.2}
$$

$$
\begin{aligned}
Y_5' &= Y_8 Y_6, \\
Y_6' &= Y_8 V[\partial U/\partial z - G(Y) Y_6], \\
Y_7' &= Y_8 U, \\
Y_8' &= 0.
\end{aligned}
$$

where U is the slowness of the medium (i.e. $U \equiv 1/V$), and $G(Y) \equiv U_x Y_2 + U_y Y_4 + U_z Y_6$. The prime "'" in (3.2) denotes differentiation with respect to ξ. The variable ξ is identified with a ratio of the local ray length s to the total ray length S (i.e. $\xi \equiv s/S$). After indroducing ξ, a particle moving from the starting point (x_0, y_0, z_0) to the receiver (x_1, y_1, z_1) will produce a change in ξ from 0 to 1. So the corresponding boundary conditions to (3.2) are:

$$
\begin{aligned}
Y_1(0) &= x_0, \\
Y_3(0) &= y_0, \\
Y_5(0) &= z_0, \\
Y_1(1) &= x_1, \\
Y_3(1) &= y_1, \\
Y_5(1) &= z_1, \\
Y_7(0) &= 0.
\end{aligned}
\tag{3.3}
$$

where

$$
Y \equiv (x, dx/ds, y, dy/ds, z, dz/ds, t, S) \ . \tag{3.4}
$$

Solving (3.2) with the boundary conditions (3.3) will give a solution for the two point ray tracing problem in 3-D space.

In the case of a two dimensional inhomogeneous medium we need only consider the two point ray tracing problem in the x-z plane. Introducing the variables

$$(3.5) \qquad Y \equiv (Y_1,Y_2,Y_3,Y_4,Y_5) \equiv (x,z,\psi,S,t) ,$$

the two point ray tracing equations may be obtained from (3.2) in the simplified form

$$\begin{aligned} Y_1' &= Y_4 \cos Y_3, \\ Y_2' &= Y_4 \sin Y_3, \\ Y_3' &= Y_4 V[U_z \cos Y_3 - U_x \sin Y_3], \qquad 0 \le \xi \le 1 \\ Y_4' &= 0, \\ Y_5' &= Y_4 U, \end{aligned} \tag{3.6}$$

where the travel angle $\psi(s)=0.5\pi-\phi(s)$ was clearly shown in Figure 2.2. The corresponding boundary conditions are:

$$\begin{aligned} Y_1(0) &= x_0, \\ Y_2(0) &= z_0, \\ Y_1(1) &= x_1, \\ Y_2(1) &= z_1, \\ Y_5(0) &= 0. \end{aligned} \tag{3.7}$$

Solving (3.6) with its boundary conditions (3.7) will give a solution for the two point ray tracing problem in two dimensional (2-D) space.

Mathematically, two point seismic-ray tracing equations (3.2) with (3.3), or (3.6) with (3.7) are usually called the nonlinear two point boundary value problems. Because the

differential equation (2.91) with its boundary condition (2.93), describing the principal component $P^{(1)}$ of the first order terms for a pure P wave propagating in vertically inhomogeneous media, is also a nonlinear boundary value problem, it may be useful to briefly outline the algorithm which was used in Zheng (1985) to deal with two point ray tracing problems and which will be employed to find the first order terms of ART in this work.

3.2 An Adaptive Finite Difference Solver for Nonlinear Boundary Value Problems

A convenient numerical method used to solve two point seismic ray tracing problems is based on an adaptive difference solver for nonlinear boundary value problems described by two mathematicians V. Pereyra and H. B. Keller and a seismologist W. H. K. Lee in 1980, which has been known as the Lentini-Pereyra Method. The mathematical details of this solver can be found by interested readers in the following mathematical papers: H. B. Keller (1968,1969,1974); V. Pereyra (1967,1968,1973); M. Lentini and V. Pereyra (1974, 1975, 1977); A. Bjorck and V. Pereyra (1970).

We are interested in developing usable software for nonlinear boundary problems for an n-dimensional system of the form:

$$\begin{aligned} &Y'(\xi) = F'(\xi, Y(\xi)) \\ &g(Y(0), Y(1)) = 0 \end{aligned} \qquad \xi \in [0, 1] \tag{3.8}$$

with the assumption that (3.8) has an isolated solution $Y^*(\xi)$. We assume also that F is smooth, so that all the necessary derivatives of $Y^*(\xi)$ exist.

Let the mesh $m = \{\xi_1, \ldots\ldots, \xi_{n+1}\}$ be a general partition of the interval [0, 1] satisfying:

$$
\begin{aligned}
&0 = \xi_1 < \xi_2 < \ldots\ldots < \xi_{n+1} = 1 \\
&h_i = \xi_{i+1} - \xi_i, \quad h = \max h_i, \quad \hat{h} = \min h_i \\
&h/\hat{h} \le K
\end{aligned}
\tag{3.9}
$$

with K a given positive constant. The condition (3.9) implies

$$1/n \le h \le K/n \tag{3.10}$$

and we can use h and 1/n interchangeably as equivalent asymptotic scales.

The basic finite difference approximation considered is the trapezoidal rule:

$$
\begin{aligned}
&\Phi_m(\mathbf{u})_i \equiv \frac{u_{i+1} - u_i}{h_i} - \frac{F(\xi_{i+1},u_{i+1}) + F(\xi_i,u_i)}{2} = 0 \\
&g(u_1,u_{n+1}) = 0, \qquad\qquad i = 0, 1, \ldots, n
\end{aligned}
\tag{3.11}
$$

As usual, the local truncation error is defined by applying the operator Φ_m to the values of the exact solution $Y^*(\xi)$ on the mesh m. Using a Taylor expansion we get:

$$\tau_m(Y^*_i) = \sum_{t=1}^{T} \frac{-t}{2^{2t-1}(2t+1)} F^{(2t)}_{i+1/2} \frac{h_i^{2t}}{(2t)!} + o(h^{2t+2}) \tag{3.12}$$

$$t = 1, 2, \ldots, n$$

where:

$$F_{i+1/2}^{(2t)} = \frac{d^{2t}}{d\xi^{2t}} F(\xi, Y^s(\xi))\,|\,\xi=\xi_i+h_i/2$$

We shorten (3.12) for further reference to

$$(3.13) \qquad \tau_m(Y^s{}_i) = \sum_{t=1}^{T} D_t(\xi_i)\, h_i{}^{2t} + o(h^{2t+2})$$

Let $\tau_{m,k}$ be the mesh function obtained by adding up the first k terms in the asymptotic expansion (3.12), and let $S_m{}^{(k)}(Y^s)$ be an $o(h^{2k+2})$ approximation to $\tau_{m,k}$.

It is well known that if $u^{(k-1)}$ is an $0(h^{2k})$ discrete approximation to $Y^s(\xi)$ on m, and if $(u^{(k-1)} - Y^s)$ has an asymptotic expansion in even powers of h, then $S_m{}^{(k)}(u^{(k-1)})$ is an $o(h^{2k+2})$ approximation to $\tau_{m,k}$. The operators $S_m{}^{(k)}$ can be readily constructed via numerical differentiation, and they are the basis of the deferred correction algorithm. They are also used in the dynamic monitoring of the global error $e^{(k)} = (u^{(k)} - Y^s)$.

We hope it will be clear from the context that we are speaking of vector mesh function on m, i.e., that an expression such as the one above means

$$(3.14) \qquad \begin{aligned} &e_j(\xi_i) = u_j{}^{(k)}(\xi_i) - Y_j{}^s(\xi_i) \\ &j = 1, 2, \ldots, d \\ &\xi_i \in \text{mesh } m \end{aligned}$$

Another important fact we shall need later is that the method is stable in the infinite norm $||\cdot||$, i.e.

$$||e^{(k)}|| \leq c||\tau_m^{(k)}|| \tag{3.15}$$

where the constant c is independent of the mesh m. The mesh function $\tau_m^{(k)}$ represents the local truncation error after the kth correction has been performed.

We recall now the deferred correction algorithm. Letting $S_m^{(0)}(u^{(-1)}) \equiv 0$, solve successively for k = 0, 1, 2, ...

$$\begin{aligned} &\Phi_m(u) = S_m^{(k)}(u^{(k-1)}) \\ &g(u_1, u_{n+1}) = 0 \end{aligned} \tag{3.16}$$

We define $u^{(k)}$ as the solution of (3.16) (closest to $Y^s(\xi)$). The main features of the deferred correction procedure are: (a) solutions of increased accuracy are obtained on the same mesh (compare with the Richardson extrapolation procedure); (b) the same system of equations is solved all the time (with different right-hand sides).

Under certain conditions, the successively corrected solutions will satisfy on the mesh

$$||e^{(k)}|| \equiv ||u^{(k)} - Y^s|| = o(h^{2k+2})$$

An asymptotic estimate for $e^{(k)}$ can be found by solving for Δ from the (linear) variational equation

$$\Phi'_m(u^{(k)})\,\Delta = S_m^{(k)}(u^{(k-1)}) - S_m^{(k+1)}(u^{(k)}) \tag{3.17}$$

where $\Phi'_m(\mathbf{u}^{(k)})$ is the Jacobian matrix of Φ_m evaluated at $\mathbf{u}^{(k)}$. If $\Delta^{(k)}$ is the solution of this linear problem, then

$$(3.18) \quad \Delta^{(k)} = e^{(k)} + o(h^{2k+4})$$

Observe that if (3.16) is being solved by Newton's interaction method, then $\Phi'_m(\mathbf{u}^{(k)})$ will be available, and since $\mathbf{S}_m^{(k)}$, $\mathbf{S}_m^{(k+1)}$ are also available, the cost of the estimate (3.18) is just that of one Newton step, i.e. the solution of a sparse system of linear equations.

For the automatic mesh placement algorithm, we will be interested in having an $o(h^{2k+4})$ estimate of the leading term in $\tau_m^{(k)}$. For this purpose, it is necessary to use in $\mathbf{S}_m^{(k)}$ formulae with a higher order interpolation error than is necessary for the rest of the process. In fact, we will insist that

$$(3.19) \quad \mathbf{S}_m^{(k)}(\mathbf{Y}^s) = \tau_{m,k}(\mathbf{Y}^s) + o(h^{2k+4})$$

i.e., the numerical differentation formula will be two orders more precise than before.

The features of this method, consisting of an automatic procedure for choosing a nonuniform mesh, have been shown in Zheng (1985) for many numerical examples. The principal component of the first order term, $P^{(1)}$, for vertically inhomogeneous elastic media can also be solved using it. As the relevant equation (2.91) with its boundary condition (2.93) is also a nonlinear boundary problem. Numerical results will be discussed in the next section.

3.3 Numerical Results for Model #2 and Model #3

In this section numerical results for two models, Model #2 and Model #3, will be presented for the zero and first order approximations. These results are essential in view of the rather complicated form of the theoretical formulae. They also provide insight into the practical implications of the theory and their application to the current needs of seismic exploration and crustal seismology.

Presented here first are the numerical results for Model #2. Using Lentini-Pereyra Method to solve (3.6) with its boundary condition (3.7), the kinematic properties along four curved rays b, c, d and e for four inhomogeneous models B, C, D and E in Model #2 may be obtained numerically. All of the kinematic characteristics such as the ray length (LNGH), the travel time (TIME) and the travel angle $\psi(s)$ (ANGLE) measured in radians at positions (X(s), Z(s)) along the ray have been summarized in Tables 3.1, 3.2, 3.3 and 3.4, respectively.

The geometrical spreading L(s), which will be employed to compute the amplitude coefficients of the zero order term, have been calculated by (2.15) based on the above kinematic data and have been summarized in the above mentioned tables under the column denoted G-SP. The amplitude coefficients of the zero order term $P^{(0)}(s)$ and the additional component of the first order $p^{(1)}(s)$ then can be calculated using expressions (2.14a) and (2.87),

respectively. Once again using the Lentini-Pereyra Method to solve the differential equation (2.91) with its boundary condition (2.93) the value of the principal component of the first order $P^{(1)}(s)$ may be obtained. All of the results of $P^{(0)}(s)$, $p^{(1)}(s)$ and $P^{(1)}(s)$ have been arranged in Tables 3.1, 3.2, 3.3 and 3.4 according to the different velocity gradients 0.02, 0.2, 0.3 and 0.5 under the columns P(0), SP(1) and LP(1), respectively.

The main results for Model #2 are shown in Figure 3.2 where the amplitude-distance curves of all three individual terms ($P^{(0)}$, $p^{(1)}$ and $P^{(1)}$), comprising the first order approximation to Asymptotic Ray Theory are presented for the 4 inhomogeneous models in this data set.

In Figure 3.2, the labelling is consistent for all models with "1" denoting plots of the zero term $P^{(0)}$. Label "2" is used for curves pertaining to the first order principal component $|P^{(1)}|/2\pi$, whereas, "3" indicates the amplitude-distance properties of the first order additional component $|p^{(1)}|/2\pi$. Label "4" is used for curves depicting the relative amplitude of the combined first order terms with respect to the zero order term. Mathematically, this dependence is expressed by the square root of the ratio $[(P^{(1)})^2+(p^{(1)})^2]/[4\pi^2(P^{(0)})^2]$, plotted as a function of the distance from the starting point S along the ray.

Fig. 3.2 shows clearly that with increasing inhomogeneity (i.e. with increasing values of the vertical velocity gradient) the importance of the combined effect of

TABLE 3.1

THE NUMERICAL SOLUTION OF THE RAY b IN MODEL 2

VELOCITY MODEL:
V(X,Z)=ZO+Z1*X+Z2*Z; WHERE: (ZO= 2.0000000 , Z1= 0 , Z2= 0.0200000 ,)

S POINT ON UNIT SPHERE: (X= 0 , Z= 0)
RECEIVER: (X= 5.0000000 , Z= 3.0000000)

ERROR= 0.0003

N= 1001

	X	Z	ANGLE	LNGH	TIME	G-SP	P(O)	SP(1)	LP(1)
N= 1	0.0000	0.0000	0.5650	1.0000	0.5000	1.0000	1.0000	-0.0148	0.6667
N= 41	0.1971	0.1247	0.5631	1.2333	0.6166	1.2334	0.8101	-0.0120	0.4334
N= 81	0.3945	0.2490	0.5611	1.4665	0.7330	1.4671	0.6806	-0.0101	0.3058
N= 121	0.5921	0.3729	0.5591	1.6998	0.8492	1.7011	0.5865	-0.0087	0.2264
N= 161	0.7900	0.4965	0.5572	1.9330	0.9654	1.9354	0.5151	-0.0077	0.1750
N= 201	0.9881	0.6196	0.5552	2.1663	1.0814	2.1699	0.4591	-0.0068	0.1386
N= 241	1.1864	0.7424	0.5532	2.3996	1.1972	2.4048	0.4139	-0.0062	0.1127
N= 281	1.3850	0.8648	0.5513	2.6328	1.3129	2.6399	0.3768	-0.0056	0.0931
N= 321	1.5838	0.9867	0.5493	2.8661	1.4285	2.8753	0.3457	-0.0052	0.0784
N= 361	1.7829	1.1083	0.5473	3.0994	1.5439	3.1111	0.3192	-0.0048	0.0668
N= 401	1.9822	1.2295	0.5453	3.3326	1.6592	3.3470	0.2965	-0.0044	0.0578
N= 441	2.1818	1.3503	0.5434	3.5659	1.7743	3.5833	0.2767	-0.0041	0.0502
N= 481	2.3816	1.4707	0.5414	3.7991	1.8893	3.8199	0.2594	-0.0039	0.0441
N= 521	2.5816	1.5907	0.5394	4.0324	2.0042	4.0567	0.2441	-0.0037	0.0390
N= 561	2.7818	1.7103	0.5375	4.2657	2.1189	4.2938	0.2304	-0.0035	0.0348
N= 601	2.9823	1.8296	0.5355	4.4989	2.2335	4.5312	0.2182	-0.0033	0.0311
N= 641	3.1831	1.9484	0.5335	4.7322	2.3480	4.7688	0.2072	-0.0031	0.0280
N= 681	3.3840	2.0668	0.5316	4.9655	2.4623	5.0068	0.1972	-0.0030	0.0253
N= 721	3.5852	2.1849	0.5296	5.1987	2.5765	5.2450	0.1881	-0.0028	0.0231
N= 761	3.7866	2.3025	0.5276	5.4320	2.6906	5.4835	0.1798	-0.0027	0.0210
N= 801	3.9883	2.4198	0.5256	5.6652	2.8045	5.7223	0.1722	-0.0026	0.0192
N= 841	4.1902	2.5366	0.5237	5.8985	2.9184	5.9613	0.1651	-0.0025	0.0177
N= 881	4.3923	2.6530	0.5217	6.1318	3.0320	6.2006	0.1587	-0.0024	0.0163
N= 921	4.5946	2.7691	0.5197	6.3650	3.1456	6.4402	0.1526	-0.0023	0.0150
N= 961	4.7972	2.8848	0.5178	6.5983	3.2590	6.6801	0.1471	-0.0022	0.0139
N=1001	5.0000	3.0000	0.5158	6.8316	3.3723	6.9202	0.1419	-0.0022	0.0129

TABLE 3.2

THE NUMERICAL SOLUTION OF THE RAY c IN MODEL 2

VELOCITY MODEL:
V(X,Z)=ZO+Z1*X+Z2*Z; WHERE: (ZO= 2.0000000 , Z1= 0 , Z2= 0.2000000 ,)

S POINT ON UNIT SPHERE: (X= 0 , Z= 0)
RECEIVER: (X= 5.0000000 , Z= 3.0000000)

ERROR= 0.0004

N= 1001

	X	Z	ANGLE	LNGH	TIME	G-SP	P(O)	SP(1)	LP(1)
N= 1	0.0000	0.0000	0.7545	1.0000	0.5000	1.0000	1.0000	-0.1275	0.6667
N= 41	0.1726	0.1595	0.7374	1.2350	0.6166	1.2369	0.8005	-0.1037	0.4102
N= 81	0.3479	0.3160	0.7202	1.4701	0.7314	1.4775	0.6638	-0.0873	0.2802
N= 121	0.5259	0.4695	0.7031	1.7051	0.8444	1.7218	0.5644	-0.0753	0.2022
N= 161	0.7065	0.6199	0.6860	1.9401	0.9559	1.9696	0.4890	-0.0662	0.1517
N= 201	0.8896	0.7673	0.6689	2.1751	1.0658	2.2210	0.4299	-0.0590	0.1173
N= 241	1.0753	0.9114	0.6517	2.4102	1.1742	2.4757	0.3825	-0.0532	0.0926
N= 281	1.2633	1.0524	0.6346	2.6452	1.2812	2.7338	0.3436	-0.0484	0.0746
N= 321	1.4538	1.1901	0.6175	2.8802	1.3869	2.9952	0.3112	-0.0444	0.0608
N= 361	1.6466	1.3245	0.6004	3.1153	1.4912	3.2598	0.2838	-0.0410	0.0501
N= 401	1.8416	1.4556	0.5832	3.3503	1.5944	3.5275	0.2604	-0.0380	0.0417
N= 441	2.0389	1.5834	0.5661	3.5853	1.6964	3.7983	0.2402	-0.0355	0.0350
N= 481	2.2383	1.7077	0.5490	3.8203	1.7973	4.0720	0.2225	-0.0332	0.0295
N= 521	2.4399	1.8286	0.5319	4.0554	1.8972	4.3486	0.2070	-0.0312	0.0250
N= 561	2.6434	1.9461	0.5147	4.2904	1.9961	4.6280	0.1933	-0.0295	0.0213
N= 601	2.8490	2.0600	0.4976	4.5254	2.0940	4.9101	0.1812	-0.0279	0.0181
N= 641	3.0565	2.1704	0.4805	4.7605	2.1910	5.1948	0.1703	-0.0264	0.0155
N= 681	3.2658	2.2773	0.4634	4.9955	2.2871	5.4821	0.1605	-0.0251	0.0132
N= 721	3.4769	2.3805	0.4462	5.2305	2.3824	5.7719	0.1516	-0.0239	0.0112
N= 761	3.6898	2.4801	0.4291	5.4655	2.4769	6.0641	0.1436	-0.0228	0.0095
N= 801	3.9044	2.5761	0.4120	5.7006	2.5707	6.3585	0.1363	-0.0219	0.0081
N= 841	4.1205	2.6684	0.3949	5.9356	2.6638	6.6552	0.1296	-0.0209	0.0068
N= 881	4.3382	2.7569	0.3777	6.1706	2.7563	6.9540	0.1235	-0.0201	0.0057
N= 921	4.5574	2.8417	0.3606	6.4057	2.8481	7.2548	0.1179	-0.0193	0.0047
N= 961	4.7780	2.9227	0.3435	6.6407	2.9393	7.5576	0.1127	-0.0186	0.0038
N=1001	5.0000	3.0000	0.3264	6.8757	3.0300	7.8622	0.1080	-0.0179	0.0030

TABLE 3.3

THE NUMERICAL SOLUTION OF THE RAY d IN MODEL 2

VELOCITY MODEL:
V(X,Z)=ZO+Z1*X+Z2*Z; WHERE: (ZO= 2.0000000 , Z1= 0 , Z2= 0.3000000 ,)

S POINT ON UNIT SPHERE: (X= 0 , Z= 0)
RECEIVER: (X= 5.0000000 , Z= 3.0000000)

ERROR= 0.0008

N= 1001

	X	Z	ANGLE	LNGH	TIME	G-SP	P(0)	SP(1)	LP(1)
N= 1	0.0000	0.0000	0.8375	1.0000	0.5000	1.0000	1.0000	-0.1757	0.6667
N= 41	0.1605	0.1740	0.8137	1.2367	0.6168	1.2398	0.7937	-0.1431	0.3875
N= 81	0.3251	0.3441	0.7900	1.4734	0.7308	1.4857	0.6522	-0.1205	0.2561
N= 121	0.4937	0.5102	0.7662	1.7101	0.8420	1.7376	0.5496	-0.1040	0.1792
N= 161	0.6662	0.6723	0.7424	1.9468	0.9507	1.9953	0.4720	-0.0913	0.1302
N= 201	0.8425	0.8302	0.7187	2.1835	1.0571	2.2587	0.4114	-0.0813	0.0973
N= 241	1.0225	0.9839	0.6949	2.4202	1.1612	2.5276	0.3630	-0.0732	0.0743
N= 281	1.2061	1.1333	0.6711	2.6569	1.2634	2.8019	0.3235	-0.0665	0.0574
N= 321	1.3932	1.2783	0.6474	2.8936	1.3636	3.0815	0.2908	-0.0609	0.0448
N= 361	1.5837	1.4188	0.6236	3.1303	1.4620	3.3661	0.2633	-0.0561	0.0352
N= 401	1.7775	1.5547	0.5998	3.3670	1.5588	3.6556	0.2400	-0.0520	0.0277
N= 441	1.9744	1.6860	0.5761	3.6037	1.6540	3.9498	0.2199	-0.0484	0.0218
N= 481	2.1744	1.8126	0.5523	3.8404	1.7477	4.2486	0.2025	-0.0453	0.0170
N= 521	2.3774	1.9344	0.5285	4.0772	1.8401	4.5519	0.1874	-0.0425	0.0131
N= 561	2.5832	2.0513	0.5048	4.3139	1.9312	4.8594	0.1740	-0.0400	0.0100
N= 601	2.7917	2.1633	0.4810	4.5506	2.0212	5.1709	0.1622	-0.0378	0.0073
N= 641	3.0029	2.2703	0.4572	4.7873	2.1100	5.4863	0.1518	-0.0357	0.0051
N= 681	3.2165	2.3723	0.4335	5.0240	2.1978	5.8055	0.1424	-0.0339	0.0033
N= 721	3.4324	2.4691	0.4097	5.2607	2.2846	6.1281	0.1340	-0.0323	0.0017
N= 761	3.6506	2.5608	0.3859	5.4974	2.3705	6.4541	0.1265	-0.0308	0.0004
N= 801	3.8710	2.6473	0.3622	5.7341	2.4556	6.7833	0.1196	-0.0294	-0.0008
N= 841	4.0933	2.7286	0.3384	5.9708	2.5400	7.1155	0.1134	-0.0281	-0.0018
N= 881	4.3175	2.8045	0.3147	6.2075	2.6236	7.4504	0.1078	-0.0269	-0.0026
N= 921	4.5434	2.8751	0.2909	6.4442	2.7066	7.7880	0.1026	-0.0258	-0.0034
N= 961	4.7710	2.9402	0.2671	6.6809	2.7890	8.1279	0.0979	-0.0248	-0.0040
N=1001	5.0000	3.0000	0.2434	6.9176	2.8709	8.4701	0.0936	-0.0238	-0.0046

TABLE 3.4

THE NUMERICAL SOLUTION OF THE RAY e IN MODEL 2

VELOCITY MODEL:
V(X,Z)=ZO+Z1*X+Z2*Z; WHERE: (ZO= 2.0000000 , Z1= 0 , Z2= 0.5000000 ,)

S POINT ON UNIT SPHERE: (X= 0 , Z= 0)
RECEIVER: (X= 5.0000000 , Z= 3.0000000)

ERROR= 0.0001

N= 1001

	X	Z	ANGLE	LNGH	TIME	G-SP	P(O)	SP(1)	LP(1)
N= 1	0.0000	0.0000	0.9670	1.0000	0.5000	1.0000	1.0000	-0.2484	0.6667
N= 41	0.1399	0.1956	0.9329	1.2405	0.6174	1.2464	0.7787	-0.2029	0.3200
N= 81	0.2863	0.3863	0.8988	1.4809	0.7295	1.5044	0.6275	-0.1709	0.1870
N= 121	0.4392	0.5719	0.8647	1.7214	0.8368	1.7736	0.5186	-0.1472	0.1145
N= 161	0.5984	0.7521	0.8305	1.9619	0.9400	2.0539	0.4372	-0.1290	0.0711
N= 201	0.7635	0.9269	0.7964	2.2023	1.0394	2.3449	0.3744	-0.1145	0.0437
N= 241	0.9346	1.0959	0.7623	2.4428	1.1353	2.6462	0.3248	-0.1028	0.0253
N= 281	1.1113	1.2589	0.7281	2.6833	1.2282	2.9575	0.2850	-0.0931	0.0127
N= 321	1.2935	1.4159	0.6940	2.9237	1.3183	3.2784	0.2524	-0.0849	0.0038
N= 361	1.4809	1.5665	0.6599	3.1642	1.4059	3.6085	0.2254	-0.0779	-0.0026
N= 401	1.6734	1.7106	0.6257	3.4047	1.4912	3.9475	0.2028	-0.0719	-0.0073
N= 441	1.8707	1.8481	0.5916	3.6451	1.5744	4.2950	0.1836	-0.0667	-0.0108
N= 481	2.0725	1.9788	0.5575	3.8856	1.6557	4.6505	0.1673	-0.0621	-0.0134
N= 521	2.2787	2.1025	0.5234	4.1261	1.7354	5.0137	0.1532	-0.0580	-0.0154
N= 561	2.4890	2.2191	0.4892	4.3665	1.8134	5.3841	0.1410	-0.0544	-0.0169
N= 601	2.7031	2.3285	0.4551	4.6070	1.8901	5.7613	0.1303	-0.0512	-0.0180
N= 641	2.9209	2.4305	0.4210	4.8475	1.9655	6.1448	0.1210	-0.0483	-0.0189
N= 681	3.1420	2.5250	0.3868	5.0879	2.0397	6.5343	0.1127	-0.0457	-0.0196
N= 721	3.3662	2.6119	0.3527	5.3284	2.1129	6.9292	0.1054	-0.0433	-0.0201
N= 761	3.5932	2.6911	0.3186	5.5689	2.1852	7.3291	0.0989	-0.0411	-0.0205
N= 801	3.8229	2.7625	0.2844	5.8093	2.2567	7.7335	0.0931	-0.0391	-0.0208
N= 841	4.0548	2.8260	0.2503	6.0498	2.3275	8.1420	0.0879	-0.0373	-0.0210
N= 881	4.2887	2.8816	0.2162	6.2903	2.3976	8.5541	0.0833	-0.0356	-0.0212
N= 921	4.5244	2.9291	0.1821	6.5307	2.4673	8.9693	0.0791	-0.0340	-0.0213
N= 961	4.7616	2.9686	0.1479	6.7712	2.5365	9.3870	0.0753	-0.0326	-0.0214
N=1001	5.0000	3.0000	0.1138	7.0117	2.6053	9.8070	0.0719	-0.0312	-0.0216

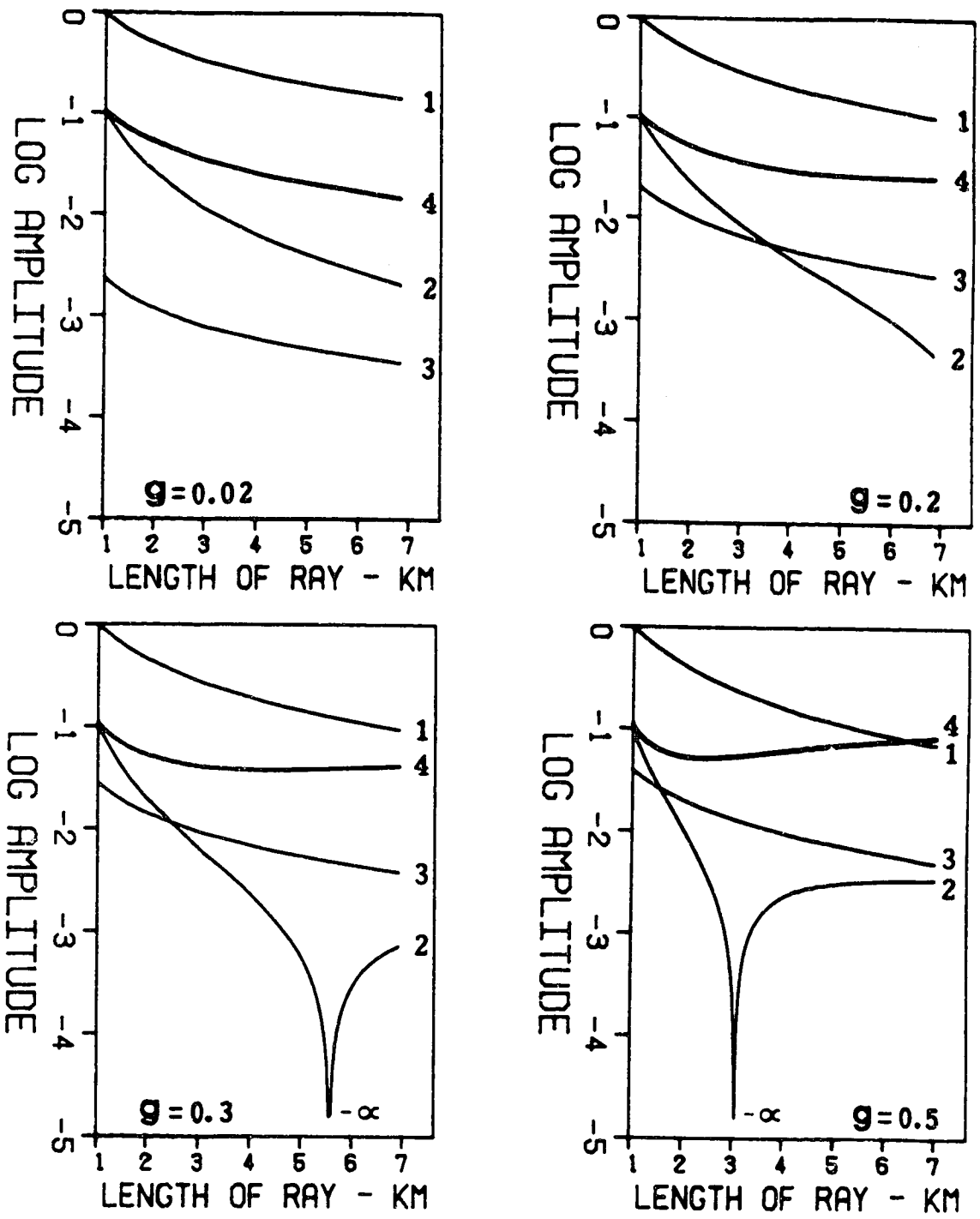

Figure 3.2 Magnitudes of the individual terms in the ray series for the four curved P rays in Model #2. With a positive increase in inhomogeneity of the media the importance of the first order effects increases steadily (see label 4).

both first order terms $P^{(1)}$ and $p^{(1)}$ increases steadily.

In Model #2 all values of the velocity gradients are positive. If the velocity gradients are negative, the inhomogeneity of media will be negatively increasing. What about the first order effects in this case? For this purpose a new model with negative velocity gradients, named Model #3 here, is introduced to be compared with Model #2 as follows (see Figure 3.3):

$$
\begin{aligned}
&A': \quad V_1(z) = 2.0 \ (km/s) \\
&B': \quad V_2(z) = 2.0 - 0.02\ z \ (km/s) \\
&C': \quad V_3(z) = 2.0 - 0.2\ z \ (km/s) \\
&D': \quad V_4(z) = 2.0 - 0.3\ z \ (km/s) \\
&E': \quad V_5(z) = 2.0 - 0.5\ z \ (km/s)
\end{aligned}
\tag{3.18}
$$

In Figure 3.3 the rays a', b', c', d' and e', corresponding to gradients 0.0, -0.02, -0.2, -0.3 and -0.5 respectively, are arranged to have the same starting point S (x=0km, z=0km) and the same receiver R (x=5km, z=3km) as Model #2.

All numerical results along four curved rays b', c', d' and e' in Model #3 have been obtained by the same way dealing with Model #2, and have been summarized into Tables 3.5, 3.6, 3.7 and 3.8, respectively. The main results are graphically shown in Fig 3.4 where the amplitude-distance curves of all three individural terms ($P^{(0)}$, $p^{(1)}$ and $P^{(1)}$) comprising the first order approximation of ART are plotted for the 4 inhomogeneous models in this data set.

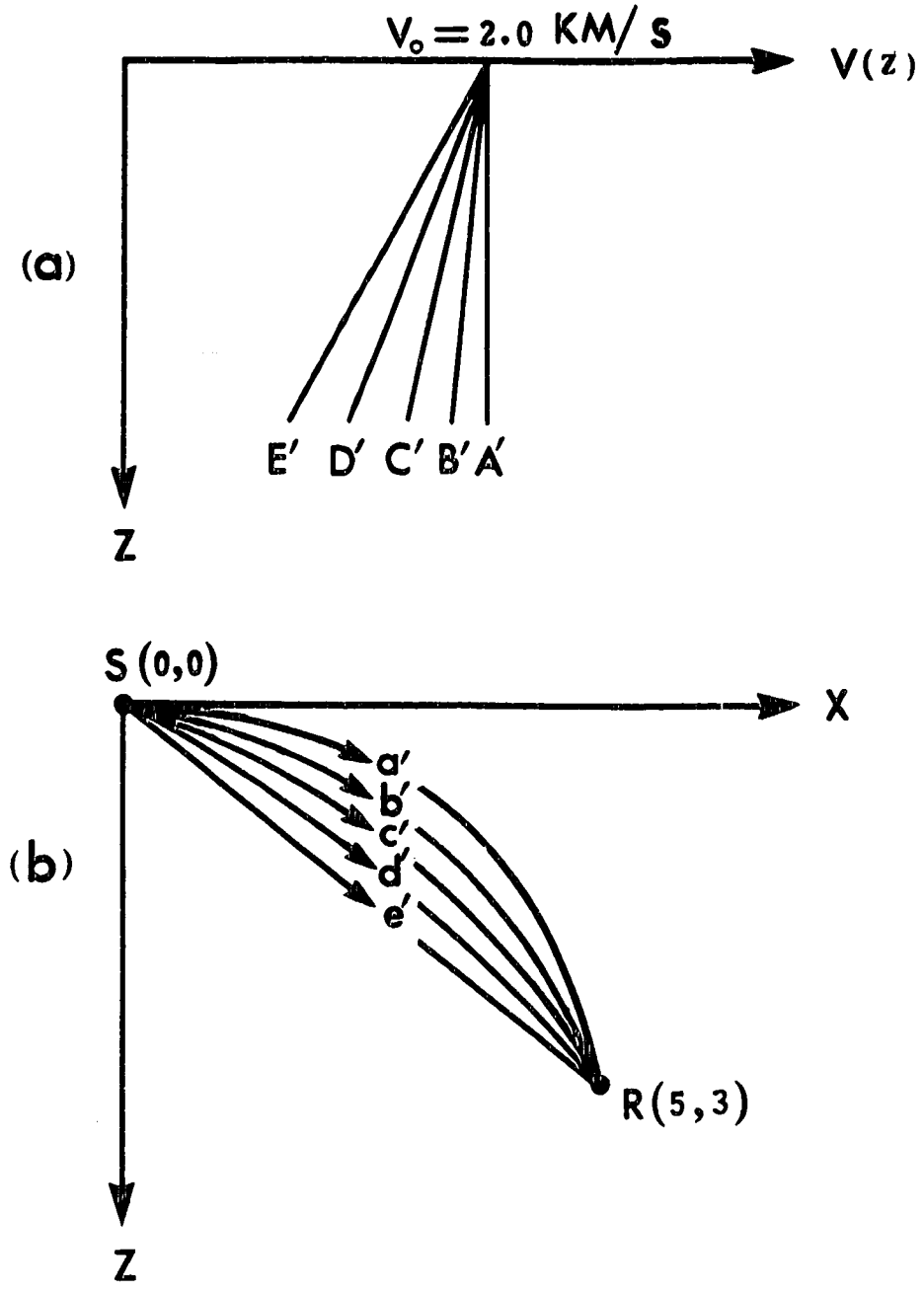

Figure 3.3 Model #3. (a) Schematic velocity-depth structures for longitudinal waves in the five models represented by the vertically inhomogeneous half spaces of five different velocity gradients "g". (b) Ray paths of the direct longitudinal rays from S to R. The individual ray paths are drawn to scale and labelled according to the text.

In Figure 3.4 the labelling is consistent for all models with "1" denoting plots of the zero term $P^{(0)}$. Label "2" is used for curves pertaining to the first order principal component $|P^{(1)}|/2\pi$, whereas, "3" indicates the amplitude-distance properties of the first order additional component $|p^{(1)}|/2\pi$. Label "4" is used for curves depicting the relative amplitude of the combined first order terms with respect to the zero order term. Mathematically, the dependence is expressed by the ratio $[(P^{(1)})^2+(p^{(1)})^2]/[4\pi^2(P^{(0)})^2]$, plotted as a function of the distance from the starting point S along the rays.

Figure 3.4 clearly shows that with a negative increase in the inhomogeneity of media the importance of the combined effect of both first order terms $P^{(1)}$ and $p^{(1)}$ also increases steadily.

TABLE 3.5

THE NUMERICAL SOLUTION OF THE RAY b' IN MODEL 3

VELOCITY MODEL:
V(X,Z)=ZO+Z1*X+Z2*Z; WHERE: (ZO= 2.0000000 , Z1= 0 , Z2= -0.0200000 ,)

S POINT ON UNIT SPHERE: (X= 0 , Z= 0)
RECEIVER: (X= 5.0000000 , Z= 3.0000000)

ERROR= 0.0003

N= 1001

	X	Z	ANGLE	LNGH	TIME	G-SP	P(0)	SP(1)	LP(1)
N= 1	0.0000	0.0000	0.5150	1.0000	0.5000	1.0000	1.0000	0.0152	0.6667
N= 41	0.2029	0.1151	0.5171	1.2333	0.6167	1.2331	0.8115	0.0123	0.4343
N= 81	0.4055	0.2306	0.5191	1.4665	0.7335	1.4660	0.6831	0.0104	0.3062
N= 121	0.6079	0.3466	0.5211	1.6998	0.8505	1.6986	0.5900	0.0090	0.2286
N= 161	0.8101	0.4629	0.5232	1.9331	0.9676	1.9309	0.5194	0.0079	0.1762
N= 201	1.0121	0.5796	0.5252	2.1663	1.0849	2.1629	0.4640	0.0070	0.1398
N= 241	1.2138	0.6968	0.5272	2.3996	1.2022	2.3947	0.4194	0.0063	0.1143
N= 281	1.4152	0.8144	0.5293	2.6329	1.3198	2.6262	0.3827	0.0058	0.0946
N= 321	1.6165	0.9323	0.5313	2.8661	1.4374	2.8575	0.3520	0.0053	0.0797
N= 361	1.8175	1.0507	0.5333	3.0994	1.5552	3.0884	0.3259	0.0049	0.0681
N= 401	2.0182	1.1695	0.5353	3.3327	1.6732	3.3191	0.3035	0.0046	0.0589
N= 441	2.2187	1.2887	0.5374	3.5659	1.7913	3.5495	0.2840	0.0043	0.0514
N= 481	2.4190	1.4083	0.5394	3.7992	1.9095	3.7797	0.2669	0.0040	0.0452
N= 521	2.6190	1.5284	0.5414	4.0325	2.0279	4.0095	0.2518	0.0038	0.0400
N= 561	2.8188	1.6488	0.5435	4.2657	2.1464	4.2391	0.2384	0.0036	0.0357
N= 601	3.0183	1.7696	0.5455	4.4990	2.2650	4.4683	0.2263	0.0034	0.0321
N= 641	3.2176	1.8908	0.5475	4.7323	2.3838	4.6973	0.2154	0.0032	0.0290
N= 681	3.4166	2.0125	0.5496	4.9655	2.5028	4.9260	0.2056	0.0031	0.0263
N= 721	3.6154	2.1345	0.5516	5.1988	2.6219	5.1545	0.1966	0.0029	0.0240
N= 761	3.8140	2.2569	0.5536	5.4321	2.7412	5.3826	0.1885	0.0028	0.0219
N= 801	4.0123	2.3798	0.5556	5.6653	2.8606	5.6105	0.1809	0.0027	0.0202
N= 841	4.2103	2.5030	0.5577	5.8986	2.9801	5.8380	0.1740	0.0026	0.0185
N= 881	4.4081	2.6267	0.5597	6.1319	3.0998	6.0653	0.1676	0.0025	0.0171
N= 921	4.6057	2.7507	0.5617	6.3652	3.2197	6.2923	0.1617	0.0024	0.0159
N= 961	4.8029	2.8752	0.5638	6.5984	3.3397	6.5190	0.1562	0.0023	0.0148
N=1001	5.0000	3.0000	0.5658	6.8317	3.4598	6.7454	0.1511	0.0022	0.0139

TABLE 3.6

THE NUMERICAL SOLUTION OF THE RAY c' IN MODEL 3

VELOCITY MODEL:
V(X,Z)=ZO+Z1*X+Z2*Z; WHERE: (ZO= 2.0000000 , Z1= 0 , Z2= -0.2000000 ,)

S POINT ON UNIT SPHERE: (X= 0 , Z= 0)
RECEIVER: (X= 5.0000000 , Z= 3.0000000)

ERROR= 0.0007

N= 1001

	X	Z	ANGLE	LNGH	TIME	G-SP	P(0)	SP(1)	LP(1)
N= 1	0.0000	0.0000	0.2544	1.0000	0.5000	1.0000	1.0000	0.1694	0.6667
N= 41	0.2281	0.0621	0.2773	1.2364	0.6186	1.2357	0.8124	0.1367	0.4226
N= 81	0.4548	0.1294	0.3001	1.4729	0.7380	1.4699	0.6859	0.1147	0.2944
N= 121	0.6799	0.2013	0.3230	1.7093	0.8582	1.7025	0.5949	0.0987	0.2157
N= 161	0.9032	0.2795	0.3459	1.9458	0.9793	1.9332	0.5265	0.0867	0.1640
N= 201	1.1247	0.3622	0.3688	2.1822	1.1014	2.1621	0.4733	0.0773	0.1282
N= 241	1.3443	0.4500	0.3917	2.4187	1.2247	2.3890	0.4308	0.0697	0.1025
N= 281	1.5618	0.5427	0.4146	2.6551	1.3491	2.6137	0.3962	0.0635	0.0833
N= 321	1.7771	0.6404	0.4374	2.8916	1.4747	2.8362	0.3675	0.0583	0.0687
N= 361	1.9901	0.7431	0.4603	3.1280	1.6017	3.0563	0.3434	0.0538	0.0573
N= 401	2.2007	0.8505	0.4832	3.3645	1.7302	3.2739	0.3229	0.0500	0.0482
N= 441	2.4088	0.9628	0.5061	3.6009	1.8602	3.4889	0.3053	0.0467	0.0409
N= 481	2 6143	1.0797	0.5290	3.8374	1.9919	3.7012	0.2902	0.0438	0.0349
N= 521	2.8170	1.2014	0.5519	4.0738	2.1253	3.9107	0.2770	0.0413	0.0299
N= 561	3.0170	1.3276	0.5747	4.3103	2.2606	4.1173	0.2655	0.0390	0.0257
N= 601	3.2139	1.4584	0.5976	4.5467	2.3980	4.3208	0.2554	0.0369	0.0222
N= 641	3.4078	1.5937	0.6205	4.7832	2.5375	4.5211	0.2465	0.0351	0.0191
N= 681	3.5986	1.7334	0.6434	5.0196	2.6793	4.7183	0.2387	0.0334	0.0165
N= 721	3.7862	1.8774	0.6663	5.2561	2.8236	4.9120	0.2318	0.0319	0.0141
N= 761	3.9704	2.0256	0.6892	5.4925	2.9705	5.1024	0.2258	0.0305	0.0121
N= 801	4.1511	2.1781	0.7121	5.7290	3.1202	5.2891	0.2204	0.0292	0.0103
N= 841	4.3283	2.3346	0.7349	5.9654	3.2728	5.4722	0.2158	0.0280	0.0087
N= 881	4.5019	2.4951	0.7578	6.2019	3.4287	5.6516	0.2117	0.0269	0.0072
N= 921	4.6718	2.6596	0.7807	6.4383	3.5880	5.8271	0.2082	0.0259	0.0059
N= 961	4.8378	2.8279	0.8036	6.6748	3.7509	5.9987	0.2052	0.0249	0.0047
N=1001	5.0000	3.0000	0.8265	6.9112	3.9177	6.1662	0.2027	0.0240	0.0036

TABLE 3.7

THE NUMERICAL SOLUTION OF THE RAY d' IN MODEL 3

VELOCITY MODEL:
V(X,Z)=ZO+Z1*X+Z2*Z; WHERE: (ZO= 2.0000000 , Z1= 0 , Z2= -0.3000000 ,)

S POINT ON UNIT SPHERE: (X= 0 , Z= 0)
RECEIVER: (X= 5.0000000 , Z= 3.0000000)

ERROR= 0.0009

N= 1001

	X	Z	ANGLE	LNGH	TIME	G-SP	P(0)	SP(1)	LP(1)
N= 1	0.0000	0.0000	0.0898	1.0000	0.5000	1.0000	1.0000	0.2614	0.6667
N= 41	0.2399	0.0260	0.1258	1.2413	0.6209	1.2409	0.8078	0.2104	0.4006
N= 81	0.4787	0.0605	0.1619	1.4826	0.7423	1.4807	0.6792	0.1760	0.2708
N= 121	0.7161	0.1037	0.1979	1.7240	0.8645	1.7190	0.5874	0.1512	0.1925
N= 161	0.9519	0.1554	0.2340	1.9653	0.9875	1.9557	0.5189	0.1325	0.1415
N= 201	1.1855	0.2156	0.2700	2.2066	1.1116	2.1903	0.4660	0.1179	0.1066
N= 241	1.4169	0.2842	0.3061	2.4479	1.2370	2.4226	0.4242	0.1062	0.0817
N= 281	1.6457	0.3610	0.3421	2.6893	1.3638	2.6523	0.3904	0.0965	0.0632
N= 321	1.8715	0.4460	0.3782	2.9306	1.4922	2.8791	0.3627	0.0885	0.0491
N= 361	2.0941	0.5392	0.4142	3.1719	1.6225	3.1026	0.3398	0.0816	0.0382
N= 401	2.3132	0.6403	0.4503	3.4132	1.7548	3.3226	0.3206	0.0758	0.0295
N= 441	2.5285	0.7492	0.4863	3.6546	1.8895	3.5388	0.3044	0.0706	0.0224
N= 481	2.7398	0.8658	0.5224	3.8959	2.0268	3.7509	0.2908	0.0662	0.0165
N= 521	2.9467	0.9900	0.5584	4.1372	2.1669	3.9586	0.2793	0.0622	0.0116
N= 561	3.1490	1.1215	0.5945	4.3785	2.3103	4.1618	0.2696	0.0586	0.0074
N= 601	3.3465	1.2602	0.6306	4.6199	2.4572	4.3600	0.2614	0.0554	0.0038
N= 641	3.5388	1.4060	0.6666	4.8612	2.6080	4.5531	0.2547	0.0525	0.0006
N= 681	3.7257	1.5586	0.7027	5.1025	2.7632	4.7408	0.2491	0.0499	-0.0022
N= 721	3.9070	1.7178	0.7387	5.3438	2.9231	4.9228	0.2447	0.0475	-0.0048
N= 761	4.0825	1.8835	0.7748	5.5852	3.0884	5.0990	0.2413	0.0453	-0.0072
N= 801	4.2519	2.0554	0.8108	5.8265	3.2597	5.2690	0.2390	0.0432	-0.0095
N= 841	4.4149	2.2333	0.8469	6.0678	3.4376	5.4328	0.2375	0.0413	-0.0117
N= 881	4.5715	2.4169	0.8829	6.3091	3.6229	5.5899	0.2370	0.0395	-0.0138
N= 921	4.7213	2.6061	0.9190	6.5505	3.8165	5.7404	0.2375	0.0378	-0.0159
N= 961	4.8642	2.8005	0.9550	6.7918	4.0195	5.8839	0.2389	0.0362	-0.0180
N=1001	5.0000	3.0000	0.9911	7.0331	4.2331	6.0202	0.2414	0.0347	-0.0202

TABLE 3.8

THE NUMERICAL SOLUTION OF THE RAY e' IN MODEL 3

VELOCITY MODEL:
V(X,Z)=ZO+Z1*X+Z2*Z; WHERE: (ZO= 2.0000000 , Z1= 0 , Z2= -0.5000000 ,)

S POINT ON UNIT SPHERE: (X= 0 , Z= 0)
RECEIVER: (X= 5.0000000 , Z= 3.0000000)

ERROR= 0.0018

N= 1001

	X	Z	ANGLE	LNGH	TIME	G-SP	P(O)	SP(1)	LP(1)
N= 1	0.0000	0.0000	-0.2450	1.0000	0.5000	1.0000	1.0000	0.4244	0.6667
N= 41	0.2531	-0.0549	-0.1821	1.2591	0.6286	1.2609	0.7863	0.3383	0.3259
N= 81	0.5092	-0.0938	-0.1193	1.5181	0.7557	1.5249	0.6464	0.2808	0.1913
N= 121	0.7672	-0.1165	-0.0565	1.7772	0.8819	1.7908	0.5485	0.2396	0.1156
N= 161	1.0262	-0.1230	0.0063	2.0362	1.0076	2.0578	0.4769	0.2086	0.0688
N= 201	1.2850	-0.1132	0.0692	2.2953	1.1334	2.3246	0.4227	0.1845	0.0378
N= 241	1.5427	-0.0872	0.1320	2.5544	1.2597	2.5902	0.3809	0.1652	0.0163
N= 281	1.7983	-0.0451	0.1948	2.8134	1.3871	2.8536	0.3480	0.1494	0.0006
N= 321	2.0507	0.0130	0.2577	3.0725	1.5161	3.1138	0.3218	0.1361	-0.0113
N= 361	2.2990	0.0869	0.3205	3.3316	1.6472	3.3697	0.3009	0.1249	-0.0205
N= 401	2.5421	0.1761	0.3833	3.5906	1.7811	3.6204	0.2841	0.1153	-0.0282
N= 441	2.7792	0.2805	0.4462	3.8497	1.9184	3.8647	0.2708	0.1069	-0.0346
N= 481	3.0092	0.3996	0.5090	4.1087	2.0600	4.1018	0.2604	0.0995	-0.0403
N= 521	3.2313	0.5328	0.5718	4.3678	2.2066	4.3308	0.2525	0.0929	-0.0455
N= 561	3.4446	0.6798	0.6347	4.6269	2.3592	4.5506	0.2469	0.0870	-0.0504
N= 601	3.6483	0.8398	0.6975	4.8859	2.5191	4.7606	0.2434	0.0816	-0.0554
N= 641	3.8415	1.0124	0.7603	5.1450	2.6876	4.9597	0.2420	0.0767	-0.0604
N= 681	4.0235	1.1967	0.8232	5.4041	2.8666	5.1473	0.2426	0.0722	-0.0658
N= 721	4.1935	1.3921	0.8860	5.6631	3.0581	5.3226	0.2455	0.0679	-0.0718
N= 761	4.3510	1.5977	0.9488	5.9222	3.2650	5.4849	0.2507	0.0639	-0.0785
N= 801	4.4952	1.8129	1.0117	6.1812	3.4909	5.6335	0.2589	0.0601	-0.0864
N= 841	4.6256	2.0367	1.0745	6.4403	3.7407	5.7680	0.2705	0.0563	-0.0959
N= 881	4.7418	2.2682	1.1373	6.6994	4.0214	5.8977	0.2866	0.0527	-0.1076
N= 921	4.8431	2.5065	1.2002	6.9584	4.3432	5.9922	0.3089	0.0490	-0.1228
N= 961	4.9293	2.7508	1.2630	7.2175	4.7219	6.0810	0.3403	0.0451	-0.1435
N=1001	5.0000	3.0000	1.3258	7.4766	5.1843	6.1539	0.3865	0.0410	-0.1739

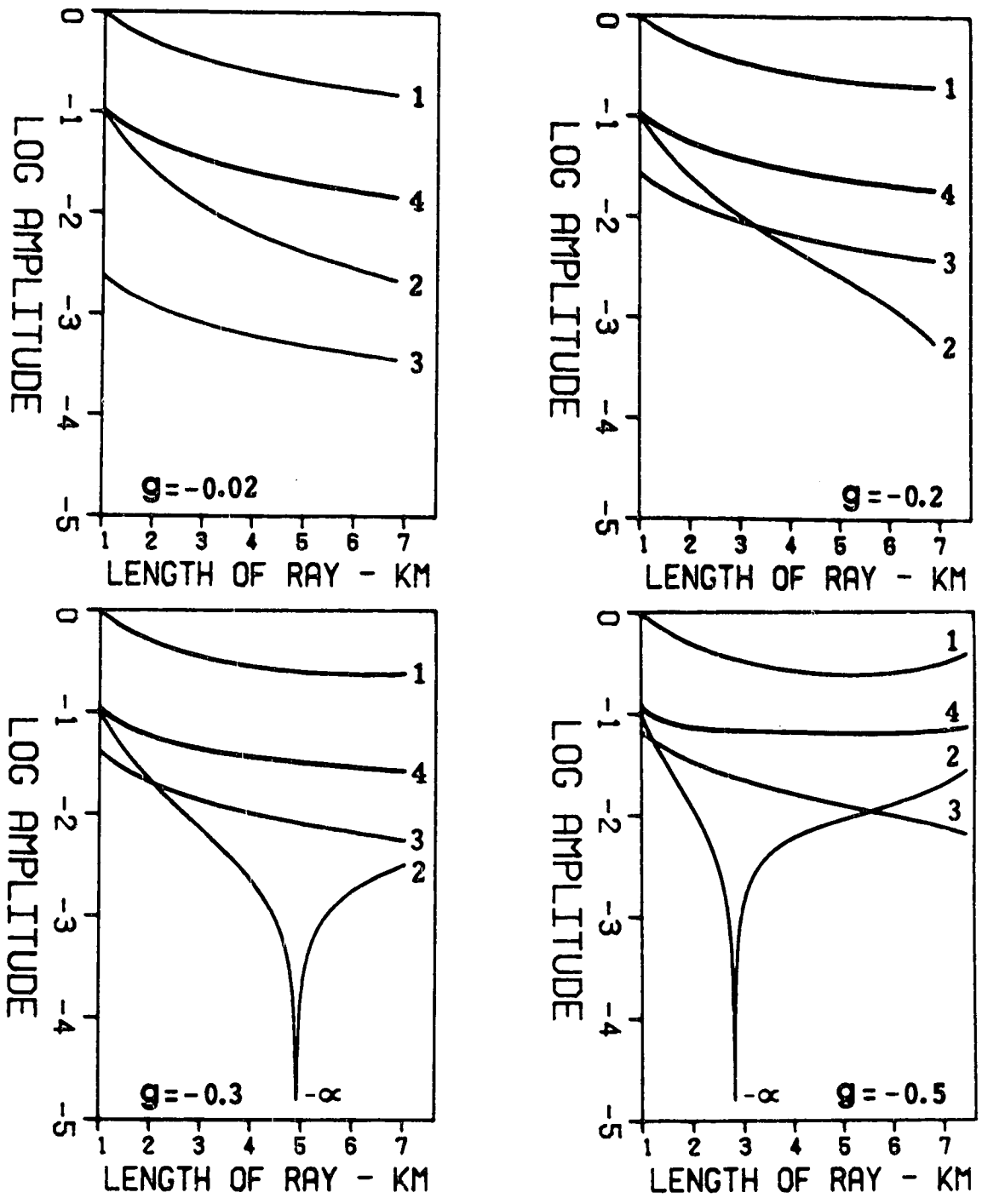

Figure 3.4 Magnitudes of the individual terms in the ray series for the four curved P rays in Model #3. With a negative increase in the inhomogeneity of the media, the importance of the first order effects also increases steadily (see label 4).

3.4 Synthetic Seismograms for Model #2 and Model #3

In the computation of synthetic seismograms, we shall assume that the form of the signal of the wave under consideration is known at a point of the ray $\tau=\tau_0$ and denoted by f(t). In the case of a point source, the function f(t) may represent the time dependence of the source function. As the wave progresses along the ray, the form of the signal f(t) remains the same if the phase shift does not change. As soon as the phase shift changes, the form of the signal also changes.

To compute the phase function $f_k(t-\tau(r))$ for $k\geq 1$ (see Eq.(1.2)), we must first evaluate the Hilbert transform of f(t), denoted by g(t). The Hilbert transform may be evaluated in an approximate computation if we take a certain source time function f(t) as follows:

$$(3.19) \quad f_0(t) = \cos(2\pi\nu t)\ \exp[-(2\pi\nu t/\gamma)^2]$$

where ν, the predominant frequency of the pulse, and γ, the damping factor. For large γ ($\gamma \geq 4$), we can obtain approximately (Cerveny et al, 1977):

$$(3.20) \quad g_0(t) \cong -\sin(2\pi\nu t)\ \exp[-(2\pi\nu t/\gamma)^2]$$

It should be noted that the above mentioned approximate formula for Hilbert transform (3.20) has been used by some authors for the computation of theoretical seismograms for a long time with satisfactory results. In the applications to

theoretical seismograms we must remember that the "zero" time corresponds to the middle of the impulse, not to the first arrivals.

The computation of the functions $f_k(t-\tau(r))$ for $k \geq 1$ in the ray series (see Eq.(1.2)) can be accomplished, when $f_0(t-\tau(r))$ is known. That is

$$\begin{aligned} f_1(\xi) &= \int f_0(x)dx \\ f_2(\xi) &= \int f_1(\eta)d\eta = \int d\eta \int f_0(x)dx \end{aligned} \tag{3.21}$$

From this, we can write the following formulae for g_1 and g_2.

$$\begin{aligned} g_1(\xi) &= \int g_0(x)dx \\ g_2(\xi) &= \int g_1(\eta)d\eta = \int d\eta \int g_0(x)dx \end{aligned} \tag{3.22}$$

Finally the source pulses which have been used in our computations of synthetic seismograms are:

$$\begin{aligned} f_0(t) &= \cos(2\pi\nu t)\ \exp[-(2\pi\nu t/\gamma)^2] \\ g_0(t) &= -\sin(2\pi\nu t)\ \exp[-(2\pi\nu t/\gamma)^2] \\ f_1(t) &= \sin(2\pi\nu t)\ \exp[-(2\pi\nu t/\gamma)^2]\ /(2\pi\nu) \\ g_1(t) &= \cos(2\pi\nu t)\ \exp[-(2\pi\nu t/\gamma)^2]\ /(2\pi\nu) \end{aligned} \tag{3.23}$$

To plot synthetic seismograms at the receiver R(x=5km, z=3km) for the five rays (a, b, c, d and e) in Model #2, the basic parameters have been builted in Table 3.9. Table 3.10 contained the basic parameters of the five rays (a', b', c', d' and e') for Model #3 at the same receiver location R(x=5km, z=3km). Both Tables 3.9 and 3.10 numerically show

that the stronger the inhomogeneity of the medium, the larger the higher order effect.

Synthetic seismograms along the vertical and horizontal directions are shown in Figures 3.5 and 3.6, respectively. The comparisons of zero order ray theory synthetic traces (I), traces computed by the first order approximation presented in this thesis (II), and the effect of the first order term only (III) for the different velocity gradients (g=0.0, 0.02, 0.2, 0.3 and 0.5) have been given in the above two Figures. The seismograms in (I) and (II) are displayed with the same plotting scale factor whereas the plotting scale factor used in (III) is 10 times than that used in (I) and (II).

For Model #3 synthetic seismograms along vertical and horizontal directions are shown in Figures 3.7 and 3.8, respectively. The comparisons of zero order ray theory synthetic traces (I), traces computed by the first order approximation presented in this thesis (II), and the effect of the first order term only (III) with different velocity gradients (g=0.0, -0.02, -0.2, -0.3 and -0.5) have been given in the above Figures. The seismograms in (I) and (II) are displayed with the same plotting scale factor whereas the plotting scale factor used in (III) is 10 times than that used in (I) and (II).

From Figures 3.5 through 3.8 we can see clearly that the first order effect is dependent on the inhomogeneity of the medium. It is also shown that generally the stronger the

Table 3.9 Parameters used to plot synthetic seismograms at point R in Model 2

RAY	g	ANGLE	LNGH	TIME	P(0)	p(1)	P(1)
a	0.0	1.0303	6.8309	3.4155	0.1464	0.0000	0.0143
b	0.02	1.0550	6.8316	3.3723	0.1419	-0.0022	0.0129
c	0.2	1.2444	6.8754	3.0300	0.1080	-0.0179	0.0030
d	0.3	1.3274	6.9176	2.8709	0.0936	-0.0238	-0.0046
e	0.5	1.4570	7.0117	2.6053	0.0719	-0.0312	-0.0216

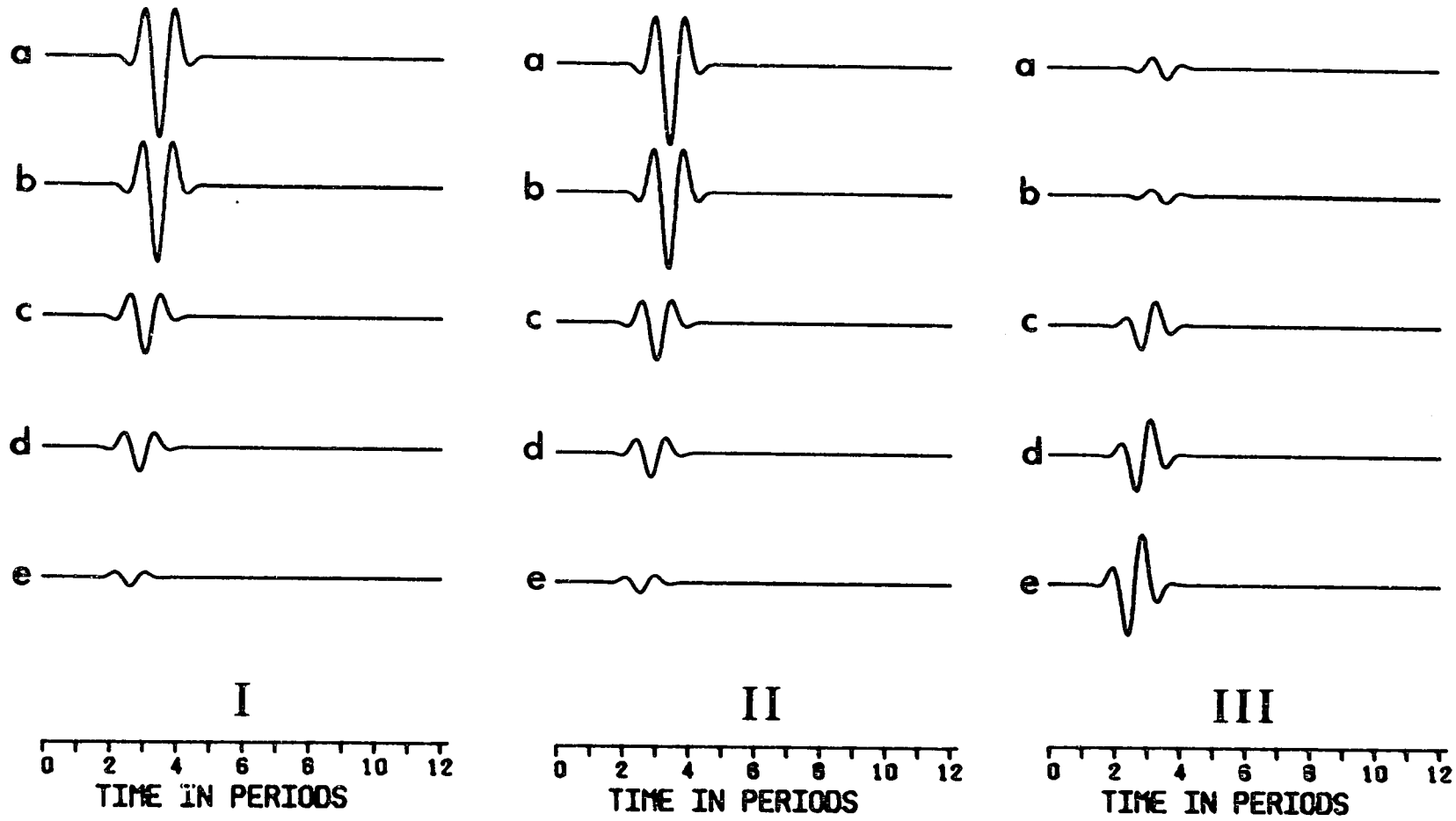

Figure 3.5 A comparison of the vertical components of displacement using zero order ray theory synthetic traces (I), traces computed using the formulas for the first order approximation presented in this thesis (II) and the effect of the first order term only (III) at point R in Model 2 described in Figure 3.1. The plotting scale factor in (III) is 10 times that used in (I) and (II).

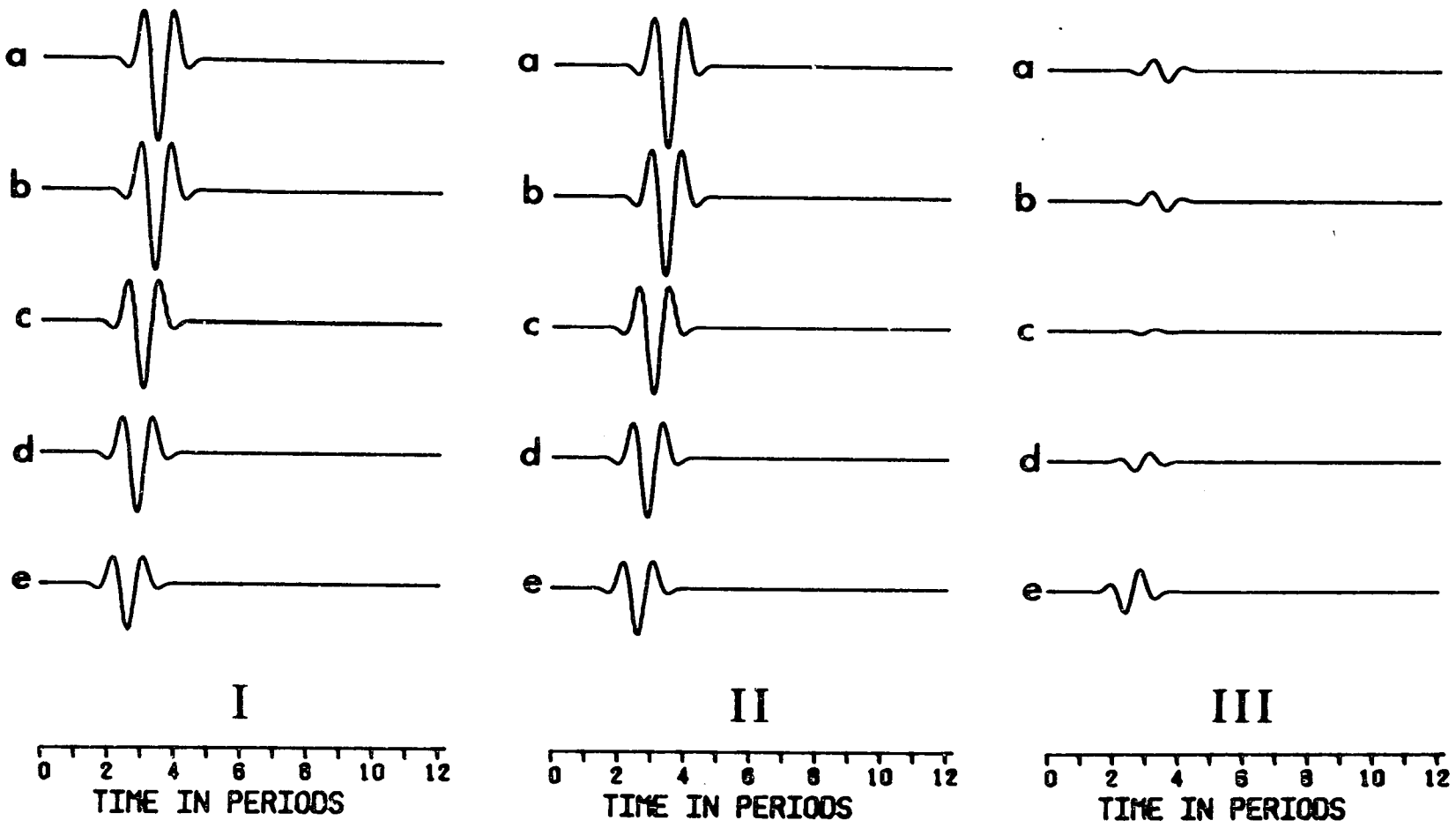

Figure 3.6 A comparison of the horizontal components of displacement using zero order ray theory synthetic traces (I), traces computed using the formulas for the first order approximation presented in this thesis (II) and the effect of the first order term only (III) at point R in Model 2 described in Figure 3.1. The plotting scale factor in (III) is 10 times that used in (I) and (II).

Table 3.10 Parameters used to plot synthetic seismograms at point R in Model 3

RAY	g	ANGLE	LNGH	TIME	P(0)	p(1)	P(1)
a'	-0.0	1.0303	6.8309	3.4155	0.1464	0.0000	0.0143
b'	-0.02	1.0050	6.8317	3.4598	0.1511	0.0022	0.0139
c'	-0.2	0.7443	6.9112	3.9177	0.2027	0.0240	0.0036
d'	-0.3	0.5797	7.0331	4.2331	0.2414	0.0347	-0.0202
e'	-0.5	0.2450	7.4766	5.1843	0.3865	0.0410	-0.1739

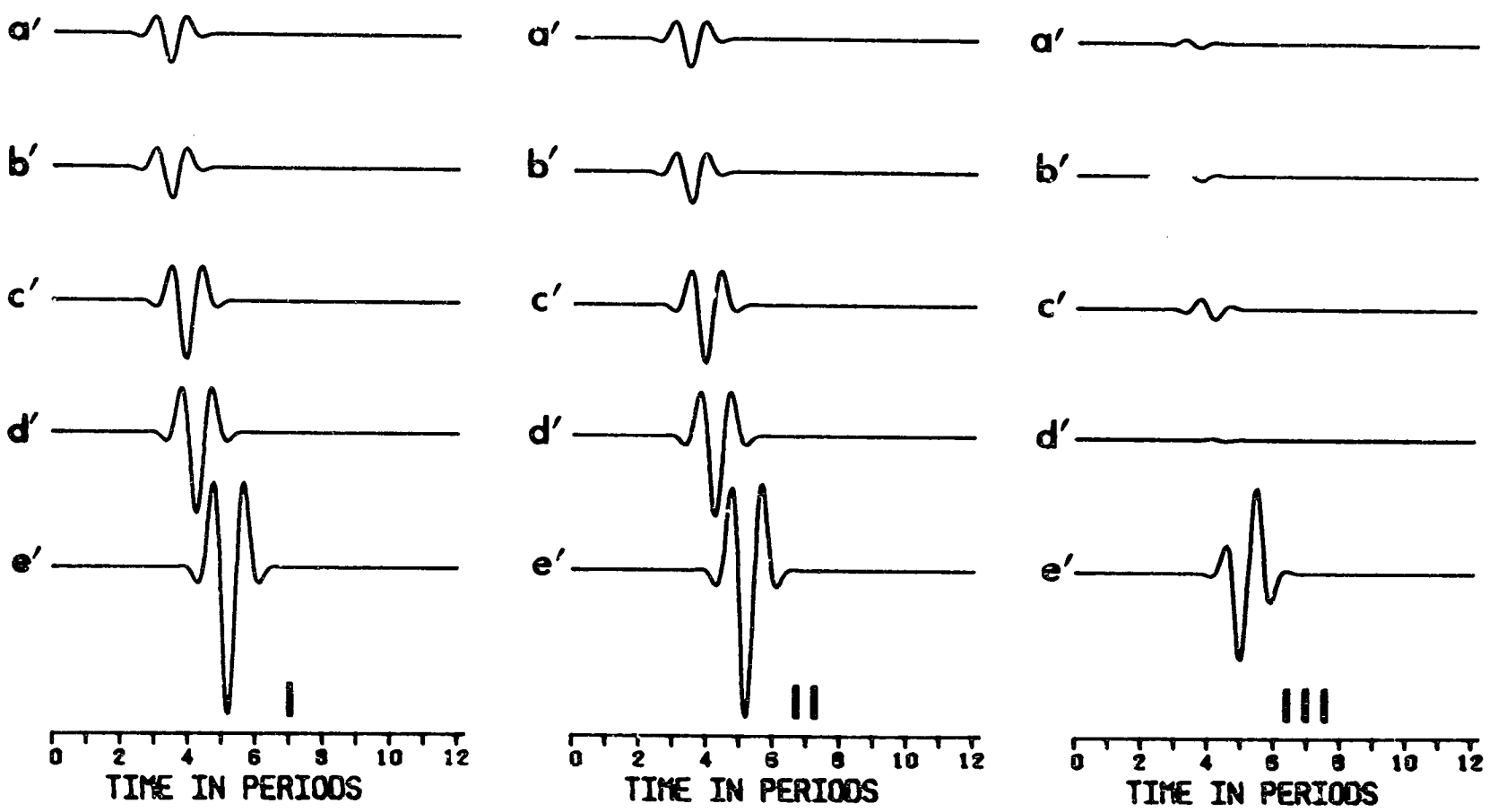

Figure 3.7 A comparison of the vertical components of displacement using zero order ray theory synthetic traces (I), traces computed using the formulas for the first order approximation presented in this thesis (II) and the effectof the first order term only (III) at point R in Model 3 described in Figure 3.3. The plotting scale factor in (III) is 10 times that used in (I) and (II).

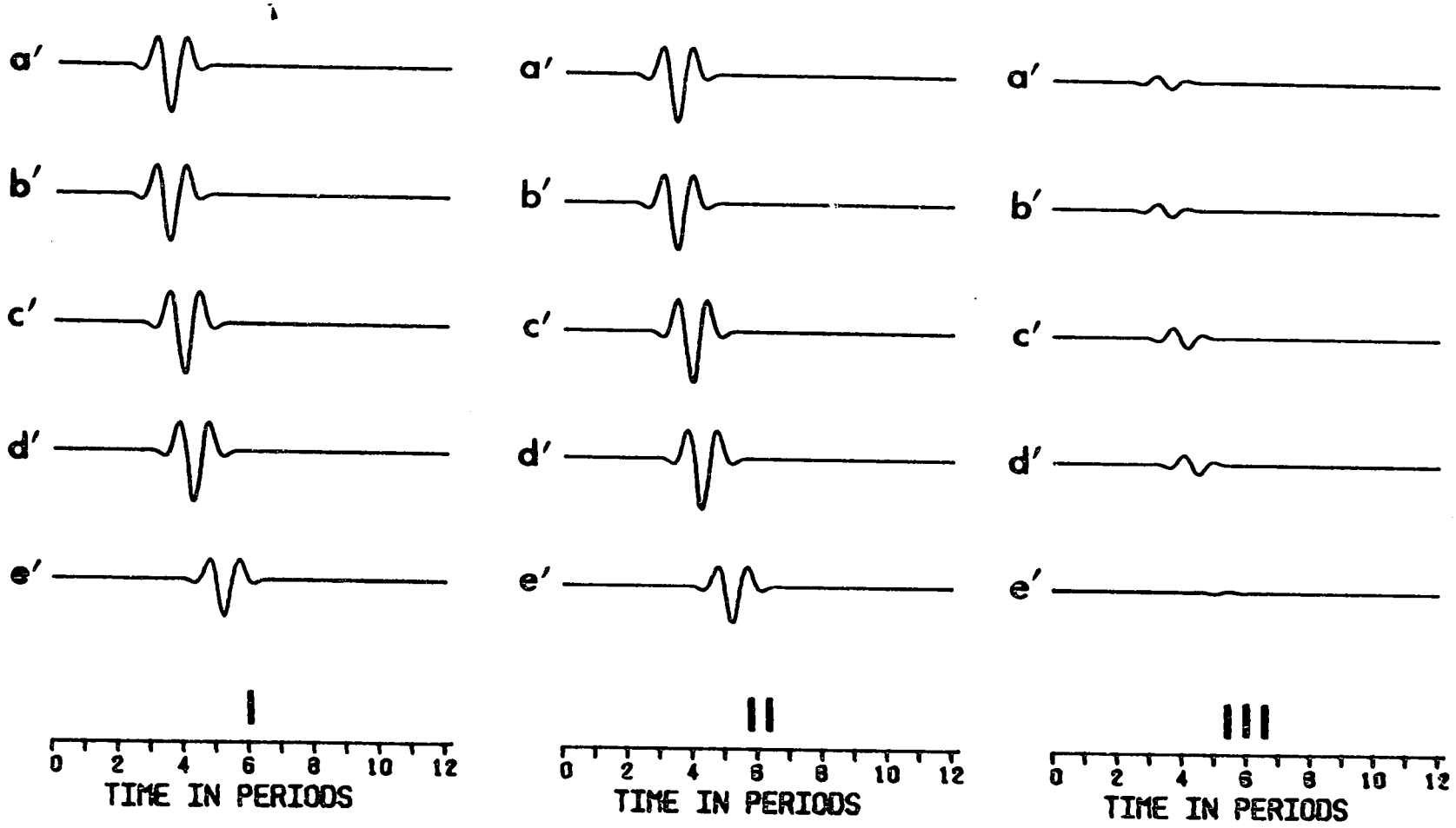

Figure 3.8 A comparison of the horizontal components of displacement using zero order ray theory synthetic traces (I), traces computed using the formulas for the first order approximation presented in this thesis (II) and the effect of the first order term only (III) at point R in Model 3 described in Figure 3.3. The plotting scale factor in (III) is 10 times that used in (I) and (II).

inhomogeneity of the medium, the larger the first order effect.

In the region near the source, the effects of higher order ART terms should be considered carefully as they should be strong enough to affect accuracies of the results. Figures 3.9 and 3.10 should be helpful to understand this point. In Figures 3.9 and 3.10, only the first order effect traces at two receiver points P(x=1km, z=0.6km) and R(x=5km, z=3km) in Model #2 and Model #3 are displayed. The labels "P-V" or "R-V" ("P-H" or "R-H") indicate traces along the vertical (horizontal) direction at the point P or R. All traces are displayed at the same scale. Comparing the synthetic traces "P-V" and "P-H" obtained at point P with the traces "R-V" and "R-H" obtained at point R, it is clear that the first order terms should be used in the computations for more accurate results whenever the Aymptotic Ray Theory is applied to inhomogeneous media. The addition of the first order terms to the solution required to produce these results may seen cumbersome and unwieldy. They are not essential for reasonably accurate results in the region far removed from the source.

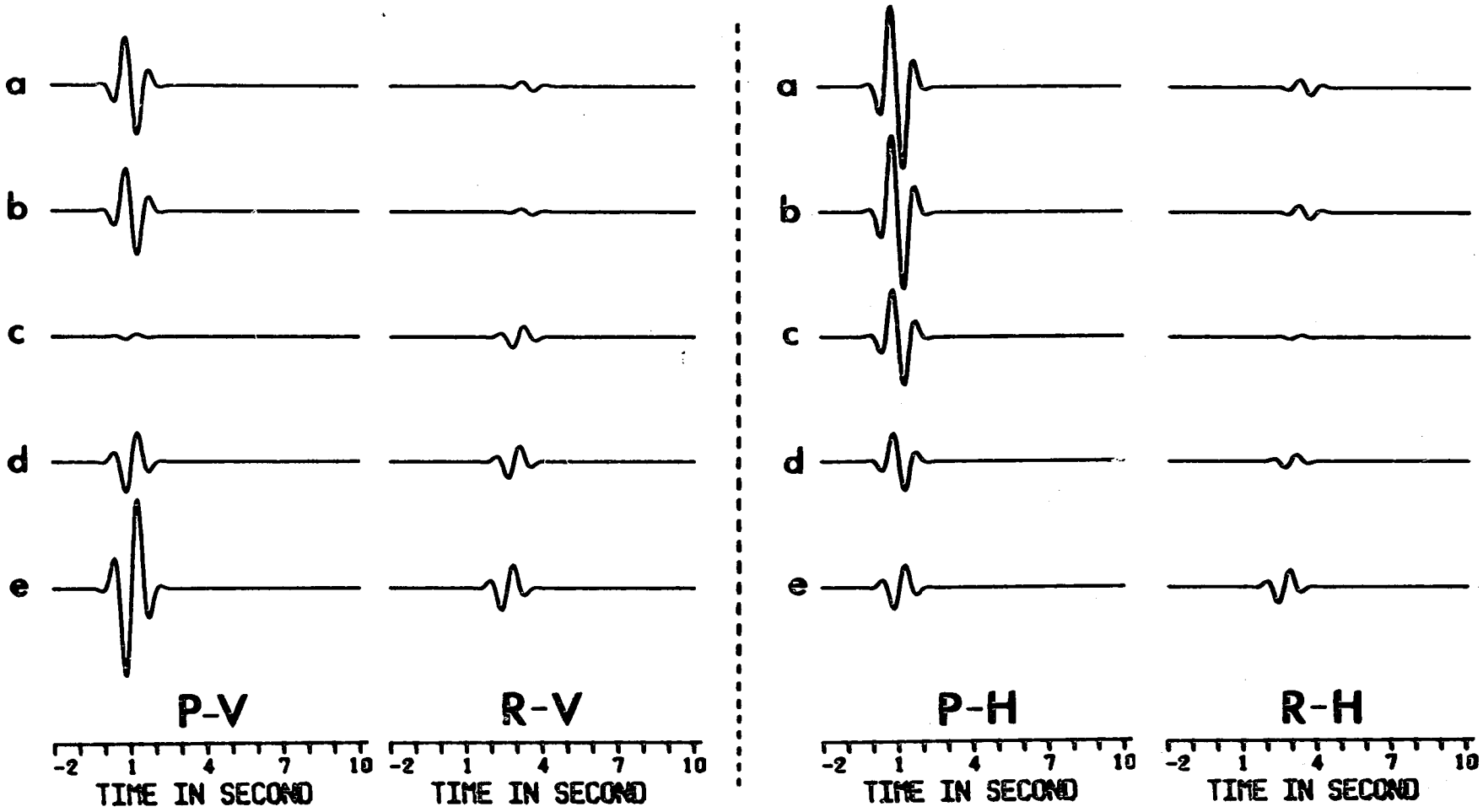

Figure 3.9 A comparison of the first order ray theory correction only for synthetic traces at two different points P(x=1 km, z=0.6 km) and R(x=5 km, z=3 km) in Model 2, where the labels "P-V" and "R-V" or "P-H" and "R-H" indicate either the vertical or horizontal components of displacement at point P or R, respectively. They were displayed in the same scale.

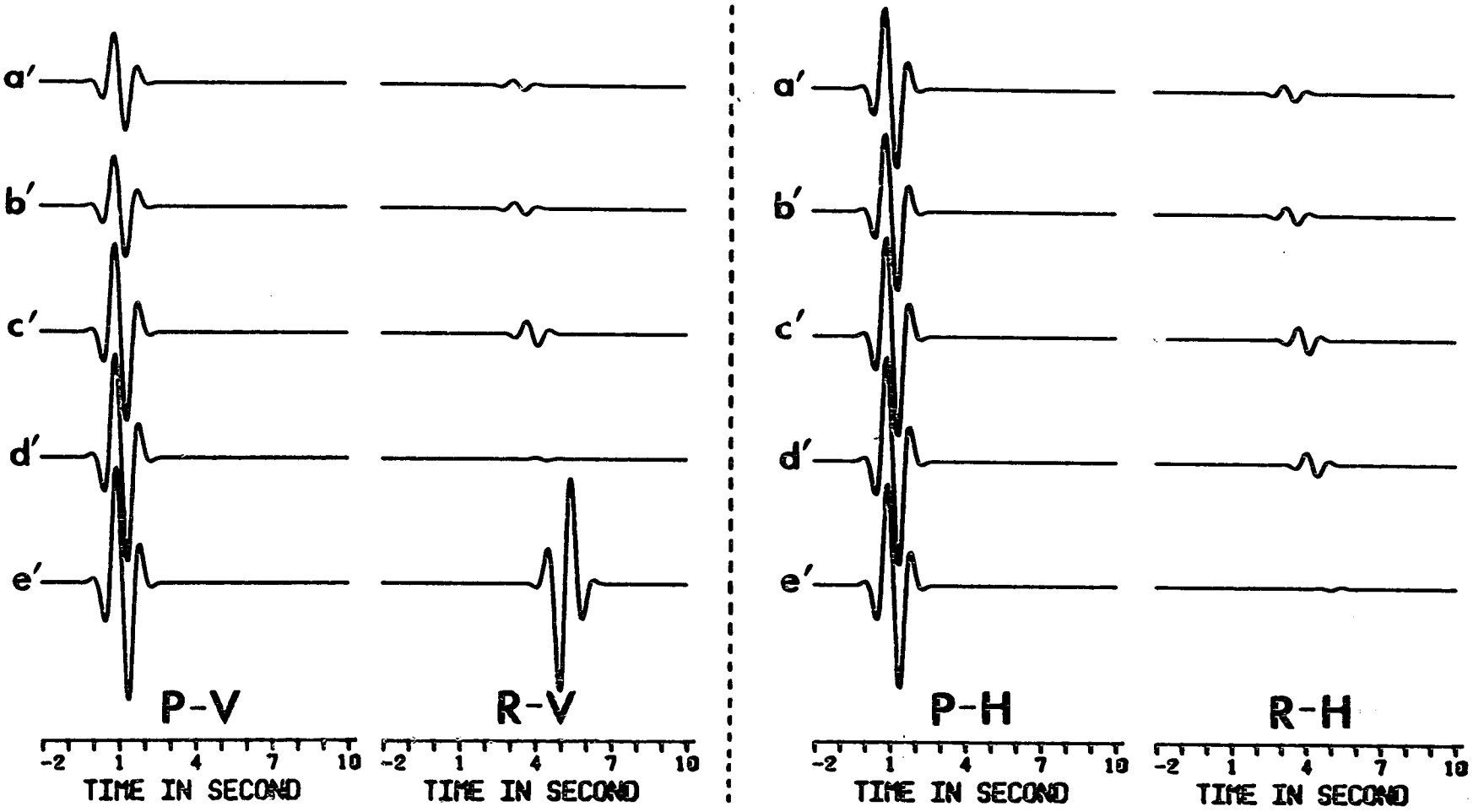

Figure 3.10 A comparison of the first order ray theory correction only for the synthetic traces at two different points P(x=1 km, z=0.6 km) and R(x=5 km, z=3 km) in model 3, where the labels "P-V" and "R-V" or "P-H" and "R-H" indicate either the vertical or horizontal components of displacement at point P or R, respectively. They were displayed in the same scale.

4. Higher Order Effects of Reflected and Transmitted Waves

It was mentioned in Chapter 3 that in Hron and Mikhailenko (1981), two phenomena were indicated in synthetic seismograms of a reflected wave for a point explosive source buried a small distance from the free surface in a homogeneous, ideally elastic isotropic half-space (Model #1). As the zero order approximation of ART does not produce very accurate results for this problem, we are going to employ the first order approximation to study it once again and to see how these results compare to the highly accurate (numerically) results produced using the AMM. In this chapter we shall pay special attention to investigating higher order effects of the reflected and transmitted waves on both sides of a interface.

To discuss the propagation properties of reflected or transmitted waves on both sides of a interface, it is first necessary to make some basic assumptions and define the notation to be used. Then some basic formulae for the general boundary conditions of two solid media in welded contact shall be given.

4.1 Boundary Conditions of Two Solid Media in Welded Contact

The intersection of the plane of incidence of the ray (i.e. the plane determined by the tangent to the ray and the normal to the surface Σ at the point of incidence) with the

boundary Σ is shown in Figure 4.1. The upper medium (layer #1) into which the Z-axis is oriented along the normal to the interface Σ at the point of incidence o, has elastic parameters λ_1, μ_1 and ρ_1 and contains the incident and reflected P and S waves whereas the lower medium (layer #2) having Lame parameters λ_2, μ_2 and volume density ρ_2 contains the transmitted (P and S) waves.

We assume the surface Σ is smooth in the vicinity of the point of incidence O allowing the construction of a tangent plane intersecting the plane of incidence in the X-axis (the case of normal incidence is considered separately). We choose the positive orientation of the X-axis in such a way that

(4.1a) $\quad \nabla r \cdot \hat{e}_x > 0$

The direction and orientation of the third Cartesian axis Y is then given by

(4.1b) $\quad \hat{e}_y = \hat{e}_z \times \hat{e}_x$

In the singular case of normal incidence the choice of X and Y axes is arbitrary as no converted phases related with them are generated upon the incidence of the ray at O.

We will write a ray series for each of the rays in the form of

$$(4.2) \qquad W_d(r,t) = \sum_k W_d^{(k)}(r)\, f_k(t-\tau_d(r))$$

where the subscript d has the following values:

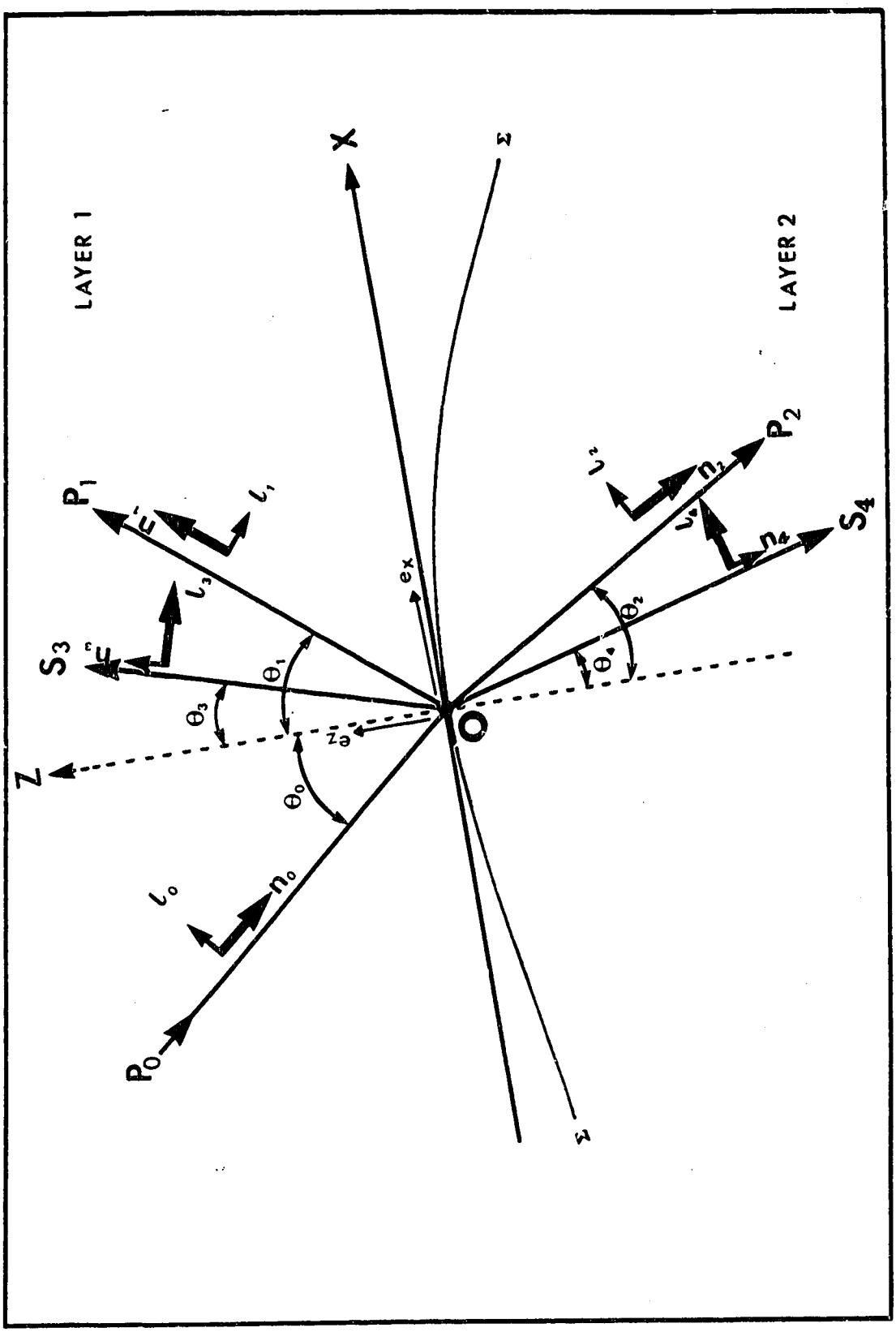

Figure 4.1 Notation and basic assumption at an intersection surface.

d = 0: incident ray (in layer 1)

d = 1: reflected P ray (in layer 1)

d = 2: transmitted P ray (in layer 2)

d = 3: reflected S ray (in layer 1)

d = 4: transmitted S ray (in layer 2).

For each ray two unit vectors $\mathbf{n}_d$ and $\mathbf{l}_d$ are defined in the plane of incidence. $\mathbf{n}_d = V_d \nabla \tau_d$ is along the ray where V_d is the wave speed. $\mathbf{l}_d$ is perpendicular to the ray (i.e. $\mathbf{l}_d \cdot \nabla \tau_d = 0$) so that $\mathbf{l}_d \cdot \hat{\mathbf{e}}_x > 0$. If the third vector is defined as $\mathbf{m}_d = \hat{\mathbf{e}}_y$ we can write each vector $W_d^{(k)}$ in (4.2) as

$$W_d^{(k)} = N_d^{(k)} \mathbf{n}_d + T_d^{(k)} \mathbf{l}_d + V_d^{(k)} \mathbf{m}_d \tag{4.3}$$

where

$N_d^{(k)} = W_d^{(k)} \cdot \mathbf{n}_d$ is the component along the ray.

$T_d^{(k)} = W_d^{(k)} \cdot \mathbf{l}_d$ is the component perpendicular to the ray in the plane of incidence.

$V_d^{(k)} = W_d^{(k)} \cdot \mathbf{m}_d$ is the component perpendicular to the plane of incidence and also perpendicular to the ray.

The boundary conditions for two solid media in welded contact require that the components of the total displacement vector U and those of the stress tensor σ_{ij} are continuous on the boundary at the point of incidence.

If we write the total displacement in layers 1 and 2 as

$$\begin{aligned} U_1 &= W_0 + W_1 + W_3 \\ U_2 &= W_2 + W_4 \end{aligned} \tag{4.4}$$

The boundary conditions imposed on the displacement vector are

$$U_1 = U_2 \tag{4.5}$$

$$\sigma_{ij}(U_1) = \sigma_{ij}(U_2), \qquad i, j = 1, 2, 3. \tag{4.6}$$

These boundary conditions must be complemented by the boundary condition for the phase function τ_d in (4.2) requiring on Σ at O that:

$$\tau_d = \tau_o \tag{4.7}$$

In our coordinate system (x,y,z) in Fig. 4.1 this leads immediately to the requirement:

$$\frac{\partial \tau_d}{\partial x} = \frac{\partial \tau_o}{\partial x} \tag{4.8}$$

which is a formulation of Snell's Law as follows:

$$\frac{\sin\theta_d}{V_d} = \frac{\sin\theta_o}{V_o} \tag{4.9}$$

with θ_d being the acute angle between the ray d and the normal direction to Σ at the point of incidence. The remaining two components of the vector $\nabla\tau_d$ at O on Σ are then easily determined as

$$\frac{\partial \tau_d}{\partial y} = 0$$

$$\frac{\partial \tau_d}{\partial z} = (-1)^{d+1} \frac{\cos\theta_d}{V_d} \tag{4.10}$$

It should be noted however that for

$$\frac{\partial \tau_0}{\partial x} = \frac{\partial \tau_d}{\partial x} > \frac{1}{V_d}$$

corresponding to the incidence angle, θ_0, which satisfy

$$\sin\theta_0 > \frac{V_0}{V_d}$$

the angle θ_d becomes complex resulting in $\sin\theta_d > 1$ and there are two complex conjugate functions $\tau_d(x,y,z)$ satisfying the fourth condition in (4.7). The uniqueness of the solution may sometimes be achieved by implementing the radiation condition requiring an exponential decrease of $f_k(t-\tau_d)$ in the direction normal to the boundary.

Once the directions of the reflected and transmitted rays at O on Σ have been established using (4.9) and (4.10), the scalar components of $W_d^{(k)}$ in (4.3) in our local coordinate system (x,y,z) can be written as:

$$W_{dx}^{(k)} = N_d^{(k)}\sin\theta_d + T_d^{(k)}\cos\theta_d$$

$$W_{dy}^{(k)} = V_d^{(k)}, \qquad d = 0, 1, 2, 3, 4 \tag{4.11}$$

$$W_{dz}^{(k)} = (-1)^{d+1}N_d^{(k)}\cos\theta_d + (-1)^d T_d^{(k)}\sin\theta_d$$

Thus the boundary condition (4.5) requiring the continuity of the displacement vector across the boundary can be written in terms of scalar components (see 4.12a, b and c for x, y and z components of vector equation, respectively) as:

$$(4.12a)\quad \sum_{d=0,1,3}(N_d^{(k)}\sin\theta_d + T_d^{(k)}\cos\theta_d) = \sum_{d=2,4}(N_d^{(k)}\sin\theta_d + T_d^{(k)}\cos\theta_d)$$

$$(4.12b)\quad \sum_{d=0,1,3}V_d^{(k)} = \sum_{d=2,4}V_d^{(k)}$$

$$(4.12c)\quad \sum_{d=0,1,3}[(-1)^{d+1}N_d^{(k)}\cos\theta_d + (-1)^d T_d^{(k)}\sin\theta_d] = \sum_{d=2,4}[(-1)^{d+1}N_d^{(k)}\cos\theta_d + (-1)^d T_d^{(k)}\sin\theta_d]$$

The boundary condition (4.6) for the continuity of the stress tensor components across the boundary requires some additional consideration. First of all the validity of Hooke's Law is assumed. This linear stress-strain relationship is given by:

$$(4.13)\quad \sigma_{ij}(\mathbf{U}) = \lambda\delta_{ij}\nabla\cdot\mathbf{U} + 2\mu\left[\frac{1}{2}\left(\frac{\partial U_i}{\partial x_j} + \frac{\partial U_j}{\partial x_i}\right)\right]$$

The stress tensor components related to the individual rays (W_d in (4.2) d=0,1,2,3,4) are evaluated below. We have, after omitting most of the intermediate algebra:

$$(4.14a)\quad \sigma_{zz}(W_d) = \sum_{k=0}[\lambda_d\nabla\cdot(W_d^{(k)}f_k) + 2\mu_d\partial(W_{dz}^{(k)}f_k)/\partial z] = \sum_{k=-1} f_k\Psi_k(W_d^{(k+1)}, W_d^{(k)})$$

where

$$(4.14b)\quad \Psi_k(W_d^{(k+1)}, W_d^{(k)}) = [\lambda_d \nabla\cdot W_d^{(k)} + 2\mu_d \partial W_{dz}^{(k)}/\partial z] + \\ - [N_d^{(k+1)} \frac{(\lambda_d + 2\mu_d \cos^2\theta_d)}{V_d} - T_d^{(k+1)} \frac{\mu_d \sin 2\theta_d}{V_d}]$$

Here, as well as in all subsequent formulae we have

$$\text{and} \qquad \begin{aligned} &\lambda_d = \lambda_1, \quad \mu_d = \mu_1, \quad \text{for} \quad d = 0, 1, 3, \\ &\lambda_d = \lambda_2, \quad \mu_d = \mu_2, \quad \text{for} \quad d = 2, 4, \end{aligned}$$

Similarly we have

$$(4.15a)\quad \sigma_{xz}(W_d) = \sum_{k=0} \mu_d [\partial(W_{dx}^{(k)} f_k)/\partial z + \partial(W_{dz}^{(k)} f_k)/\partial x] \\ = \sum_{k=-1} f_k \, T_k(W_d^{(k+1)}, W_d^{(k)})$$

where

$$(4.15b)\quad T_k(W_d^{(k+1)}, W_d^{(k)}) = \mu_d \{[\frac{\partial W_{dx}^{(k)}}{\partial z} + \frac{\partial W_{dz}^{(k)}}{\partial x}] + \\ + (-1)^d [N_d^{(k+1)} \frac{\sin 2\theta_d}{V_d} + T_d^{(k+1)} \frac{\cos 2\theta_d}{V_d}]\}$$

and

$$(4.16a)\quad \sigma_{yz}(W_d) = \sum_{k=0} \mu_d [\partial(W_{dy}^{(k)} f_k)/\partial z + \partial(W_{dz}^{(k)} f_k)/\partial y] \\ = \sum_{k=-1} f_k \, \Phi_k(W_d^{(k+1)}, W_d^{(k)})$$

where

$$(4.16b)\quad \Phi_k(W_d^{(k+1)},W_d^{(k)}) = \mu_d\{[\frac{\partial W_{dy}^{(k)}}{\partial z} + \frac{\partial W_{dz}^{(k)}}{\partial y}] + + (-1)^d V_d^{(k+1)}\frac{\cos\theta_d}{V_d}\}$$

Applying the derived formulae to the resultant displacement vectors on both sides of the boundary at the point of incidence O, the requirement of the continuity of the stress tensor components σ_{xz}, σ_{yz}, and σ_{zz} yields the following three scalar equations:

$$(4.17a)\quad \sum_{d=0,1,3}\mu_1\{(-1)^d[N_d^{(k+1)}\frac{\sin2\theta_d}{V_1} + T_d^{(k+1)}\frac{\cos2\theta_d}{V_1}] + + [\frac{\partial W_{dx}^{(k)}}{\partial z} + \frac{\partial W_{dz}^{(k)}}{\partial x}]\} = \sum_{d=2,4}\mu_2\{[N_d^{(k+1)}\frac{\sin2\theta_d}{V_2} + T_d^{(k+1)}\frac{\cos2\theta_d}{V_2}] + + [\frac{\partial W_{dx}^{(k)}}{\partial z} + \frac{\partial W_{dz}^{(k)}}{\partial x}]\}$$

$$(4.17b)\quad \sum_{d=0,1,3}\mu_1[(-1)^d V_d^{(k+1)}\frac{\cos\theta_d}{V_1} + \frac{\partial W_{dy}^{(k)}}{\partial z} + \frac{\partial W_{dz}^{(k)}}{\partial y}] = \sum_{d=2,4}\mu_2[V_d^{(k+1)}\frac{\cos\theta_d}{V_2} + \frac{\partial W_{dy}^{(k)}}{\partial z} + \frac{\partial W_{dz}^{(k)}}{\partial y}]$$

$$(4.17c)\quad \sum_{d=0,1,3}\{- N_d^{(k+1)}[\frac{\lambda_1+2\mu_1\cos^2\theta_d}{V_1}] + \lambda_1\nabla\cdot W_d^{(k)} + + T_d^{(k+1)}[\frac{\mu_1\sin2\theta_d}{V_1}] + 2\mu_1\frac{\partial W_{dz}^{(k)}}{\partial z}\}$$

$$= \sum_{d=2,4} \{- N_d^{(k+1)}[\frac{\lambda_2+2\mu_2\cos^2\theta_d}{V_2}] + \lambda_2\nabla\cdot W_d^{(k)} +$$

$$+ T_d^{(k+1)}[\frac{\mu_2\sin2\theta_d}{V_2}] + 2\mu_2\frac{\partial W_{dz}^{(k)}}{\partial z}\}$$

Obviously the two sets (4.12) and (4.17) can be combined into one set of six inhomogeneous linear equations for six principal components $N_1^{(k)}$ (reflected P-wave); $N_2^{(k)}$ (transmitted P-wave); $T_3^{(k)}$, $V_3^{(k)}$ (reflected S-wave) and $T_4^{(k)}$, $V_4^{(k)}$ (transmitted S-wave). The system is (4.18) as follows: [1]

(4.18-1):

$$\sum_{d=1}^{2} (-1)^d N_d^{(k)}\sin\theta_d + \sum_{d=3}^{4} (-1)^d T_d^{(k)}\cos\theta_d =$$

$$\sum_{d=0,3,4} (-1)^{d+()+1} N_d^{(k)}\sin\theta_d + \sum_{d=0}^{2} (-1)^{d+()+1} T_d^{(k)}\cos\theta_d$$

(4.18-2):

$$\sum_{d=1}^{2} N_d^{(k)}\cos\theta_d - \sum_{d=3}^{4} T_d^{(k)}\sin\theta_d =$$

$$\sum_{d=0,3,4} (-1)^{1+()} N_d^{(k)}\cos\theta_d + \sum_{d=0}^{2} (-1)^{()} T_d^{(k)}\sin\theta_d$$

(4.18-3) $$\sum_{d=1}^{2} \mu_d \frac{\sin2\theta_d}{V_d} N_d^{(k)} + \sum_{d=3}^{4} \mu_d \frac{\cos2\theta_d}{V_d} T_d^{(k)} = \Phi_1^{(k)}$$

---

[1] In this section the character set () arising in superscript means Dirac function δ_{d0}.

(4.18-4):

$$\sum_{d=1}^{2}(-1)^{d}\frac{\lambda_d+2\mu_d\cos^2\theta_d}{V_d}N_d^{(k)}+\sum_{d=3}^{4}(-1)^{1+d}\mu_d\frac{\sin2\theta_d}{V_d}T_d^{(k)}=\Phi_2^{(k)}$$

(4.18-5) $$\sum_{d=3}^{4}(-1)^{d}V_d^{(k)}=\sum_{d=0}^{2}(-1)^{d+()+1}V_d^{(k)}$$

(4.18-6):

$$\sum_{d=3}^{4}\mu_d\frac{\cos\theta_d}{V_d}V_d^{(k)}=\sum_{d=0}^{2}(-1)^{1+()}\mu_d\frac{\cos\theta_d}{V_d}V_d^{(k)}+\sum_{d=0}^{4}(-1)^{d+()+1}\cdot\mu_d\left[\frac{\partial W_{dy}^{(k-1)}}{\partial z}+\frac{\partial W_{dz}^{(k-1)}}{\partial y}\right]$$

$$k = 0,\ 1,\ 2,\ .....$$

where

(4.19):

$$\Phi_1^{(k)}=\sum_{d=0,3,4}(-1)^{1+()}\mu_d\frac{\sin2\theta_d}{V_d}N_d^{(k)}+\sum_{d=0}^{2}(-1)^{1+()}\mu_d\cdot\frac{\cos2\theta_d}{V_d}T_d^{(k)}+\sum_{d=0}^{4}(-1)^{d+()+1}\mu_d\left[\frac{\partial W_{dx}^{(k-1)}}{\partial z}+\frac{\partial W_{dz}^{(k-1)}}{\partial x}\right]$$

and

(4.20):

$$\Phi_2^{(k)}=\sum_{d=0}^{4}(-1)^{d+()}\left[\lambda_d\nabla\cdot W_d^{(k-1)}+2\mu_d\frac{\partial W_{dz}^{(k-1)}}{\partial z}\right]+\sum_{d=0}^{2}(-1)^{d+()}\cdot\mu_d\frac{\sin2\theta_d}{V_d}T_d^{(k)}+\sum_{d=0,3,4}(-1)^{d+()+1}\left[\frac{\lambda_d+2\mu_d\cos^2\theta_d}{V_d}\right]N_d^{(k)}$$

In the case of two dimensional problems the system (4.18) simply becomes one consisting of (4.18-1), (4.18-2), (4.18-3), and (4.18-4), in which the first two equations describe the continuity of displacements, and the second two the continuity of stresses.

4.2 Determination of Amplitude Coefficients for Model #1

As mention above Model #1 is an elastic isotropic homogeneous half-space with a P wave point source buried in the half-space. Based on the formulae for the higher order terms of ART for an elastic isotropic homogeneous medium derived in Chapter 2, and the basic formulae for the boundary conditions given in the last section, we shall be able to investigate the higher order effects of ART for Model #1 in detail now.

The so called free surface mathematically means that at an interface with a vacuum, the three stress components (σ_{zz}, σ_{xz}, σ_{yz}) are all zero, and this is effectively the case also for the surface of the Earth or the oceans, since the elastic constants for the atmosphere are several orders of magnitude less than the elastic constants of rock or the bulk modulus of sea water. The case of (σ_{zz}, σ_{xz}, σ_{yz}) = (0, 0, 0) at z=0 is referred to as the "free-surface boundary condition" at z=0.

For an elastic homogeneous half-space with a free surface, noticing $\lambda_2=\lambda_4=\mu_2=\mu_4=0$, $\lambda_0=\lambda_1=\lambda_3$, and $\mu_0=\mu_1=\mu_3$, the

boundary conditions (4.18-3) and (4.18-4), describing the continuity of stresses, become:

$$(4.21)\qquad \mu_1 \frac{\sin 2\theta_1}{V_1} N_1^{(k)} + \mu_1 \frac{\cos 2\theta_3}{V_3} T_3^{(k)} = \Phi_1^{(k)}$$

$$(4.22)\qquad \mu_1 \frac{\sin 2\theta_3}{V_3} T_3^{(k)} - \left[\frac{\lambda_1 + 2\mu_1 \cos^2\theta_1}{V_1}\right] N_1^{(k)} = \Phi_2^{(k)}$$

where $\Phi_1^{(k)}$ and $\Phi_2^{(k)}$ were given by (4.19) and (4.20) respectively.

In accordance with the definition of Model #1, the above two boundary conditions may be further simplified for the zero order approximation as follows:

$$(4.23)\qquad \frac{\cos 2\theta_3}{\beta} S_3^{(0)} = \frac{\sin 2\theta_0}{\beta} \left[P_0^{(0)} - P_1^{(0)}\right]$$

$$(4.24)\qquad \frac{\sin 2\theta_3}{\beta} S_3^{(0)} = \left[\frac{\lambda_1 + 2\mu_1 \cos^2\theta_0}{\mu_1 \beta}\right]\left[P_0^{(0)} + P_1^{(0)}\right]$$

Defining $\lambda \equiv \lambda_1$, $\mu \equiv \mu_1$ and the ratio of S wave speed to P wave speed as follows:

$$(4.25a)\qquad \Omega \equiv \beta/\alpha$$

we have

$$(4.25b)\qquad \begin{aligned} \mu &= \beta^2 \rho = \Omega^2 \alpha^2 \rho \\ \lambda &= (\alpha^2 - 2\beta^2)\rho = (1 - 2\Omega^2)\alpha^2 \rho \end{aligned}$$

Solving the set consisting of (4.23) and (4.24), and using (4.25) in the solution, the amplitude coefficients of

the zeroth order term at the reflected point may be obtained as follows:

$$(4.26)\quad P_1^{(0)}(\iota_0) = \frac{\sin 2\theta_3 \sin 2\theta_0 \Omega^2 - (1-2\Omega^2\sin^2\theta_0)\cos 2\theta_3}{\sin 2\theta_3 \sin 2\theta_1 \Omega^2 + (1-2\Omega^2\sin^2\theta_1)\cos 2\theta_3} P_0^{(0)}(\iota_0)$$

$$(4.27)\quad S_3^{(0)}(\iota_0) = \frac{\Omega \sin 2\theta_0 [P_0^{(0)}(\iota_0) - P_1^{(0)}(\iota_0)]}{\cos 2\theta_3}$$

Note that the angles θ_1 and θ_3 are known as functions of the incidence angle θ_0 and the ratio Ω using Snell's Law, and that ι_0 expresses the distance from the source point to the reflection point.

The amplitude cofficient of the zeroth order term for the incident P wave, $P_0^{(0)}$, can be directly written from (2.12a) and (2.13) as follows:

$$(4.28)\quad P_0^{(0)}(r) = \frac{P_0^{(0)}(r_0)\, r_0}{r} = \frac{1}{r}$$

where r_0 stands for the distance from the source point to the reference point.

The formulae suitable for the zeroth order terms of the reflected $P_1^{(0)}$ wave and the reflected $S_3^{(0)}$ wave have been given by Cerveny and Ravindra (1971) as follows:

$$(4.29)\quad P_1^{(0)}(r) = \frac{P_1^{(0)}(\iota_0)\, \iota_0}{r}$$

$$(4.30)\quad S_3^{(0)}(r) = \frac{S_3^{(0)}(\iota_0)\, \iota_0}{L_s(r)}$$

where the geometrical spreading of the reflected S_3 wave, $L_s(r)$, is given by

$$(4.31)\quad L_s(r) = \cos\theta_0\left[\left(\frac{h_1}{\cos\theta_1} + \frac{\Omega h_2}{\cos\theta_3}\right)\left(\frac{h_1}{\cos^3\theta_1} + \frac{\Omega\, h_2}{\cos^3\theta_3}\right)\right]^{1/2}$$

where h_1 and h_2 are the vertical distances from the source point and the receiver point to the free surface, respectively.

The principal component of the first order incidence P wave, $P_0^{(1)}$, can be obtained from (2.45') as follows:

$$(4.32)\quad P_0^{(1)}(r) = (1-2\Omega^2)\ \alpha\ P_0^{(0)}(r)\ /\ r$$

Also, the additional component of the first order incidence P wave can be obtained from (2.34) as follows:

$$(4.33)\quad p_0^{(1)}(r) = 0$$

Noticing that the expressions $\nabla\cdot\hat{e}_-$ and $\nabla\cdot\hat{e}_+$ needed by the reflected P wave have forms similar to the case of the incident P wave:

$$(4.34)\quad \begin{aligned} \nabla\cdot\hat{e}_{-(1)} &= 2\ /\ \gamma \\ \nabla\cdot\hat{e}_{+(1)} &= \operatorname{cotan}\theta_1\ /\ \gamma \end{aligned}$$

where $\gamma=\iota_0+r$ stands for the total length of the ray from the source to the receiver via the reflected point. To find the expression of the principal component of the first order reflected PP wave, we integrate (2.43) by substituting

(4.34) into it, and finally obtain:

$$(4.35)\quad P_i^{(1)}(\gamma) = P_i^{(1)}(\iota_0)\frac{\iota_0}{\gamma} + \frac{\lambda}{\alpha\rho\gamma}[P_i^{(0)}(\gamma)-P_i^{(0)}(\iota_0)]$$

where $P_i^{(1)}(\iota_0)$ will be determined from the boundary conditions of the first order terms which will be discussed later in detail. The additional component of the first order term for the reflected PP wave can be directly produced from (2.26) as follows:

$$(4.36)\quad p_i^{(1)}(\gamma) = 0$$

Now let us concentrate on the reflected PS wave reflected from the free surface in Model #1. The key in the investigation of the first order terms of the reflected S wave is how to evaluate $\nabla\cdot\hat{e}_{+(3)}$ and $\nabla\cdot\hat{e}_{=(3)}$ in this case, because we have to employ their values in the general expression (2.32) for the additional component $s_3^{(1)}$, or (2.55) for the principal component $S_3^{(1)}$, respectively.

Wavefront surfaces of the reflected PS wave in three dimensional space expressed as functions of time t in Cartesian coordinates (X(t), Y(t), Z(t)) should be transformed to the following set of equations, by choosing Γ, θ_3 and ψ as three independent parameters (explained in Figure 4.2) instead of X(t), Y(t) and Z(t).

$$\begin{aligned} X &= \cos\psi\ \sin\theta_3\ \Gamma \\ (4.37)\quad Y &= \sin\psi\ \sin\theta_3\ \Gamma \\ Z &= \cos\theta_3\ \Gamma - h_1\cos\theta_3/[\Omega^2-\sin^2(\theta_3)]^{1/2} \end{aligned}$$

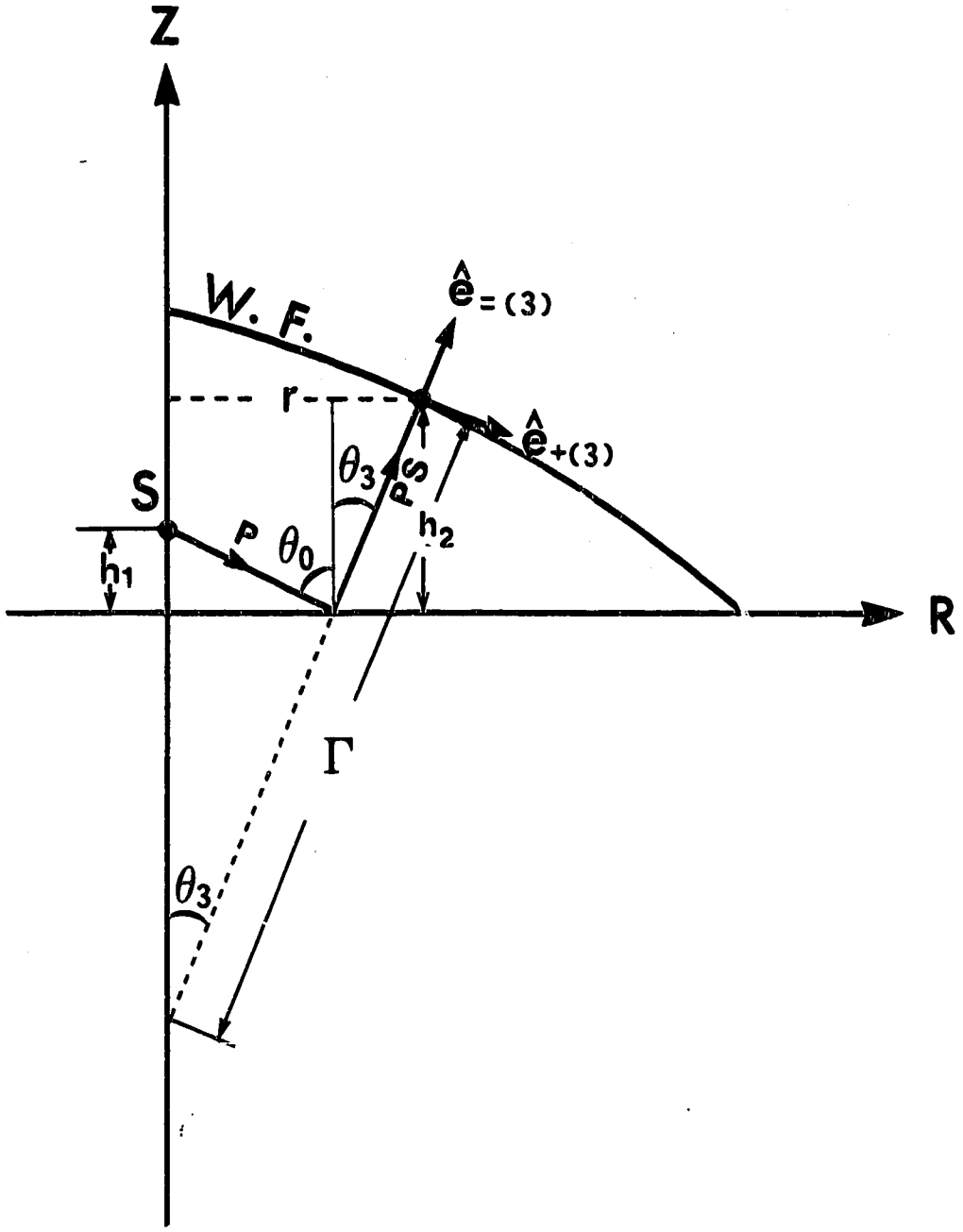

Figure 4.2 Signs and notation used to evaluate $\nabla\cdot\hat{e}_{=(3)}$ and $\nabla\cdot\hat{e}_{+(3)}$ for the reflected PS wave in Model #1.

where $\Omega \equiv \beta/\alpha$. Lame's coefficients according to the above transformed coordinate system are:

$$
\begin{aligned}
H(\Gamma) &= 1 \\
H(\psi) &= \sin(\theta_3)\,\Gamma \\
H(\theta_3) &= \left[\Gamma^2 + \frac{[h_1 \sin\theta_3 (1-\Omega^2)]^2}{(\Omega^2-\sin^2\theta_3)^3} + \frac{2h_1\Gamma\sin^2\theta_3(1-\Omega^2)}{(\Omega^2-\sin^2\theta_3)^{3/2}}\right]^{1/2}
\end{aligned}
\tag{4.38}
$$

Then it is easy to show that:

$$
\begin{aligned}
\hat{e}_{=(3)} &= (e(\Gamma), e(\theta_3), e(\psi)) = (1,0,0) \\
\hat{e}_{+(3)} &= (e(\Gamma), e(\theta_3), e(\psi)) = (0,1,0)
\end{aligned}
\tag{4.39}
$$

Finally we have the following expressions necessary to compute the reflected PS wave:

$$
\begin{aligned}
\nabla\cdot\hat{e}_{=(3)} &= \frac{1}{\Gamma} + \frac{\Gamma + B\sin\theta_3}{(\Gamma^2+B^2+2\Gamma B\sin\theta_3)} \\
\nabla\cdot\hat{e}_{+(3)} &= \frac{\operatorname{cotan}(\theta_3)}{(\Gamma^2+B^2+2\Gamma B\sin\theta_3)^{1/2}}
\end{aligned}
\tag{4.40}
$$

where

$$
B \equiv \frac{h_1\sin\theta_3(1-\Omega^2)}{(\Omega^2-\sin^2\theta_3)^{3/2}} \qquad \Gamma \equiv \frac{h_1\tan\theta_o}{\sin\theta_3} + \frac{h_2}{\cos\theta_3} \tag{4.41}
$$

Now we are able to present the additional component of the first order reflected PS wave from its general expression (2.32) as follows:

$$
s_3^{(1)}(\gamma) = \beta\, S_3^{(0)}(\gamma)\, \nabla\cdot\hat{e}_{+(3)} \tag{4.42}
$$

For the special case when the incident P wave is

perpendicular to the free surface, in another words, when $\theta_0=\theta_3=0$, (4.42) becomes:

$$(4.43) \qquad s_3^{(1)}(h_2) = \frac{4\beta\Omega}{(h_1+h_2\Omega)^2} ,$$

where h_1 and h_2 indicate the perpendicular distance from the source and the receiver to the free surface, respectively.

To determine the principal component of the first order reflected PS wave, substituting (4.40) into its general expression (2.55) yields the following differential equation:

$$(4.44) \qquad \frac{dS_3^{(1)}(r)}{dr} = - S_3^{(1)}(r)\frac{\nabla\cdot\hat{e}_{=(3)}}{2} + \frac{d^2S_3^{(0)}(r)}{dr^2}\frac{\beta}{2}$$

The general solution of the above differential equation can be obtained after some tedious mathematical operations as:

(4.45)

$$S_3^{(1)}(\gamma) = [S_3^{(1)}(\iota_0)+S_3^{(0)}(\iota_0)\frac{\beta(E+F)}{4EF}]\frac{[F(F^2+2FA+B^2)^{1/2}]^{1/2}}{RBR} +$$

$$+ S_3^{(0)}(\iota_0)\frac{\beta(EF)^{1/2}}{4}[\frac{IBI}{2RBR} - \frac{(F+E+2r)}{[(E+r)(F+r)]^{3/2}}],$$

where

$$RBR = \{(F+r)[(F+r)^2+2(F+r)A+B^2]^{1/2}\}^{1/2}$$

$$IBI = \int \frac{(F+E+2r)}{[(E+r)(F+r)]^{3/2}}\cdot\frac{2(F+r)^2+3A(F+r)+B^2}{RBR\cdot[(F+r)^2+2(F+r)A+B^2]^{1/2}}\,dr$$

$$F = \frac{\iota_0}{\Omega}$$

$$E = F \frac{\cos^2\theta_3}{\cos^2\theta_0}$$

$$A = B \sin\theta_3$$

and B given in (4.41).

Here $\gamma \equiv \iota_0 + r$ once again stands for the total length of the reflected S ray from the source point to the receiver via the reflected point.

When the incident P wave is perpendicular to the free surface, or equivalently when $\theta_0=\theta_3=0$, due to $S_3^{(0)}(\iota_0)=0$ and B=0 in (4.45), the principal component of the first order reflected PS wave now is given by:

$$(4.46) \quad S_3^{(1)}(\gamma) = S_3^{(1)}(\iota_0) \frac{F}{F+r}$$

Here $S_3^{(1)}(\iota_0)$ in both (4.45) and (4.46) stands for the boundary value of the principal component of the first order reflected PS wave at the reflected point, which will be determined by the boundary conditions of the first order terms.

Next we shall show how to evaluate the principal components of the first order reflected P and S waves, $P_1^{(1)}(\iota_0)$ and $S_3^{(1)}(\iota_0)$, at the reflected point in Model #1. Substituting k=1 into the general boundary conditions (4.21) and (4.22) yields the first order boundary conditions as

follow:

$$(4.47)\quad \mu\frac{\cos 2\theta_3}{\beta}S_3^{(1)}(\iota_0)+\mu\frac{\sin 2\theta_1}{\alpha}P_1^{(1)}(\iota_0)=\Phi_1^{(1)}(\iota_0)$$

$$(4.48)\quad \mu\frac{\sin 2\theta_3}{\beta}S_3^{(1)}(\iota_0)-\left[\frac{\lambda+2\mu\cos^2\theta_1}{\alpha}\right]P_1^{(1)}(\iota_0)=\Phi_2^{(1)}(\iota_0)$$

where $\Phi_1^{(1)}(\iota_0)$ and $\Phi_2^{(1)}(\iota_0)$ are obtained from (4.19) and (4.20) after some tedious algebraic operations:

$$(4.49)\quad \Phi_1^{(1)}(\iota_0)=\mu\{\frac{\sin 2\theta_0}{\alpha}P_0^{(1)}(\iota_0)-\frac{\sin 2\theta_3}{\beta}S_3^{(1)}(\iota_0)+2\frac{\partial P_1^{(0)}}{\partial x}\cos\theta_1 + \frac{dS_3^{(0)}}{dr}-2\sin\theta_3\frac{\partial S_3^{(0)}}{\partial x}-\Omega\frac{S_3^{(0)}}{\iota_0}\}$$

$$(4.50)\quad \Phi_2^{(1)}(\iota_0)=\rho\{\frac{4\beta^2R_{01}-\alpha^2(1+R_{01})}{\iota_0^2}+2\beta^2(1-R_{01})\frac{\cos^2\theta_0}{\sin\theta_0}\cdot\frac{\partial P_0^{(0)}}{\partial x} +2\beta^2\cos^2\theta_3 S_3^{(0)}\nabla\cdot\hat{e}_{+(3)}+(\alpha-2\beta^2\Omega\sin^2\theta_0)P_0^{(1)} -2\beta^2\frac{\sin^2\theta_3}{\cos\theta_3}\cdot\frac{\partial S_3^{(0)}}{\partial x}+2\beta^2\tan\theta_3\frac{dS_3^{(0)}}{dr}\}$$

where $R_{01}\equiv P_1^{(0)}(\iota_0)/P_0^{(0)}(\iota_0)$ denotes the reflection coefficient of the reflected PP wave.

For the sake of simplicity we introduce AAA and BBB defined by:

$$AAA=\frac{\beta}{\mu}\Phi_1^{(1)}(\iota_0)$$

(4.51)
$$BBB = \frac{1}{\rho}\,\Phi_2^{(1)}(\iota_0)$$

Notice that when the incident P wave is perpendicular to the free surface, i.e. when $\theta_0=\theta_1=\theta_3=0$, the above (4.51) becomes:

$$AAA(\iota_0) = 0$$

(4.52)
$$BBB(\iota_0) = \alpha\cdot P_0^{(1)}(\iota_0) + \frac{4(2\Omega-1)\beta^2}{h_1^2}$$

Then equations (4.47) and (4.48) may be rewritten as follows:

(4.53) $\cos(2\theta_3)S_3^{(1)}(\iota_0) + \Omega\sin(2\theta_1)P_1^{(1)}(\iota_0) = AAA$

(4.54) $\beta\sin(2\theta_3)S_3^{(1)}(\iota_0) - \alpha(1-2\Omega^2\sin^2\theta_1)P_1^{(1)}(\iota_0) = BBB$

By solving the above set of equations we are able to find the values of the principal components of the first order reflected PP and PS waves at the point of incidence on the free surface boundary. They are:

$$P_1^{(1)}(\iota_0) = \frac{AAA\Omega\alpha\sin2\theta_3 - BBB\cos2\theta_3}{\alpha(1-2\Omega^2\sin^2\theta_1)\cos2\theta_3 + \Omega^2\alpha\sin2\theta_3\sin2\theta_1}$$

(4.55)
$$S_3^{(1)}(\iota_0) = \frac{AAA - \Omega\sin2\theta_1 P_1^{(1)}(\iota_0)}{\cos2\theta_3}$$

At vertical incidence, where $\theta_0=\theta_1=\theta_3=0$, we will take the following values instead of the ones given above:

$$
\begin{aligned}
P_1^{(1)}(\iota_0) &= -\frac{\lambda}{\alpha\rho h_1^2} - \frac{4(2\Omega-1)\Omega\beta}{h_1^2} \\
S_3^{(1)}(\iota_0) &= 0 \ .
\end{aligned}
\tag{4.56}
$$

Finally substituting the above values into either (4.35) or (4.45) will give the principal components of the reflected PP or PS waves along whole relected rays.

Up until now the derivation of expressions for the zero order and the first order approximations to ART for Model #1 have been done analytically. In the next section the numerical implementation of these formulae will be presented.

4.3 Synthetic Seismograms Related with Model #1

Based on the formulae obtained in the last section we are now able to compute synthetic seismograms including the first order effects for Model #1. Many of the synthetic seismograms computed using ART will be compared with those computed using the Alekseev-Mikhailenko Method (AMM).

A wavelength is defined as the ratio of the compressional wave velocity in the half-space to the predominant frequency of the source pulse. The predominant frequency ν, of the source pulse was chosen as 1.0 wavelength/period. The time dependence of the source pulse used in all synthetic seismogram computations is:

$$
\begin{aligned}
f_0(t) &= \exp[-(2\pi\nu t/\gamma)^2] \sin(2\pi\nu t) \\
g_0(t) &= \exp[-(2\pi\nu t/\gamma)^2] \cos(2\pi\nu t) \\
f_1(t) &= -\exp[-(2\pi\nu t/\gamma)^2] \cos(2\pi\nu t) /(2\pi\nu) \\
g_1(t) &= \exp[-(2\pi\nu t/\gamma)^2] \sin(2\pi\nu t) /(2\pi\nu)
\end{aligned} \qquad (4.57)
$$

where the damping factor γ, was chosen as 4. For the sake of simplicity all distances and times were measured in terms of the predominant wavelength WL, and period T, respectively. The velocity ratio of S wave to P wave was taken to be $\Omega \equiv \beta/\alpha = 0.5$.

Two cases in Model #1 shall be discussed in this section. In the first case, the P source was buried at small distance, h=0.25 WL, from the free surface in homogeneous isotropic half-space. For this situation the vertical components of the displacement vector obtained from the AMM for a receiver depth z=3 WL at 12 epicentral distances are shown in Figure 4.3. The solution of the zero order approximation of ART is shown in Figure 4.4. If we consider not only the zero order but also the first order effects, the corresponding solution of ART shown in Figure 4.5 should match that computed using the AMM more closely. From Figure 4.5 we can see that even in the case of normal incidence a nonzero vertical component of the converted PS wave exists as predicted by the AMM's results. To clearly show only the first order effect a set of synthetic seismograms shown in Figure 4.6 is helpful in understanding that the higher order terms of ART should be considered when computing the wave fields in the region near vertical incidence in order to

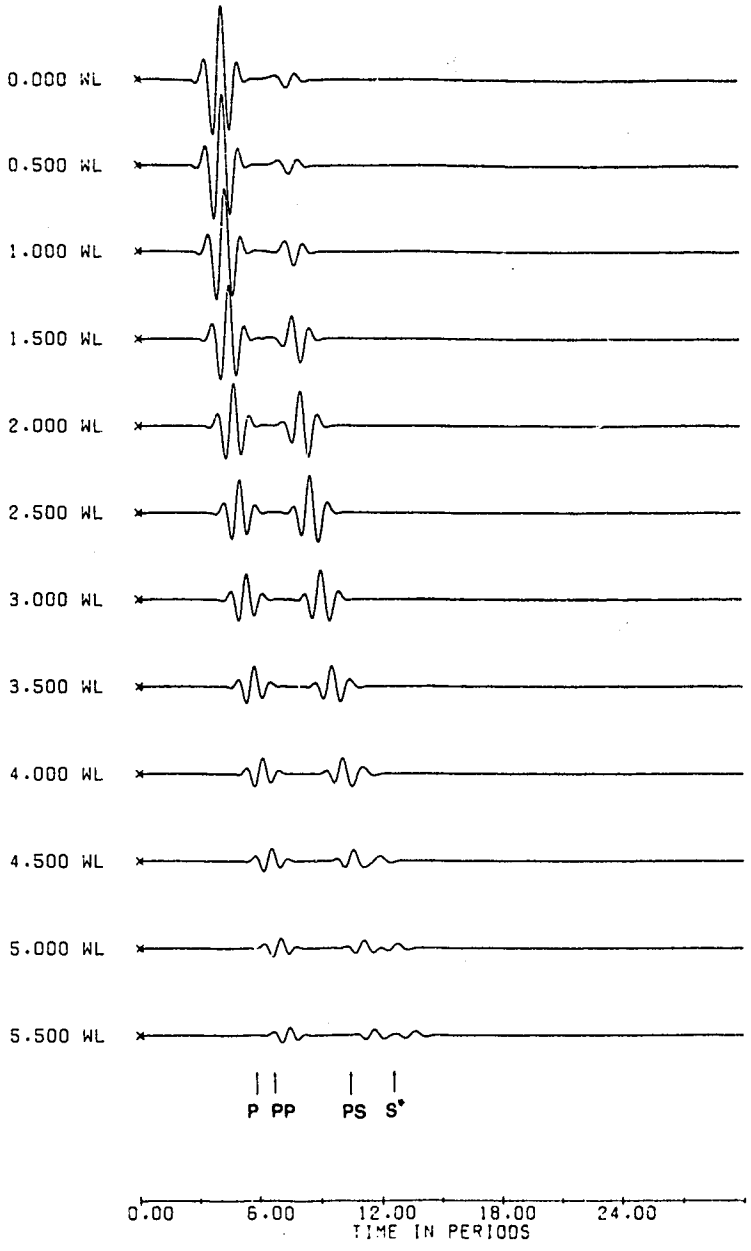

Figure 4.3 Vertical components computed using the Alekseev-Mikhailenko Method for Model #1. Vertical components of the displacement vector were computed for depth z=3 WL at all epicentral distances. The P source was buried at the depth h=0.25 WL. The ratio of S to P velocities was taken to be $\beta/\alpha=0.5$.

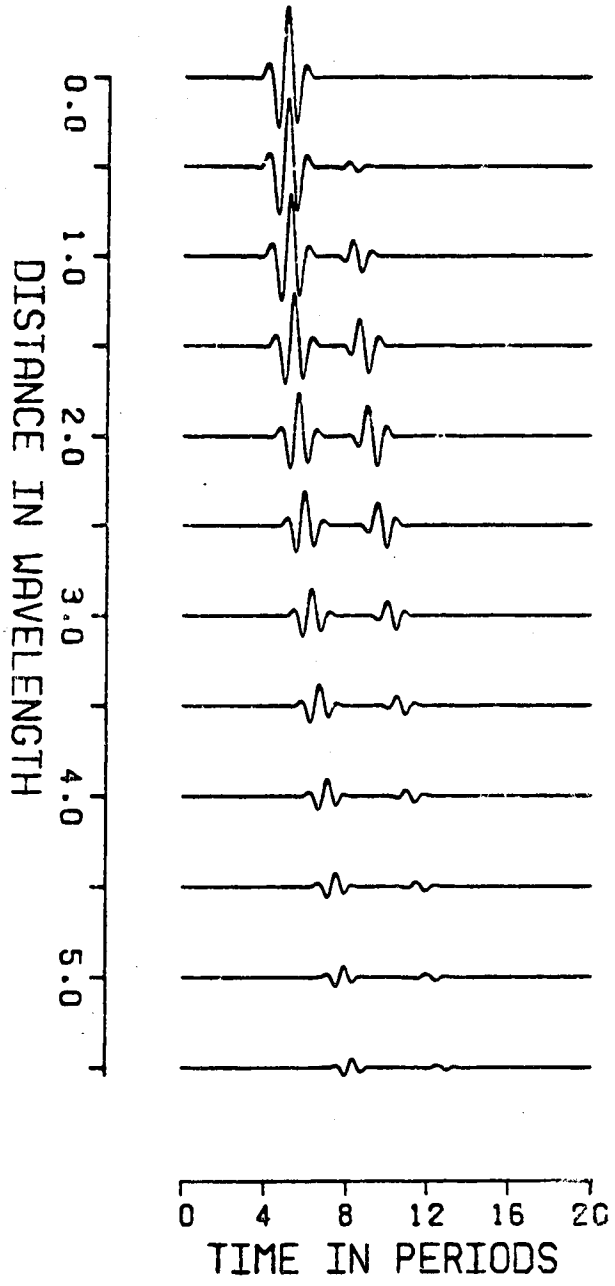

Figure 4.4 Vertical components computed using the zero order approximation of ART for Model #1. Vertical components of the displacement vector were computed for the depth z=3 WL at all epicentral distances. The P source was buried at the depth h=0.25 WL. The ratio of S to P velocities was taken to be β/α=0.5 .

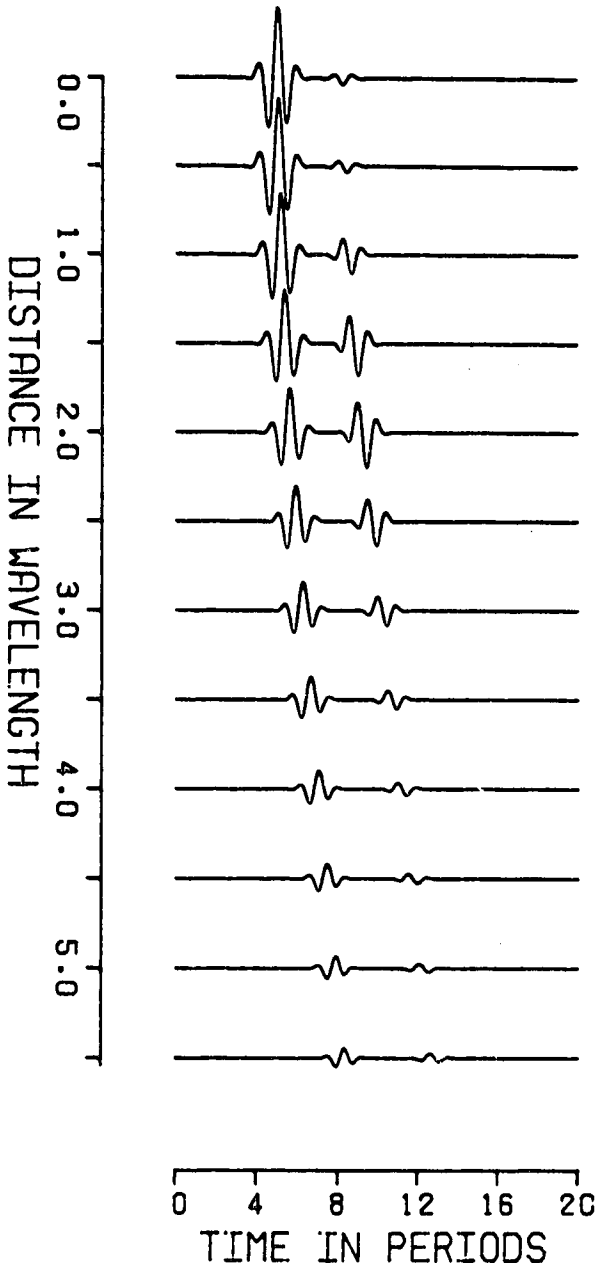

Figure 4.5 Vertical components computed using the formulae derived for the first order approximation of ART for Model #1. Vertical components of the displacement vector were computed for the depth z=3 WL at all epicentral distances. The P source was buried at the depth h=0.25 WL. The ratio of S to P velocities was taken to be $\beta/\alpha=0.5$.

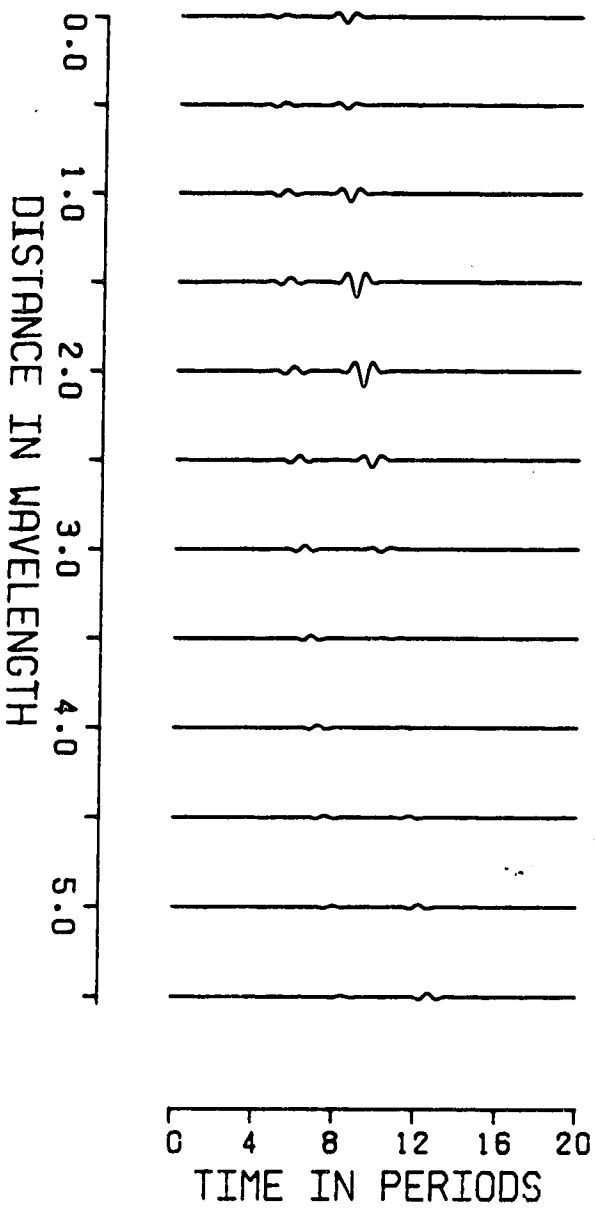

Figure 4.6 Vertical components including the effect of the first order term only in ART for Model #1. Vertical components of the displacement vector were computed for the depth z=3 WL at all epicentral distances. The P source was buried at the depth h=0.25 WL. The ratio of S to P velocities was taken to be β/α=0.5 .

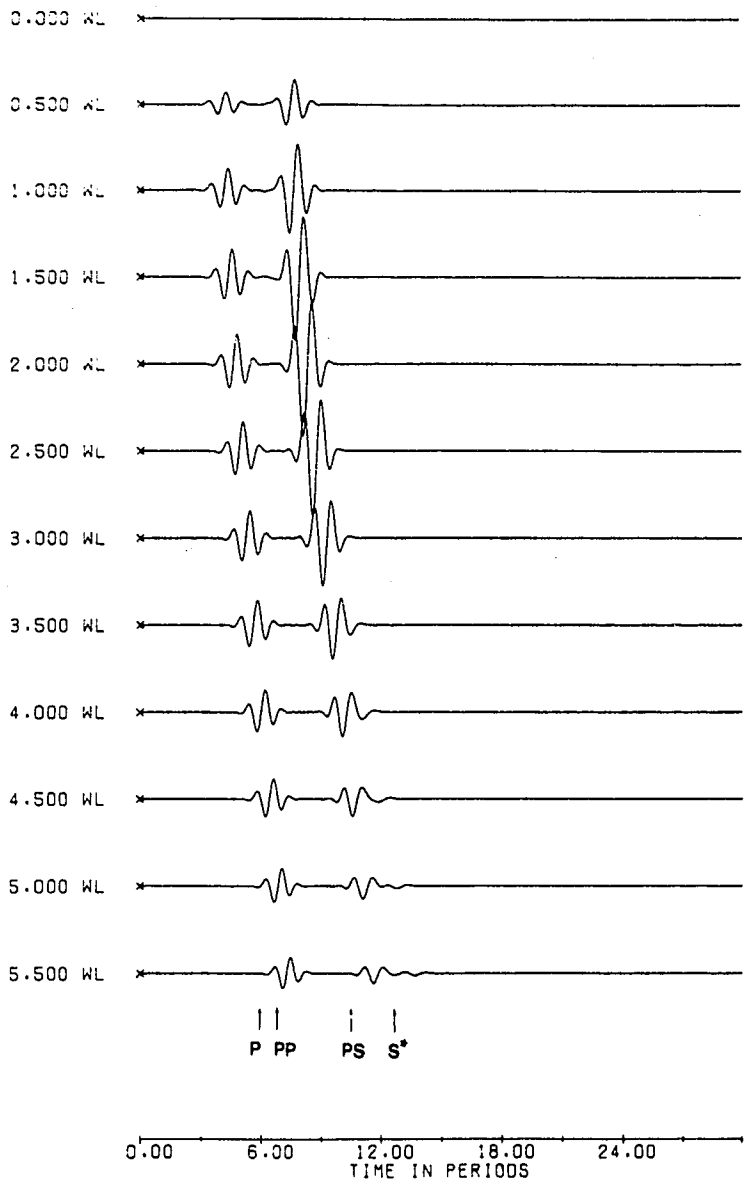

Figure 4.7 Horizontal components obtained from the Alekseev-Mikhailenko Method for Model #1. Horizontal components of the displacement vector were computed for the depth z=3 WL at all epicentral distances. The P source was buried at the depth h=0.25 WL. The ratio of S to P velocities was taken to be $\beta/\alpha=0.5$.

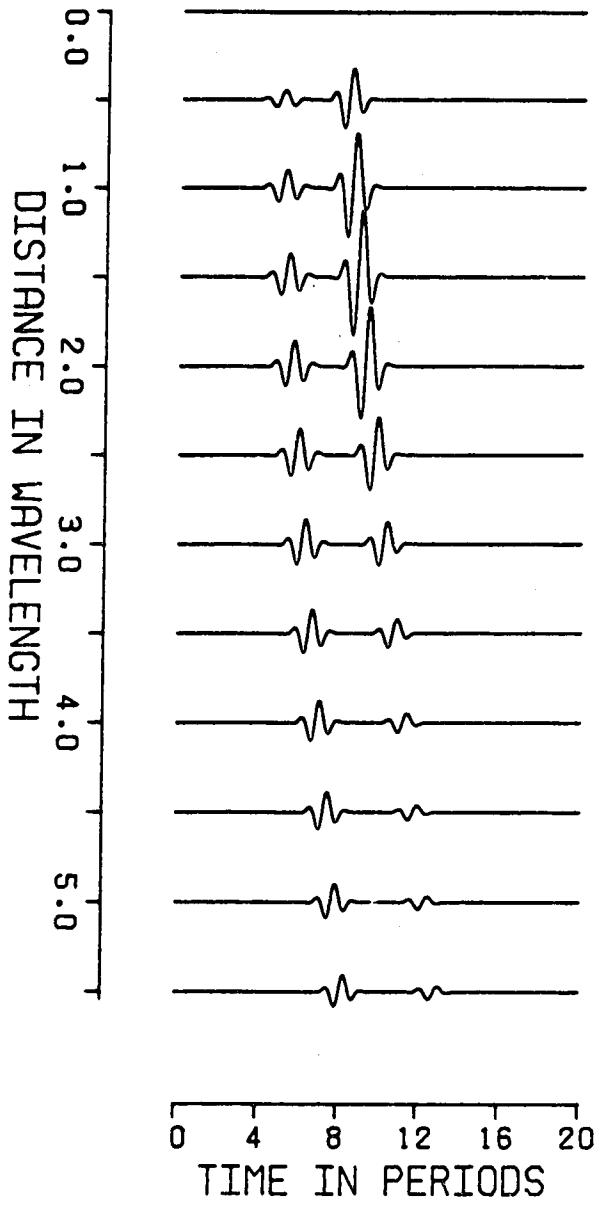

Figure 4.8 Horizontal components computed using the formulae derived for the first order approximation of ART for Model #1. Horizontal components of the displacement vector were computed for the depth z=3 WL at all epicentral distances. The P source was buried at the depth h=0.25 WL. The ratio of S to P velocities was taken to be β/α=0.5 .

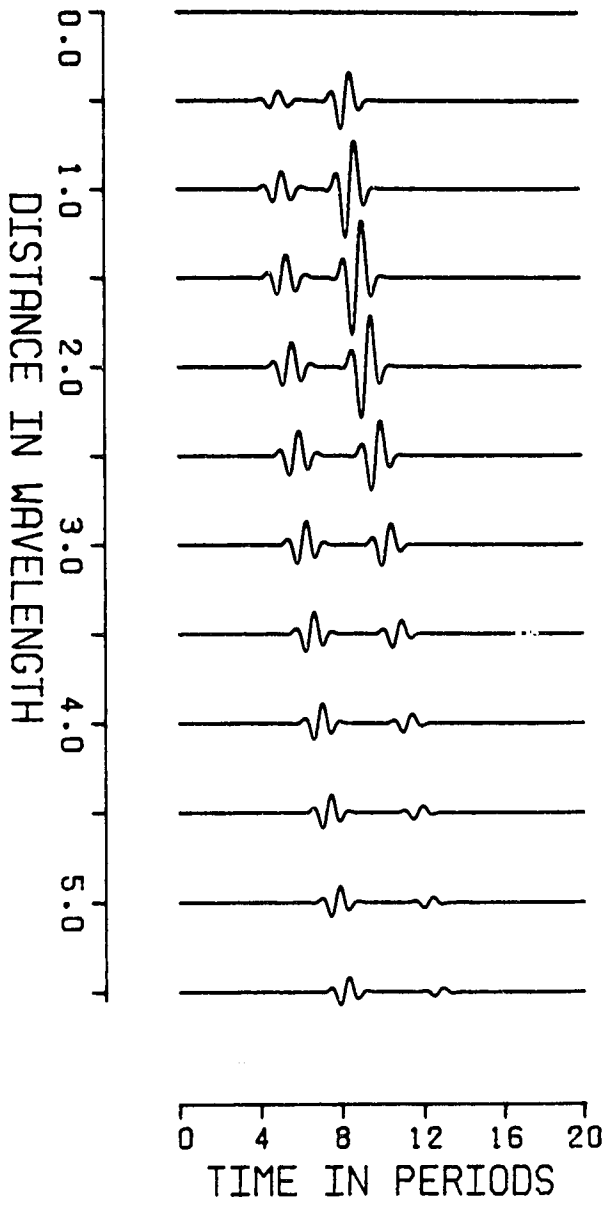

Figure 4.9 Horizontal components computed using the zero order approximation of ART for Model #1. Horizontal components of the displacement vector were computed for the depth z=3 WL at all epicentral distances. The P source was buried at the depth h=0.25 WL. The ratio of S to P velocities was taken to be $\beta/\alpha=0.5$.

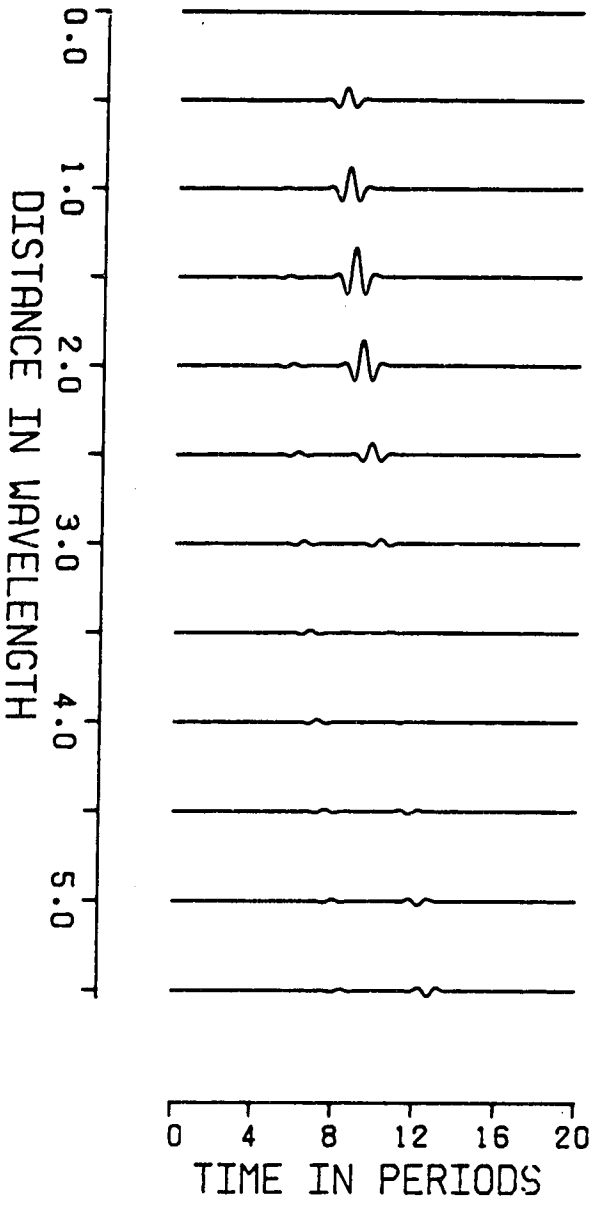

Figure 4.10 Horizontal components including the effect of the first order term only in ART for Model #1. Horizontal components of the displacement vector were computed for the depth z=3 WL at all epicentral distances. The P source was buried at the depth h=0.25 WL. The ratio of S to P velocities was taken to be $\beta/\alpha=0.5$.

obtain more accurate results.

We will now consider the relative horizontal components. Figure 4.7 shows the AMM's solution for Model #1, whereas the solution of the first order approximation of ART is shown in Figure 4.8. The similarity of these two Figures clearly indicates that the first order result of ART for Model #1 is more acceptable. To express the difference in horizontal components between the zero order and the first order approximations of ART we have shown both instances in Figures 4.9 and 4.10, respectively.

In the second case we take the source depth in model #1 from 0.25 WL (case 1) to 0.125 WL to see what effect this has on the results?

The vertical components in this case obtained from the AMM are shown in Figure 4.11, whereas the solution of the first order approximation of ART is shown in Figure 4.12. The similarity between Figures 4.11 and 4.12 once again indicates that using the first order approximation of ART to deal with Model #1 may gives a more acceptable solution. For the sake of comparison the results of the zero order approximation and the effect of the first order terms only of ART have been shown in Figures 4.13 and 4.14, respectively.

The relative horizontal components of the first order result, the zero order result and the effect of the first order terms only are shown in Figures 4.15, 4.16 and 4.17, respectively.

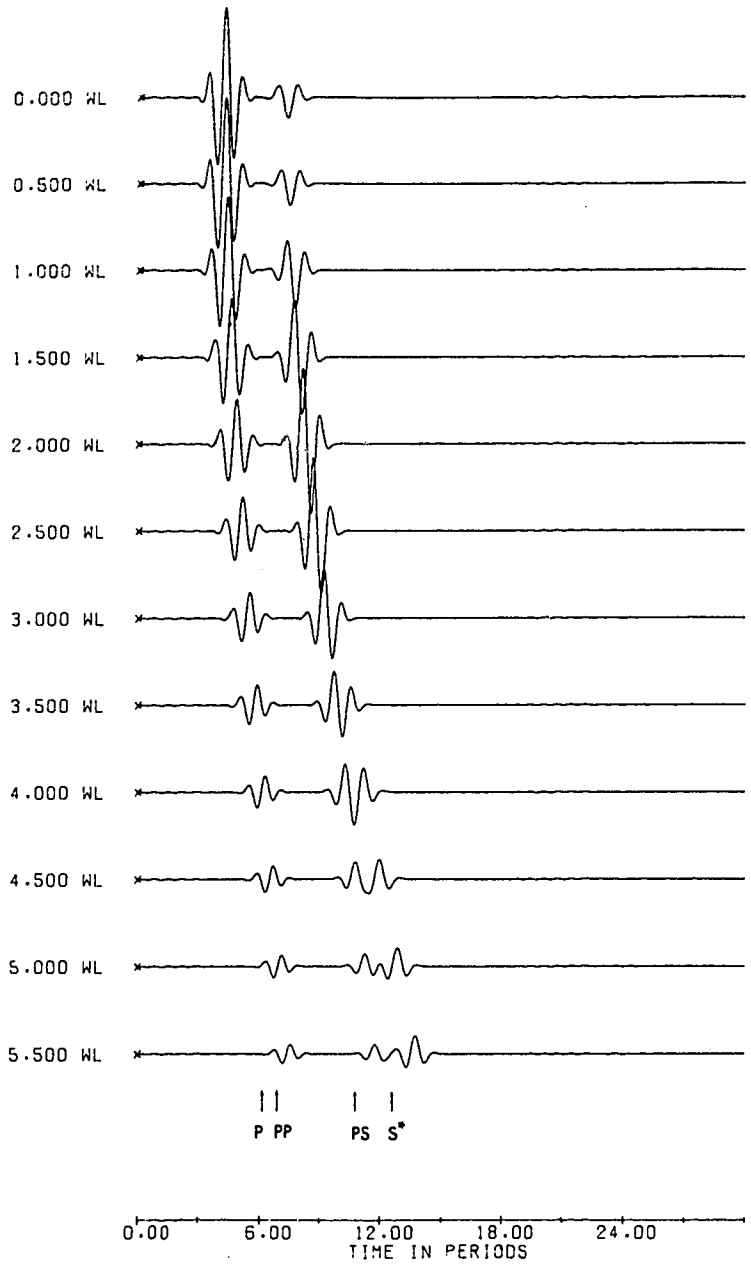

Figure 4.11 Vertical components computed using the Alekseev-Mikhailenko Method for Model #1. Vertical components of the displacement vector were computed for the depth z=3 WL at all epicentral distance. The P source was buried at the depth h=0.125 WL. The ratio of S to P velocities was taken to be $\beta/\alpha=0.5$.

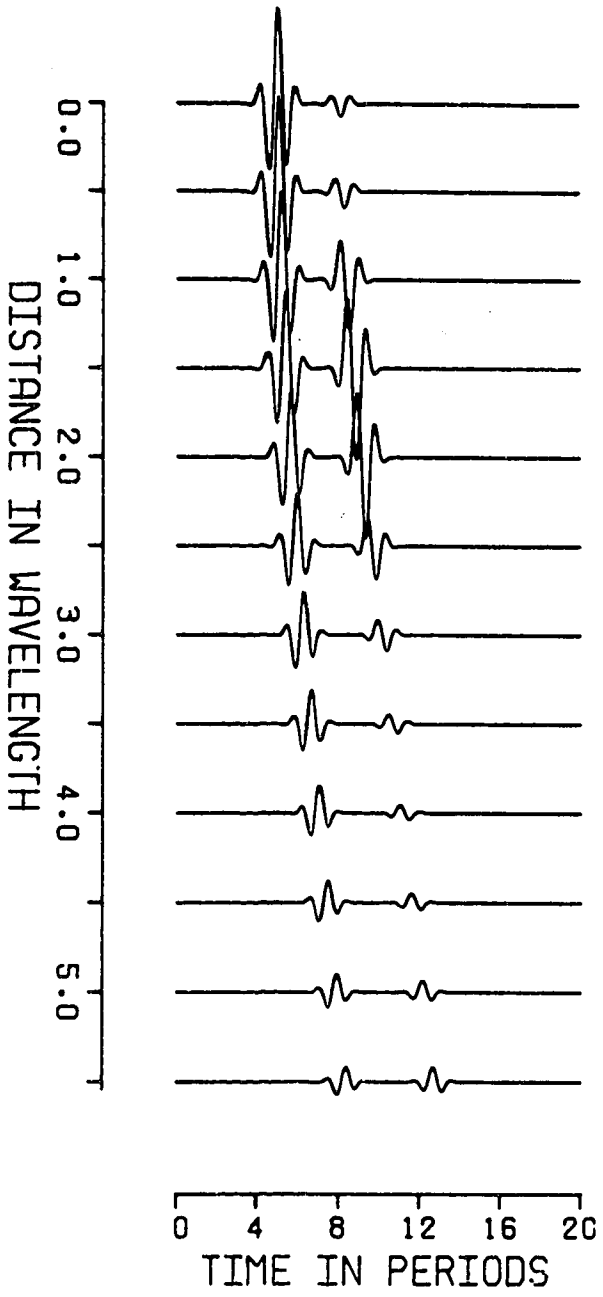

Figure 4.12 Vertical components computed using the formulae derived for the first order approximation of ART for Model #1. Vertical components of the displacement vector were computed for the depth z=3 WL at all epicentral distances. The P source was buried at the depth h=0.125 WL. The ratio of S to P velocities was taken to be β/α=0.5 .

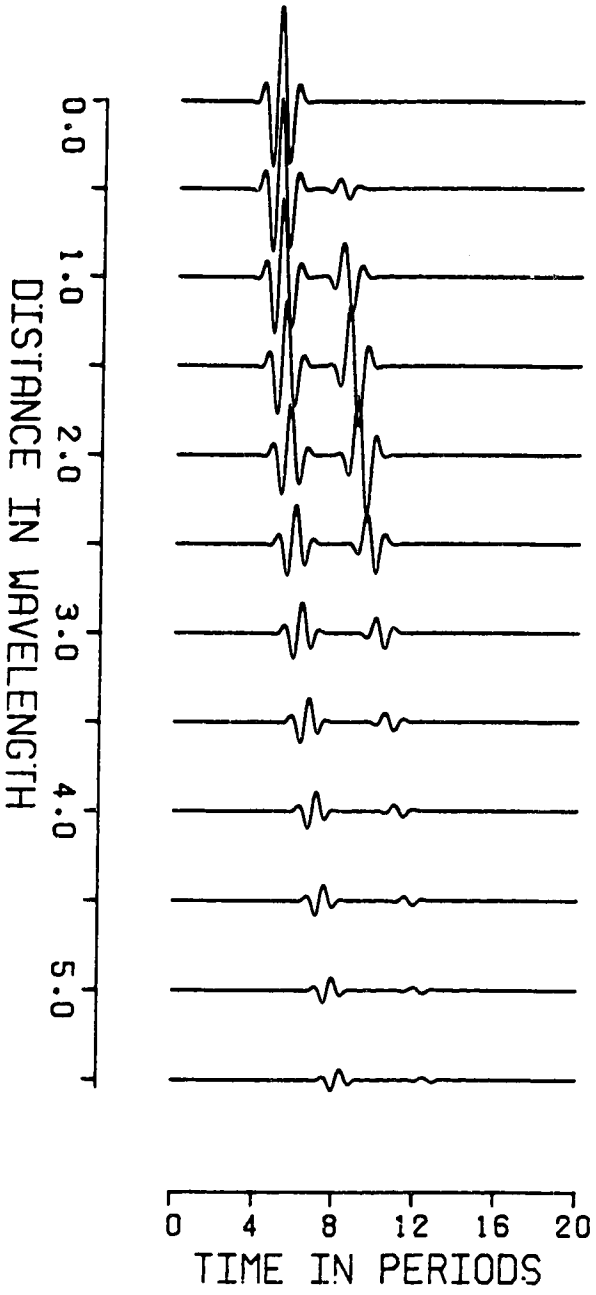

Figure 4.13 Vertical components computed using the zero order approximation of ART for Model #1. Vertical components of the displacement vector were computed for the depth z=3 WL at all epicentral distances. The P source was buried at the depth h=0.125 WL. The ratio of S to P velocities was taken to be β/α=0.5 .

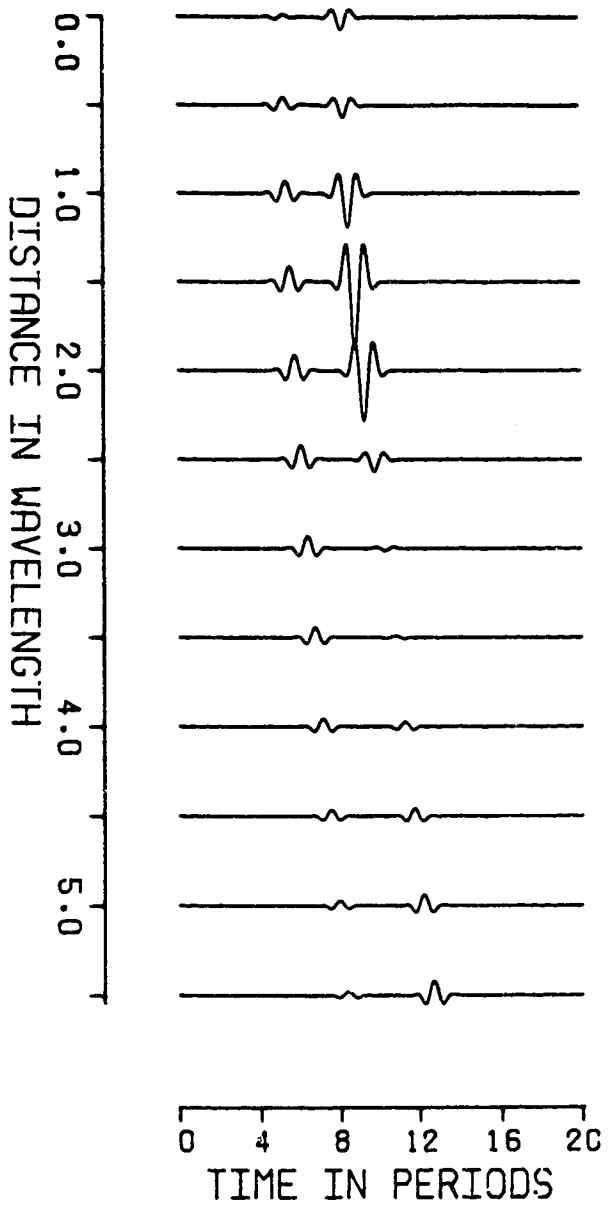

Figure 4.14 Vertical components including the effect of the first order term only in ART for Model #1. Vertical components of the displacement vector were computed for the depth z=3 WL at all epicentral distances. The P source was buried at the depth h=0.125 WL. The ratio of S to P velocities was taken to be β/α=0.5 .

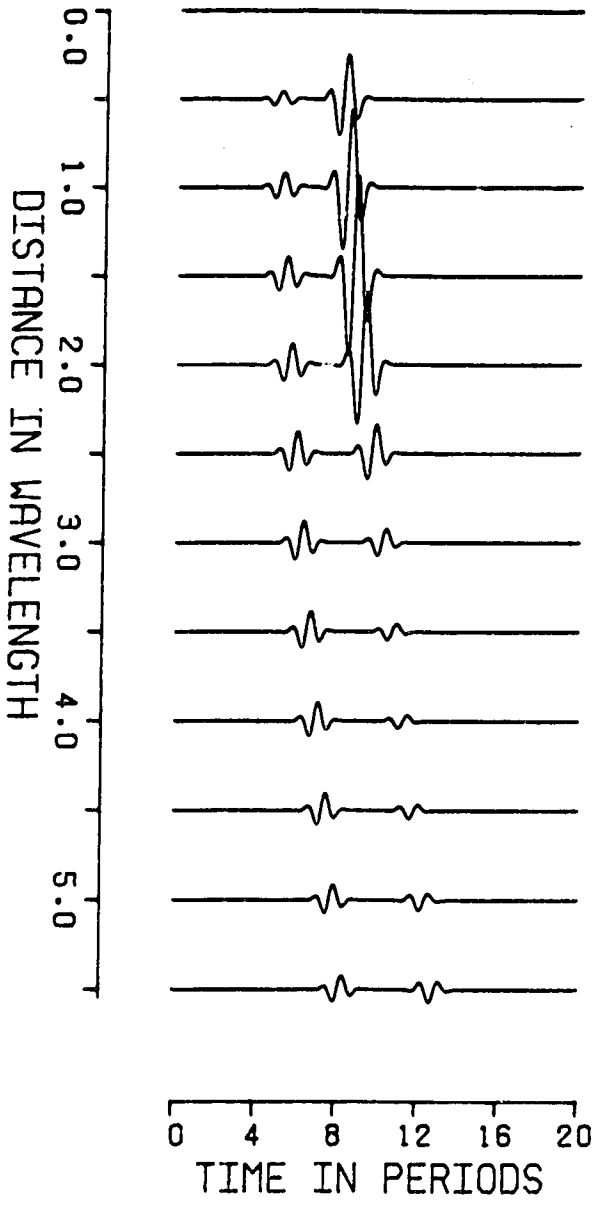

Figure 4.15 Horizontal components computed using the formulae derived for the first order approximation of ART for Model #1. Horizontal components of the displacement vector were computed for the depth z=3 WL at all epicentral distances. The P source was buried at the depth h=0.125 WL. The ratio of S to P velocities was taken to be $\beta/\alpha=0.5$.

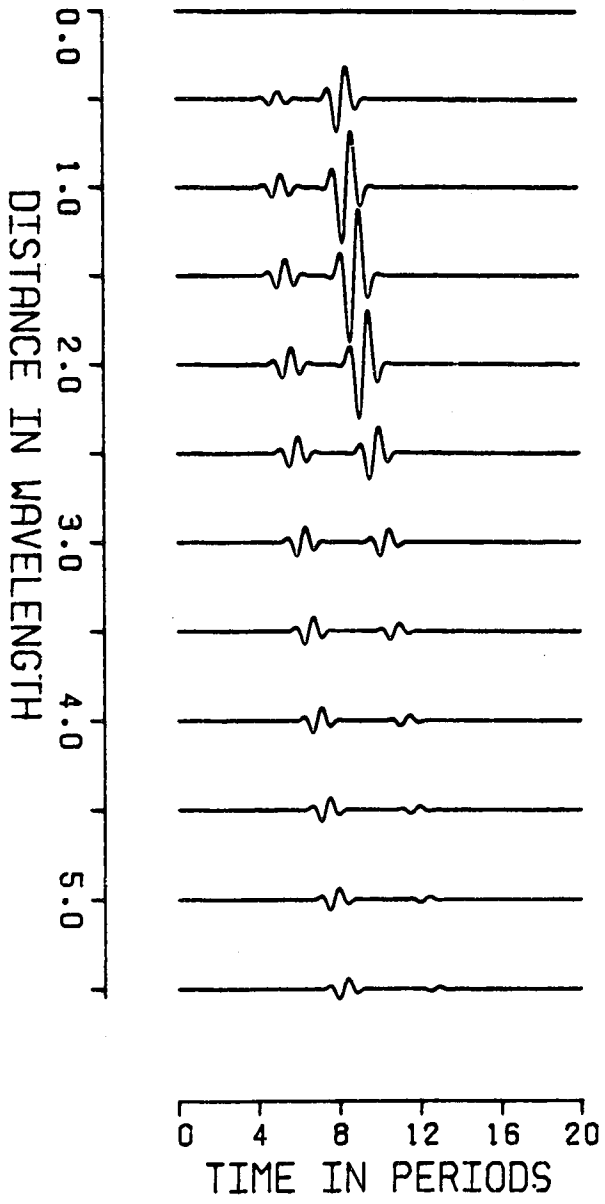

Figure 4.16 Horizontal components computed using the zero order approximation of ART for Model #1. Horizontal components of the displacement vector were computed for the depth z=3 WL at all epicentral distances. The P source was buried at the depth h=0.125 WL. The ratio of S to P velocities was taken to be β/α=0.5 .

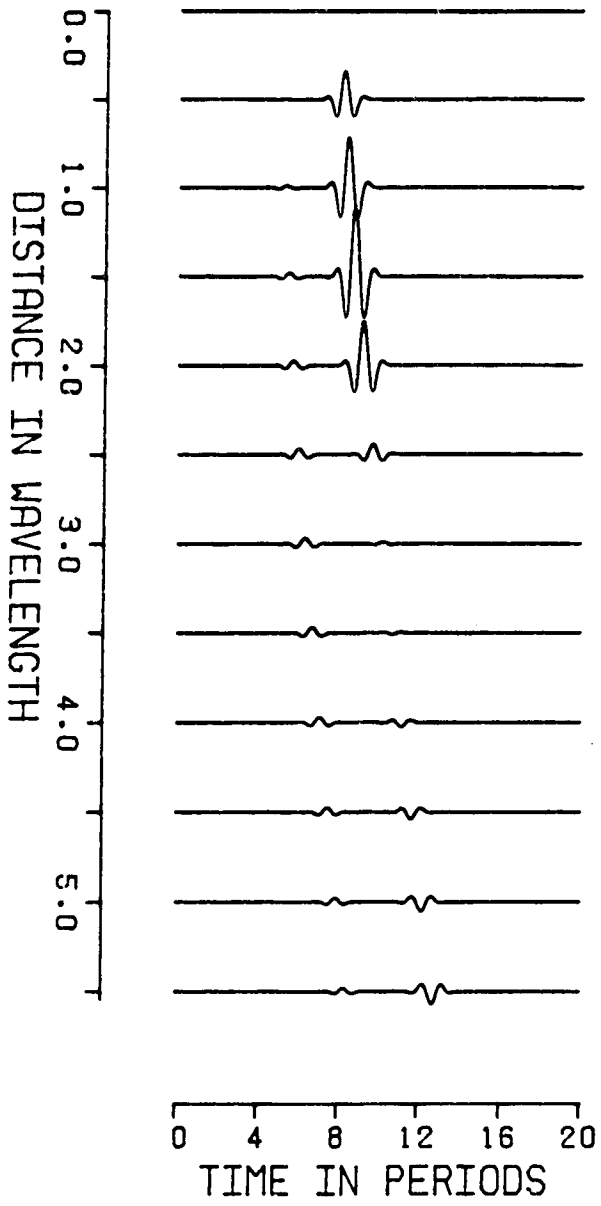

Figure 4.17 Horizontal components including the effect of the first order term only in ART for Model #1. Horizontal components of the displacement vector were computed for the depth z=3 WL at all epicentral distances. The P source was buried at the depth h=0.125 WL. The ratio of S to P velocities was taken to be $\beta/\alpha=0.5$.

From all of these figures we may once again reach the same conclusion as obtained before for case 1, that the first order effects have to be taken into consideration in the wave fields near vertical incidence.

It should be noticed that the nonzero effect of the converted PS wave in the normal incidence case is related to the source depth if we carefully study the results of the above two cases in model #1. Now we choose a set of different source depths in Model #1 and employ AMM and ART to investigate this case in detail.

All traces were computed for the same receiver location (x=0 WL, z=3 WL) but different source locations. The traces A, B, C and D in Figs. 4.18 to 4.21 correspond to the source depths 0.125 WL, 0.25 WL, 0.5 WL and 1.0 WL, respectively. Figure 4.18 shows the vertical components computed using the AMM, whereas Figure 4.19 gives the results of the first order approximation of ART. The results of the zero order approximation and the effect of the first order terms only of ART are shown in Figures 4.20 and 4.21, respectively.

Figure 4.21 shows that the smaller the source depth in model #1, the larger the nonzero vertical component of the converted PS wave reflected from the free surface. To more clearly express this phenomenon, a plot of the converted PS waves versus the source depth is displayed in Figure 4.22, in which the solid line indicates the first order effect only, while the dashed line the zeroth order effect.

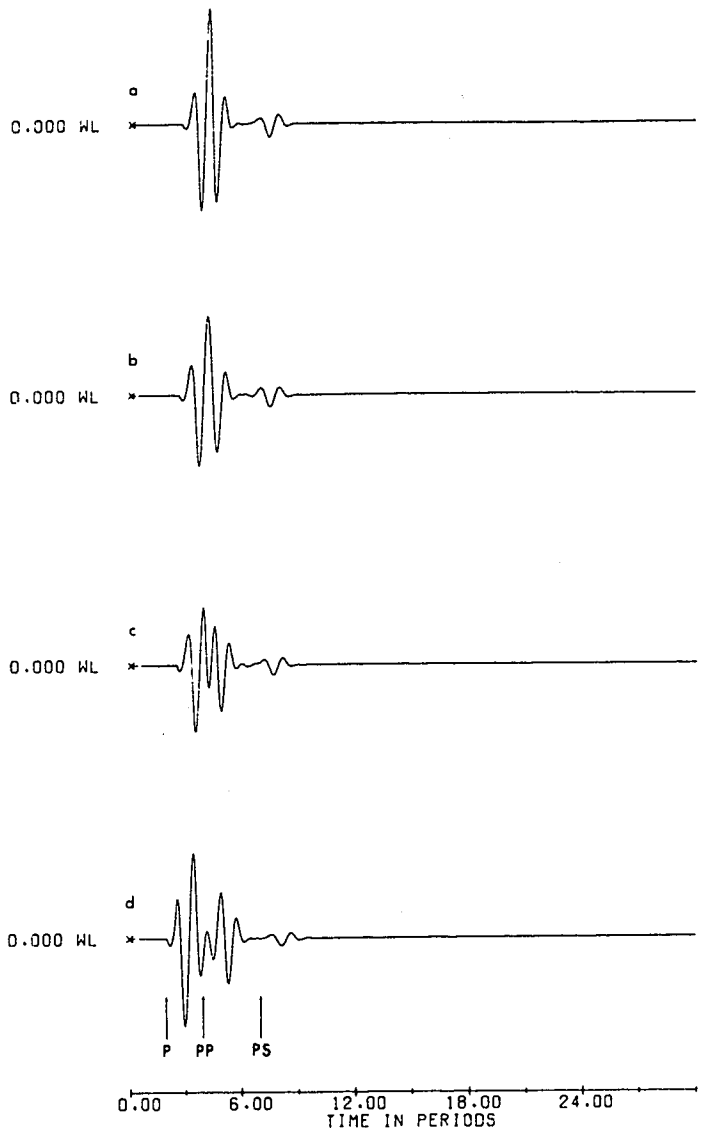

Figure 4.18 A nonzero vertical component of the converted PS wave reflected from the free surface at normal incidence computed by the Alekseev-Mikhailenko Method. All traces were computed for the same receiver location (x=0WL, z=3WL) but different source locations. The source depths corresponding to the individual traces from a to d were equal to 0.125WL, 0.25WL, 0.5WL, and 1.0WL, respectively.

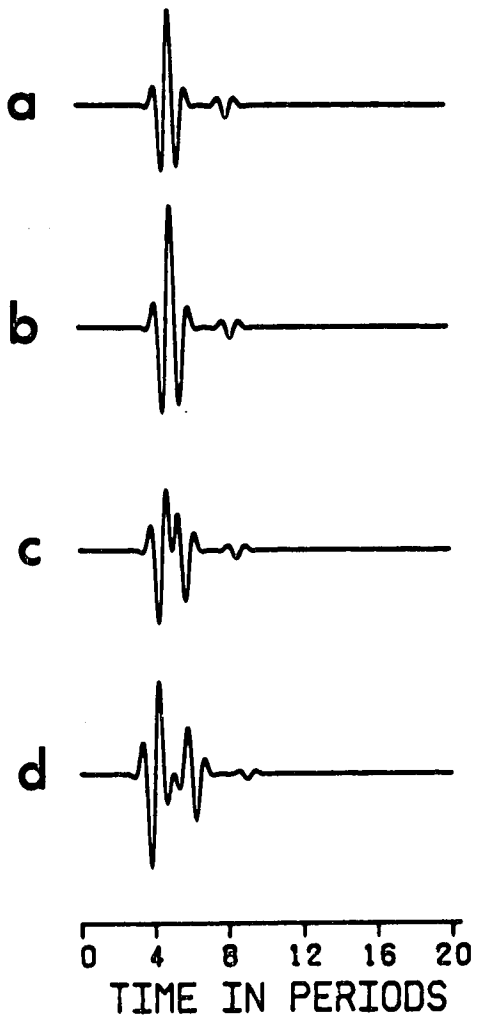

Figure 4.19 A nonzero vertical component of the converted PS wave reflected from the free surface at normal incidence computed by the first order approximation of ART. All traces were computed for the same receiver location (x=0WL, z=3WL) but different source locations. The source depths corresponding to the individual traces from a to d were equal to 0.125WL, 0.25WL, 0.5WL, and 1.0WL, respectively.

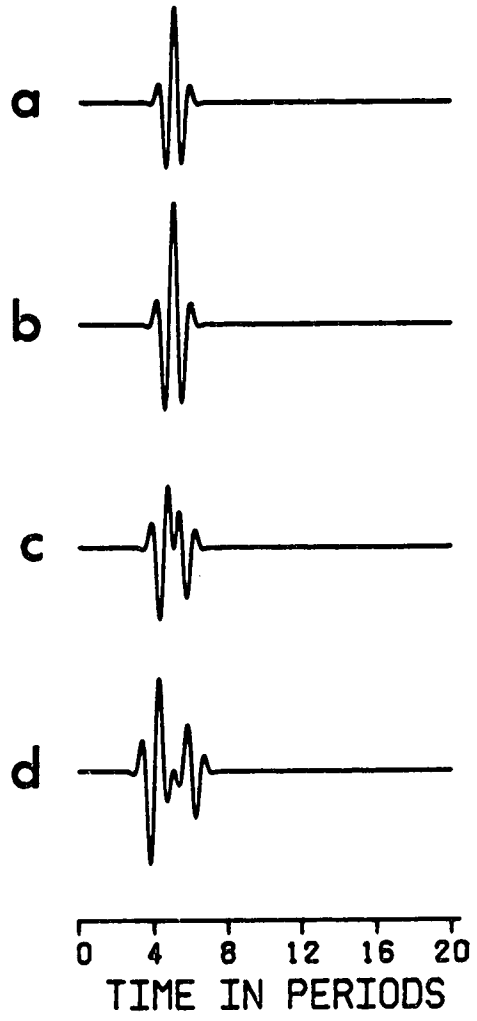

Figure 4.20 A zero vertical component of the converted PS wave reflected from the free surface at normal incidence computed by the zero order approximation of ART. All traces were computed for the same receiver location (x=0WL, z=3WL) but different source locations. The source depths corresponding to the individual traces from a to d were equal to 0.125WL, 0.25WL, 0.5WL, and 1.0WL, respectively.

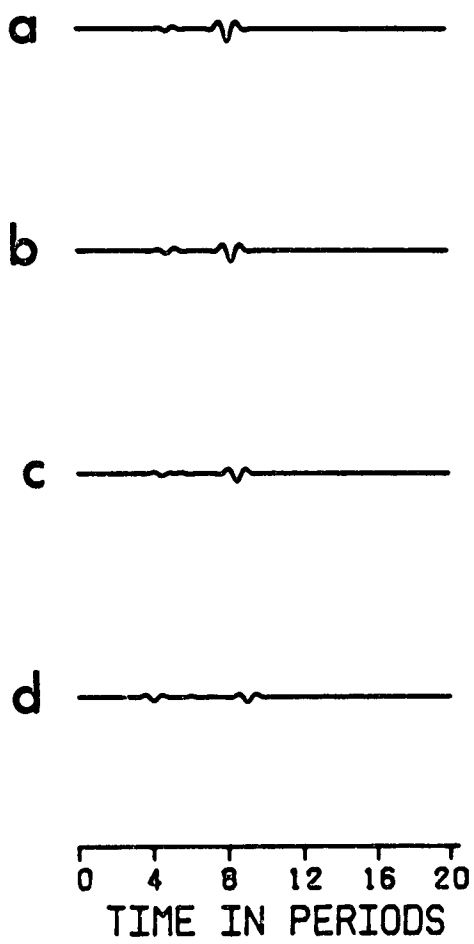

Figure 4.21 A nonzero vertical component of the converted PS wave reflected from the free surface at normal incidence computed by the only first order terms. All traces were computed for the same receiver location (x=0WL, z=3WL) but different source locations. The source depths corresponding to the individual traces from a to d were equal to 0.125WL, 0.25WL, 0.5WL, and 1.0WL, respectively.

We have seen from the above figures that the first order effect in Model #1 is related to the point source depth. In fact the higher order effect is also related to the medium in which the converted waves are propagating. Although this point of view has been mentioned before in Chapter 3, it could be more helpful to understand it if we considered a new example by investigating the relation between the first order effect and the velocity ratio $\Omega=\beta/\alpha$ in Model #1.

For this purpose we set the point source in Model #1 to be at a fixed depth (X=0WL, Z=0.125WL) and set the receivers all at the same depth of Z=3WL, whereas the velocity ratio Ω is varied from 0.2 to 0.7 by an increment 0.1. Graphically drawing the magnitudes of the zero order and the first order approximations versus the epicentral distances for each value of Ω (0.2, 0.3, 0.4, 0.5, 0.6 and 0.7) gives a set of 6 figures, which have been arranged in Figure 4.23. In Fig.4.23 the solid lines express the zeroth order magnitudes $PS^{(0)}(\iota)$, and the dashed lines the combined magnitudes of the zeroth order and the first order terms, which is mathematically equal to $PS^{(0)}(\gamma)$ + $[Ps^{(1)}(\gamma)^2+PS^{(1)}(\gamma)^2]^{1/2}/2\pi$.

Figure 4.23 generally indicates that the greater the velocity ratio $\Omega\equiv\beta/\alpha$, the greater the higher order effect.

So far a lot of attention has been paid in discussing the higher order effect for Model #1. Before ending this section some major conclusions should be summarized as follows:

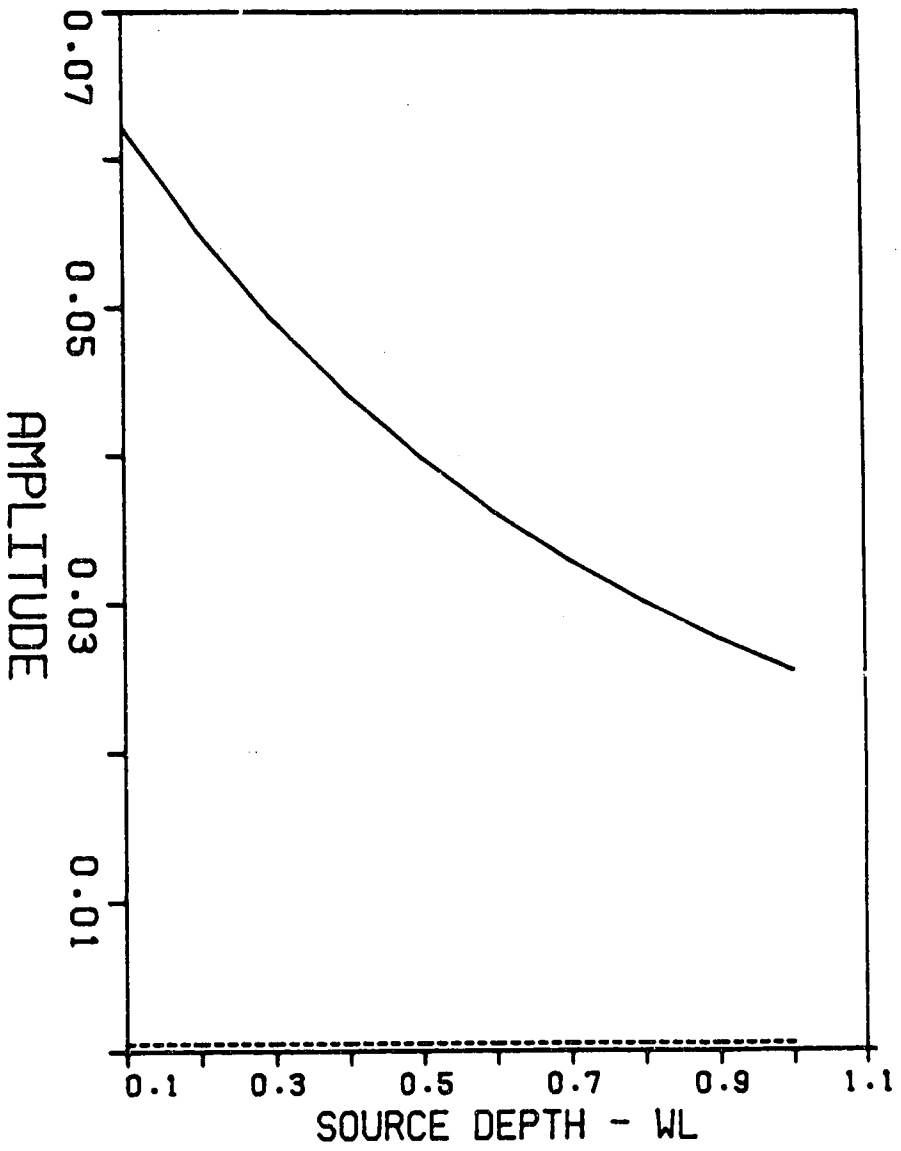

Figure 4.22 Relationship between the converted PS waves and source depths. The converted PS waves reflected from the free surface were computed for the same receiver location (x=0WL, z=3WL) but different source locations. The dashed line indicates the zero order effect, while the solid line the first order effect only.

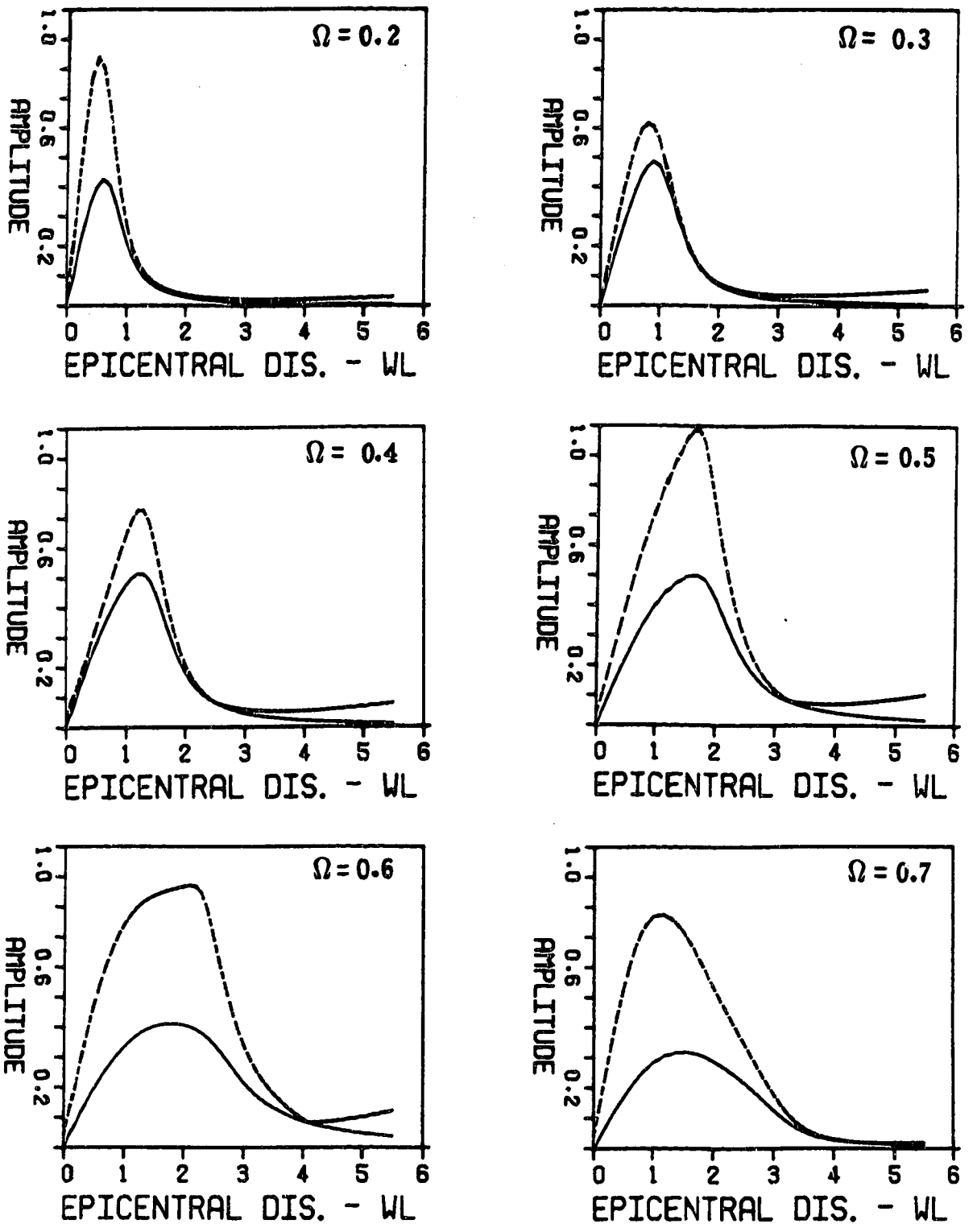

Figure 4.23 Relationship between magnitudes of converted PS waves and velocity ratios Ω. The solid and dashed lines indicate the zero and the first approximation, respectively.

(1) The first order approximation of ART can give a more acceptable result which is similar to AMM's for Model #1.

(2) The first order terms of ART should be considered in the computation of the reflected wave field in the region near the relection point.

(3) The shallower the source depth in Model #1, the larger the nonzero vertical component of the converted PS wave reflected at normal incidence on the free surface.

(4) The PS reflection response is strongly dependent on the velocity ratio Ω in such way that the larger the velocity ratio, the greater the first order effects.

4.4 Model #4 and Related synthetic Seismograms

In the synthetic seismograms computed using Alekseev-Mikhailenko Method (AMM) for Model #1, there are two interesting phenomena:

(1) There is a nonzero vertical component of the converted PS wave reflected at normal incidence from the free surface.

(2) At large epicentral distances we can see S* and PS wave are already well separated from one another.

Although the first phenomenon has been found in results computed using the first order approximation of ART, we have not found the S* wave in them at all. To more clearly show the first order effect and avoid the confusion due to S*

wave, a new model named Model #4 is introduced into this thesis (see Figure 4.24). In Model #4, both the source and receivers were set at depth 2.5 WL, as the S* arrival decays exponentially with the depth of the source (Hron and Mikhailenko, 1981; Daley and Hron, 1983a, b, 1985) and the direct P arrival does not make any contribution to the vertical components of the synthetic traces. The ratio of β/α was chosen as 0.6. The Model #4 chosen for discussion is similar to that used in the paper of Daley and Hron (1987), in which a high-frequency first order Saddle Point Approximation (SPA) was derived and used to compute the PP and PS reflected disturbance. The main purpose of introducing Model #4 is to produce synthetic seismograms computed using three different approaches (AMM, SPA and ART) for the same model. It should be helpful to confirm some conclusions we have obained in the last section.

The time dependence of the source pulse used in all synthetic seismogram computations is

$$
\begin{aligned}
f_0(t) &= \exp[-(2\pi\nu t/\gamma)^2]\cos(2\pi\nu t) \\
g_0(t) &= -\exp[-(2\pi\nu t/\gamma)^2]\sin(2\pi\nu t) \\
f_1(t) &= \exp[-(2\pi\nu t/\gamma)^2]\sin(2\pi\nu t)/(2\pi\nu) \\
g_1(t) &= \exp[-(2\pi\nu t/\gamma)^2]\cos(2\pi\nu t)/(2\pi\nu)
\end{aligned}
\tag{4.58}
$$

where the predominant frequency ν of the source pulse was chosen as 1.0 and the damping factor γ was chosen as 4.

It should also be mentioned that there is no contribution from the direct P arrival to the vertical

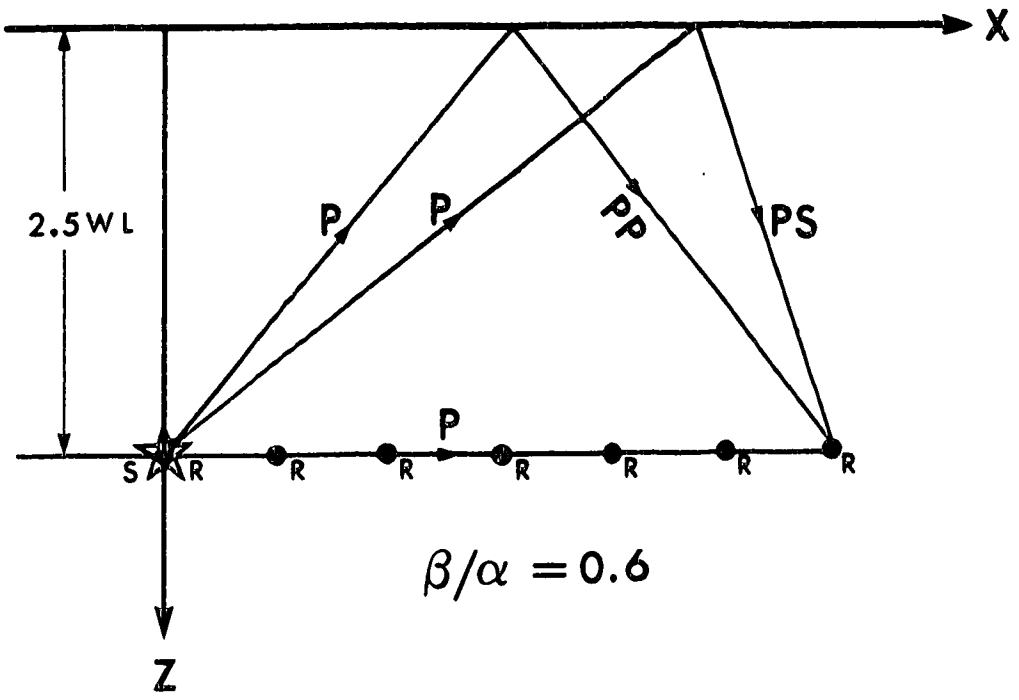

Figure 4.24 Model #4. Both the source and receivers were chosen at depth 2.5WL, such that both effects of the S* wave and the direct P arrival on the vertical direction can be neglected.

component of displacement, so that only this case will be considered for Model #4 in this section.

A comparison of zero order Asymptotic Ray Theory synthetic traces (a), traces computed using the Saddle Point Approximation (SPA) for the first order correction (b), and the Alekseev-Mikhailenko Method (AMM) traces (c) for Model #4 is presented in Figure 4.25. The synthetic traces computed using the formulae for the first order approximation of ART derived in this thesis are presented in Figure 4.26, whereas the zero order ART synthetic traces are shown in Figure 4.27. The effect of the first order approximation is well demonstrated, as there is a very good match with the AMM's and the first order SPA's results.

From this set of synthetic seismograms we may once again understand that if the first order terms in ART are considered into the synthetic seismogram computation, the results will be much better, although the zero order terms are usually reasonably accurate results at all offsets.

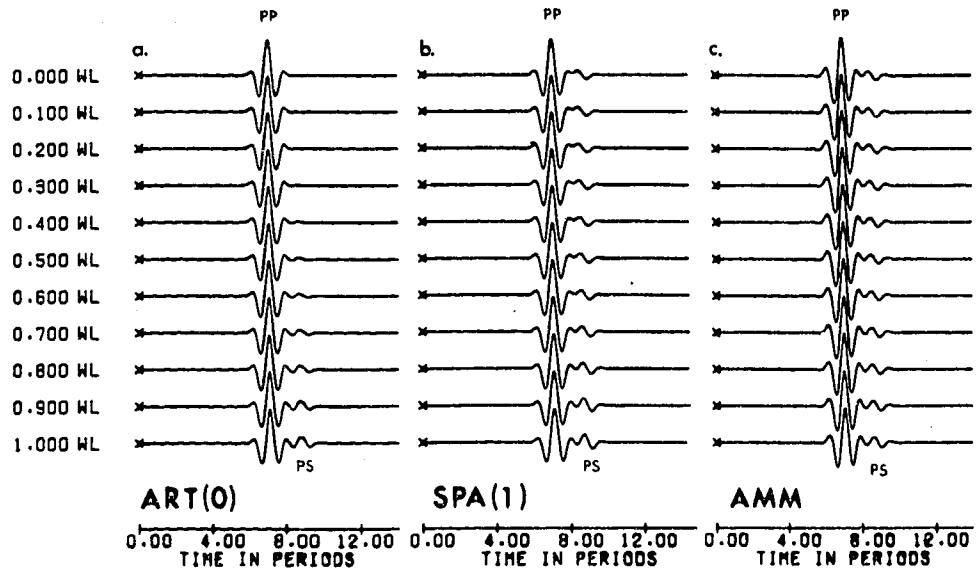

Figure 4.25 A comparison of zero order ART synthetic traces (a), traces computed using the Saddle Point Approximation (SPA) for the first order correction (b), and Alekseev-Mikhailenko Method (AMM) traces (c) for Model #4. Only the PP and PS arrivals are present here, and WL = wavelength (with author's permission).

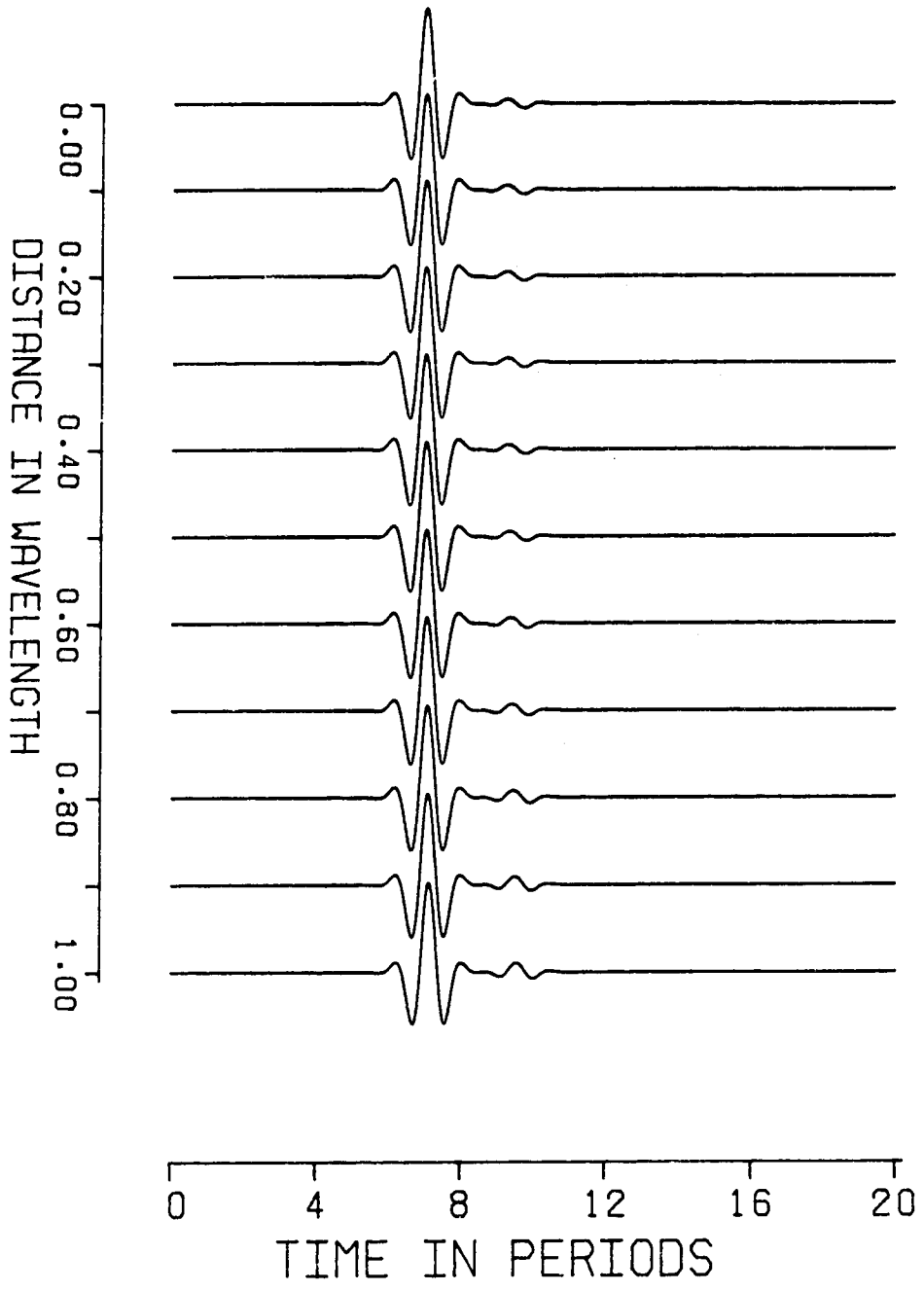

Figure 4.26 Vertical components computed using the first order approximation of ART for Model #4.

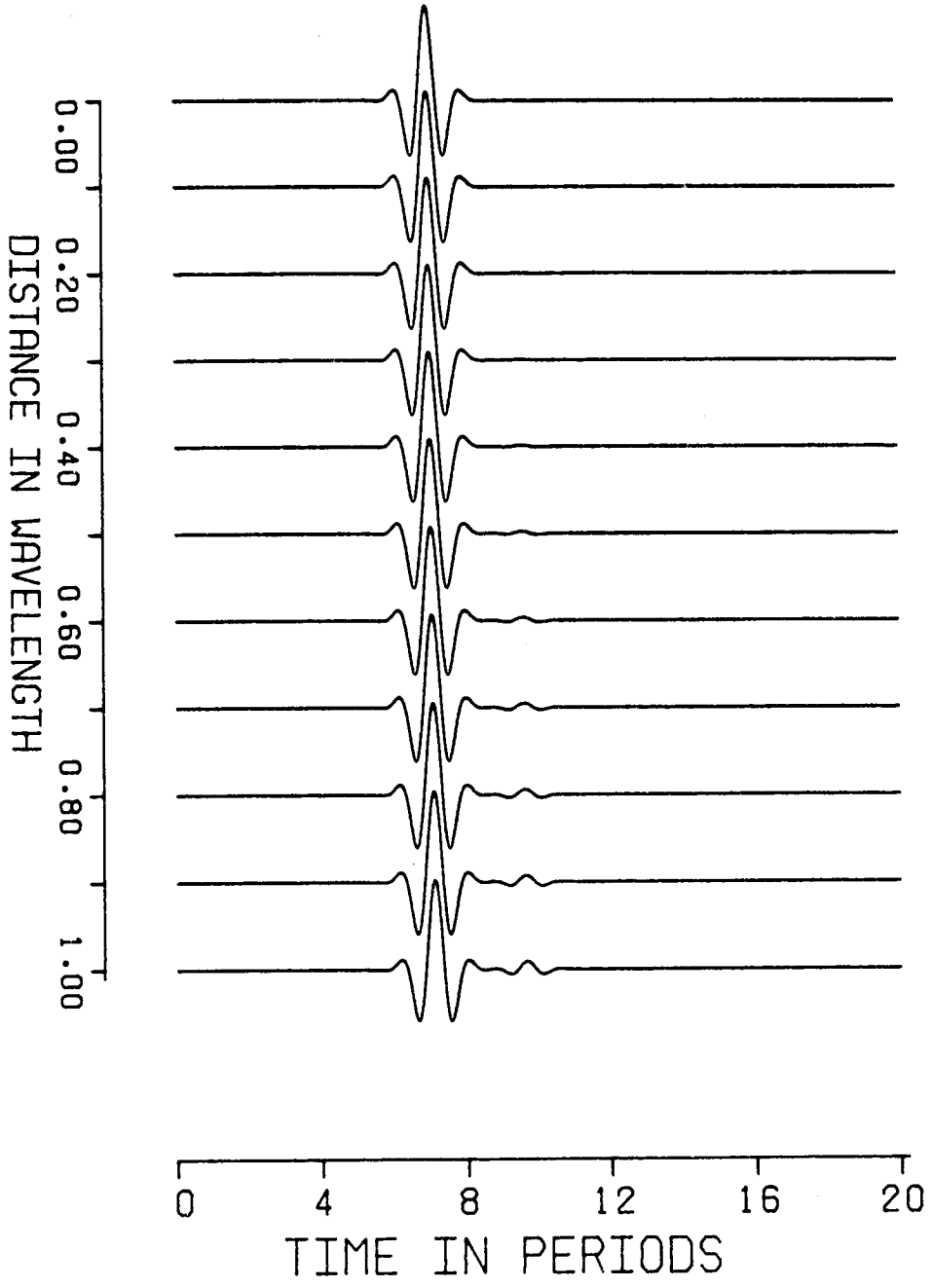

Figure 4.27 Vertical components computed using the zero order approximation of ART for Model #4.

4.5 Model #5 and Related Seismograms for the Transmitted Waves

In this section, we benefit from the high accuracy of the Alekseev-Mikhailenko Method against which we will check the suitability of our first order approximation of ART to the transmitted PP and PS arrivals due to highly concentrated sources adjacent to interfaces between elastic media. More precisely, we will investigate a case of a P wave point explosive source located less than onehalf of a predominant wavelength from the interface in a medium, whose compressional (P) and shear (S) velocities are higher than those on the other side of the interface, where a receiver is located. We will call it as Model #5 in this thesis (see Figure 4.28).

Since our investigations are based on the method discussed in great detail in earlier sections, we will restrict ourself to the discussion of results produced in our numerical experiments. A brief derivation will be presented for our first order approximation of ART to a wave field transmitted across a plane interface from a high-velocity elastic half-space into a medium of lower velocity, after being radiated from a point explosive source adjacent to the interface.

In Figure 4.28, a cylindrical coordinate system (r,ϕ,z) is centered at the point O directly below the impulsive point source situated at $S = (0,0,-h_1)$ in the upper

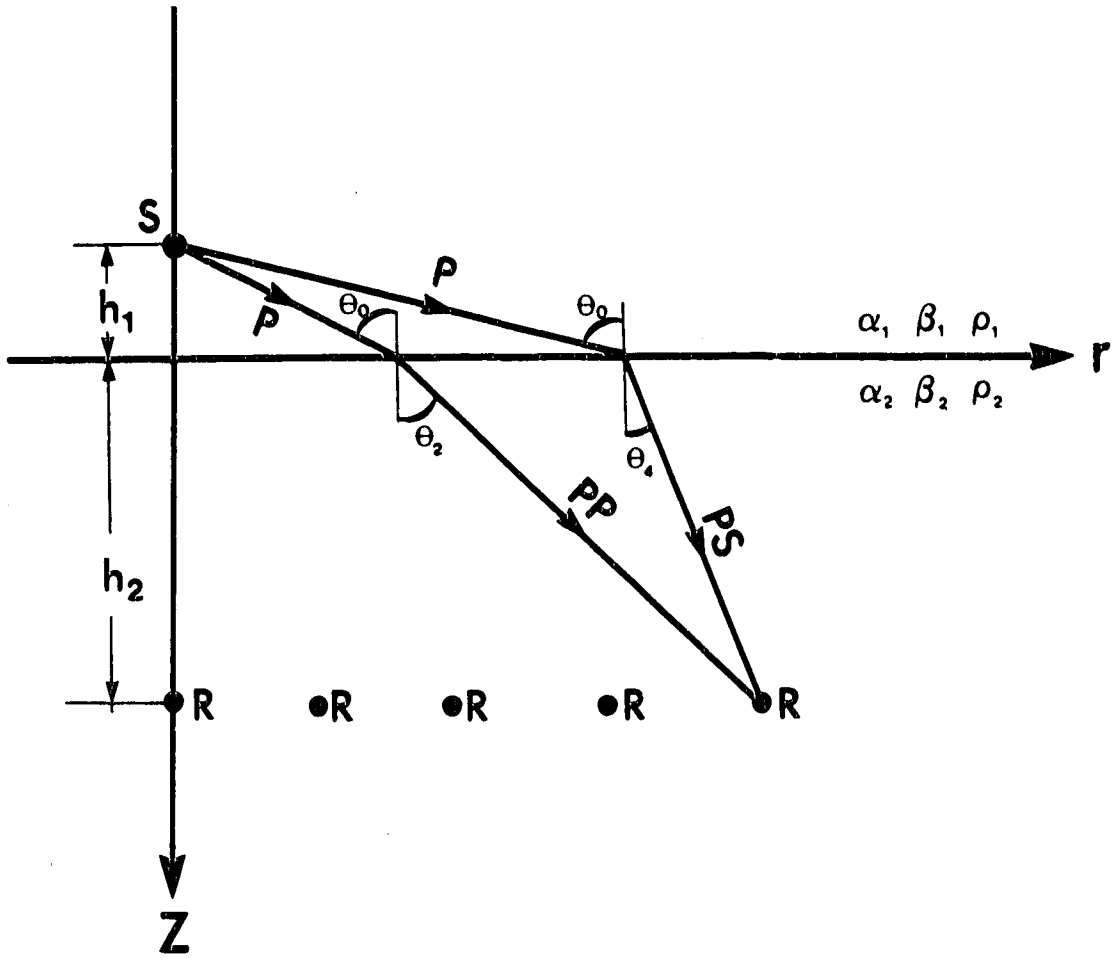

Figure 4.28 Model #5. A cylindrical coordinate system (r,ϕ,z) is centered at the point O directly below the impulsive point source situated at $S = (0,0,-h_1)$ in the upper half-space medium. The properties of the upper (medium 1) and lower (medium 2) media are characterized by α_i, the compressional velocity, β_i, the shear velocity and ρ_i, the volume density (i=1,2). The total transmitted wave field will be evaluated at the receiver location in the lower half-space (medium 2) at point $R = (r,0,h_2)$. α_1=1.3355 WL/T, β_1=0.771 WL/T, α_2=1.000 WL/T, β_2=0.577 WL/T, $\rho_1=\rho_2$=1.0 gm/cc, h_1=0.25 WL and h_2=5.0 WL.

half-space medium. The properties of the upper (medium 1) and lower (medium 2) media are characterized by α_i, the compressional velocity, β_i, the shear velocity and ρ_i, the volume density (i=1,2). The total transmitted wave field will be evaluated at the receiver location in the lower half-space (medium 2) at point R = $(r,0,h_2)$. Further, it will be assumed that $\alpha_1 > \alpha_2 > \beta_1 > \beta_2$ and that the depth of the source h_1 amounts to only a fraction of the predominant wavelength of the source pulse.

We shall evaluate the zero order approximation of ART for the transmitted PP and PS waves first in Model #5. Taking k=0 in the general boundary conditions (4.18-1), (4.18-2), (4.18-3) and (4.18-4) finally yields the following set of equations as the zero order boundary conditions:

$$\sin\theta_1 P_1^{(0)} - \sin\theta_2 P_2^{(0)} + \cos\theta_3 S_3^{(0)} - \cos\theta_4 S_4^{(0)} = -\sin\theta_0 P_0^{(0)}$$

$$\cos\theta_1 P_1^{(0)} + \cos\theta_2 P_2^{(0)} - \sin\theta_3 S_3^{(0)} - \sin\theta_4 S_4^{(0)} = \cos\theta_0 P_0^{(0)}$$

(4.59)

$$\beta_1\Omega\sin2\theta_1 P_1^{(0)} + \beta_2\Omega\sin2\theta_2 P_2^{(0)} + \beta_1\cos2\theta_3 S_3^{(0)} + \beta_2\cos2\theta_4 S_4^{(0)} = \beta_1\Omega\sin2\theta_0 P_0^{(0)}$$

$$(2\Omega\beta_1\sin^2\theta_1-\alpha_1)P_1^{(0)} + (\alpha_2-2\Omega\beta_2\sin^2\theta_2)P_2^{(0)} + \beta_1\sin2\theta_3 S_3^{(0)} - \beta_2\sin2\theta_4 S_4^{(0)} = (\alpha_1-2\Omega\beta_1\sin^2\theta_0)P_0^{(0)}$$

where Ω, the ratio of β/α.

Solving the above set of equations will produce the values of the zero order reflected and transmitted waves at the point of incidence on the interface boundary, $P_i^{(0)}(\iota_0)$,

$S_3^{(0)}(\iota_0)$, $P_2^{(0)}(\iota_0)$ and $S_4^{(0)}(\iota_0)$.

The transmitted PP and PS waves in the zero order approximation, $P_2^{(0)}(r)$ and $S_4^{(0)}(r)$, are determined by the following formulas gived by Cerveny and Ravindra (1971):

$$P_2^{(0)}(r) = \frac{P_2^{(0)}(\iota_0)\ \iota_0}{L_{02}(r)}$$

(4.60)

$$S_4^{(0)}(r) = \frac{S_4^{(0)}(\iota_0)\ \iota_0}{L_{04}(r)}$$

where $L_{02}(r)$ and $L_{04}(r)$ indicate the geometrical spreadings of the transmitted PP and PS waves, respectively.

$$L_{02}(r) = \frac{\cos\theta_0}{\alpha_1}\left[\left(\frac{\alpha_1 h_1}{\cos\theta_0} + \frac{\alpha_2 h_2}{\cos\theta_2}\right)\left(\frac{\alpha_1 h_1}{\cos^3\theta_0} + \frac{\alpha_2 h_2}{\cos^3\theta_2}\right)\right]^{1/2}$$

(4.61)

$$L_{04}(r) = \frac{\cos\theta_0}{\alpha_1}\left[\left(\frac{\alpha_1 h_1}{\cos\theta_0} + \frac{\beta_2 h_2}{\cos\theta_4}\right)\left(\frac{\alpha_1 h_1}{\cos^3\theta_0} + \frac{\beta_2 h_2}{\cos^3\theta_4}\right)\right]^{1/2}$$

Now let us investigate the first order approximation of the tansmitted waves. The principal component of the first order incidence P wave, $P_0^{(1)}(r)$, is similar to (4.32) as follows:

(4.62) $\quad P_0^{(1)}(r) = (1-2\Omega^2)\ \alpha\ P_0^{(0)}(r)\ /\ r$

The additional component of the first order incidence P wave is similar to (4.33) as follows:

(4.63) $\quad p_0^{(1)}(r) = 0$

To determine the first order terms for the transmitted PS wave, we have to evaluate $\nabla\cdot\hat{e}_{=(4)}$ and $\nabla\cdot\hat{e}_{+(4)}$ on the transmitted wavefront surfaces, where $\hat{e}_{=(4)}$ and $\hat{e}_{+(4)}$ are the unit vectors along the rays and in the plane normal to the rays for the transmitted PS wave, respectively. The wavefront surfaces of the transmitted PS wave in three dimensional space may be expressed in a special transformed coordinate system (Γ_4,θ_4,ψ) in the following way (see Figure 4.29):

$$
\begin{aligned}
X &= \cos\psi\,\sin\theta_4\,\Gamma_4 \\
Y &= \sin\psi\,\sin\theta_4\,\Gamma_4 \\
Z &= \cos\theta_4\Gamma_4 - h_1\cos\theta_4/[\Lambda^2-\sin^2(\theta_4)]^{1/2}
\end{aligned}
\tag{4.64}
$$

where $\Lambda \equiv \beta_2/\alpha_1$. Lame's coefficients according to the above transformed system are:

$$
\begin{aligned}
H(\Gamma_4) &= 1 \\
H(\psi) &= \sin(\theta_4)\,\Gamma_4 \\
H(\theta_4) &= \left[\Gamma_4^2+\frac{[h_1\sin\theta_4(1-\Lambda^2)]^2}{(\Lambda^2-\sin^2\theta_4)^3}+\frac{2h_1\Gamma_4\sin^2\theta_4(1-\Lambda^2)}{(\Lambda^2-\sin^2\theta_4)^{3/2}}\right]^{1/2}
\end{aligned}
\tag{4.65}
$$

Then it is easy to show that:

$$
\begin{aligned}
\hat{e}_{=(4)} &= (e(\Gamma_4),e(\theta_4),e(\psi)) = (1,0,0) \\
\hat{e}_{+(4)} &= (e(\Gamma_4),e(\theta_3),e(\psi)) = (0,1,0)
\end{aligned}
\tag{4.66}
$$

Finally we have the following expressions necessary to compute the transmitted PS wave:

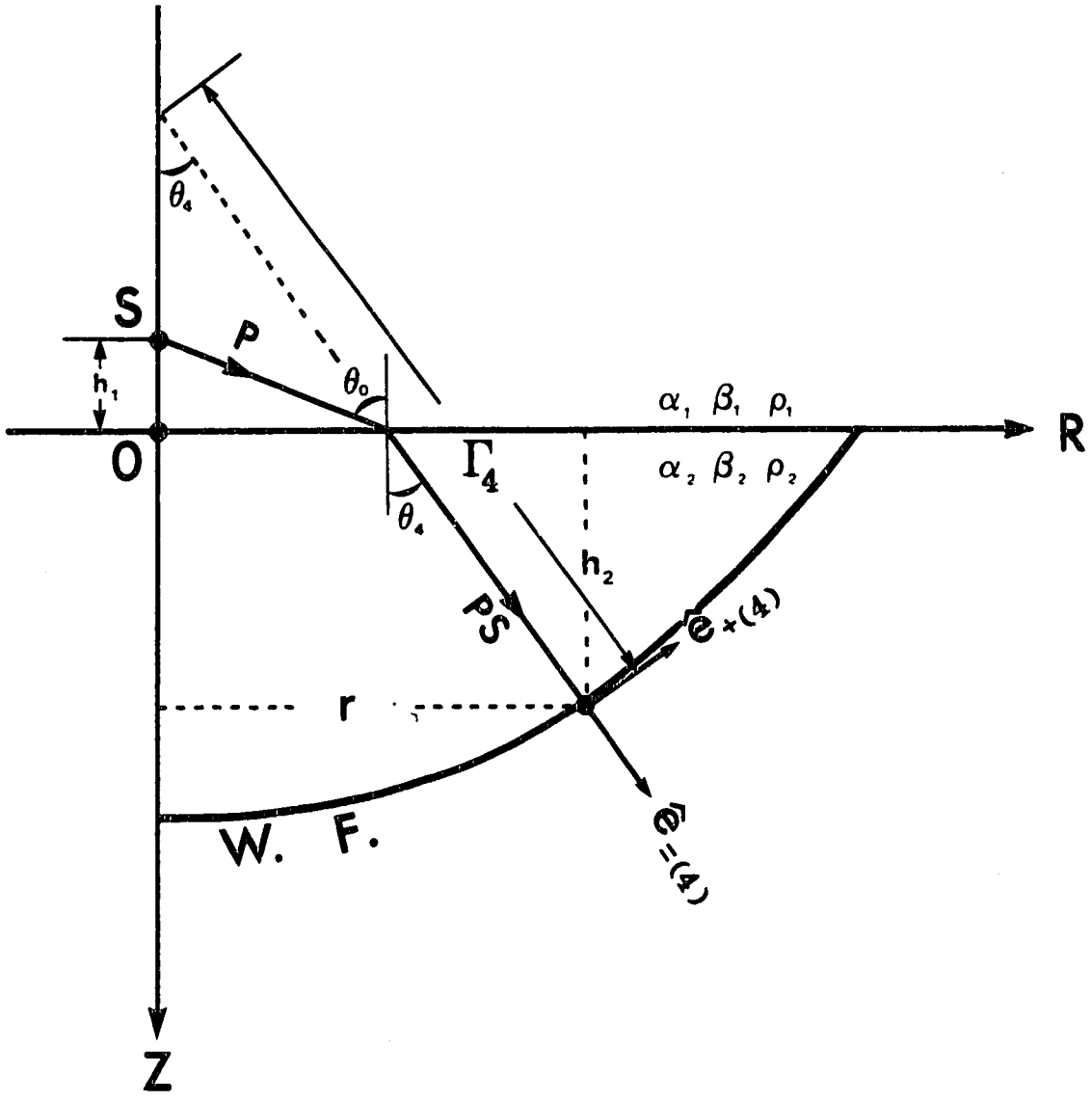

Figure 4.29 Signs and notation used to evaluate $\nabla\cdot\hat{e}_{-(4)}$ and $\nabla\cdot\hat{e}_{+(4)}$ for the transmitted PS wave in Model #5.

$$
\begin{aligned}
\nabla\cdot\hat{e}_{=(4)} &= \frac{1}{\Gamma_4} + \frac{\Gamma_4 + C\sin\theta_4}{(\Gamma_4^2+C^2+2\Gamma_4 C\sin\theta_4)} \\
\nabla\cdot\hat{e}_{+(4)} &= \frac{\cot an\theta_4}{(\Gamma_4^2+C^2+2\Gamma_4 C\sin\theta_4)^{1/2}}
\end{aligned}
\tag{4.67}
$$

where

$$
C \equiv \frac{h_1\sin\theta_4(1-\Lambda^2)}{(\Lambda^2-\sin^2\theta_4)^{3/2}} \qquad \Gamma_4 \equiv \frac{h_1\tan\theta_0}{\sin\theta_4} + \frac{h_2}{\cos\theta_4} \tag{4.68}
$$

Based on the similarity between the transmitted PS and PP wavefront surfaces, we are able to write the following expressions for the transmitted PP waves:

$$
\begin{aligned}
\nabla\cdot\hat{e}_{=(2)} &= \frac{1}{\Gamma_2} + \frac{\Gamma_2 + D\sin\theta_2}{(\Gamma_2^2+D^2+2\Gamma_2 D\sin\theta_2)} \\
\nabla\cdot\hat{e}_{+(2)} &= \frac{\cot an\theta_2}{(\Gamma_2^2+D^2+2\Gamma_2 D\sin\theta_2)^{1/2}}
\end{aligned}
\tag{4.69}
$$

where

$$
D \equiv \frac{h_1\sin\theta_2(1-\Pi^2)}{(\Pi^2-\sin^2\theta_2)^{3/2}} \qquad \Gamma_2 \equiv \frac{h_1\tan\theta_0}{\sin\theta_2} + \frac{h_2}{\cos\theta_2} \tag{4.70}
$$

with $\Pi \equiv \alpha_2/\alpha_1$.

The additional components of the first order transmitted PS and PP waves then can be presented from their general formula (2.32) and (2.34) as follows:

$$
\begin{aligned}
s_4^{(1)}(\gamma) &= \beta\, S_4^{(0)}(\gamma)\, \nabla\cdot\hat{e}_{+(4)} \\
p_2^{(1)}(\gamma) &= 0
\end{aligned}
\tag{4.71}
$$

To determine the principal component of the first order transmitted PS wave, substituting (4.67) into its general expression (2.55) yields the following differential equation:

$$(4.72)\qquad \frac{dS_4^{(1)}(r)}{dr} = -S_4^{(1)}(r)\frac{\nabla\cdot\hat{e}_{=(4)}}{2} + \frac{d^2S_4^{(0)}(r)}{dr^2}\frac{\beta_2}{2}$$

The general solution of the above differential equation can be obtained after some integrating operations as:

(4.73)

$$S_4^{(1)}(\gamma) = [S_4^{(1)}(\iota_0) + S_4^{(0)}(\iota_0)\frac{\beta_2(E+F)}{4EF}]\cdot\frac{[F(F^2+2FH+C^2)^{1/2}]^{1/2}}{RCR}$$

$$+ S_4^{(0)}(\iota_0)\frac{\beta_2(EF)^{1/2}}{4}\cdot[\frac{IPS}{2RCR} - \frac{F+E+2r}{[(E+r)(F+r)]^{1/2}}]$$

where

$$RCR = \{(F+r)[(F+r)^2+2(F+r)H+C^2]^{1/2}\}^{1/2}$$

$$PCP = (RCR)\cdot[(F+r)^2+2(F+r)H+C^2]^{1/2}$$

$$IPS = \int \frac{(F+E+2r)}{[(E+r)(F+r)]^{3/2}}\cdot\frac{2(F+r)^2+3H(F+r)+C^2}{PCP}\,dr$$

$$F = \frac{\alpha_1\iota_0}{\beta_2}$$

$$E = F\frac{\cos^2\theta_4}{\cos^2\theta_0}$$

$$H = C\sin\theta_4$$

and C given in (4.68).

Here $\gamma \equiv \iota_0+r$ denotes the total length of the transmitted PS ray from the source point to the receiver via the transmitted point, and $S_4^{(1)}(\iota_0)$ the principal component of the first order transmitted PS wave at the transmitted point which will be determined later by using the first order boundary conditions.

When the incident P wave is perpendicular to the free surface, or equivalently when $\theta_0=\theta_4=0$, the principal component of the first order transmitted PS wave is given by:

$$(4.74)\quad S_4^{(1)}(\gamma) = S_4^{(0)}(\iota_0)\beta_2\cdot\left[\frac{1}{F+r} - \frac{F}{(F+r)^2}\right] + S_4^{(1)}(\iota_0)\,\frac{F}{F+r}$$

To determine the principal component of the first order transmitted PP wave, substituting (4.69) into its general expression (2.43) yields the following differential equation:

$$(4.75)\quad \frac{dP_2^{(1)}(r)}{dr} = -P_2^{(1)}(r)\frac{\nabla\cdot\hat{e}_{=(2)}}{2} + \frac{d^2P_2^{(0)}(r)}{dr^2}\cdot\frac{\alpha_2}{2} +$$

$$+ \frac{dP_2^{(0)}(r)}{dr}\cdot\frac{\alpha_2^2-\beta_2^2}{2\alpha_2}\nabla\cdot\hat{e}_{=(2)} + P_2^{(0)}(r)\,\frac{\alpha_2^2-\beta_2^2}{2\alpha_2}\cdot\frac{d(\nabla\cdot\hat{e}_{=(2)})}{dr}$$

The general solution of the above differential equation can be obtained after some tedious integrating operations as:

(4.76)

$$P_2^{(1)}(\gamma) = \left[P_2^{(1)}(\iota_0)+P_2^{(0)}(\iota_0)\frac{\alpha_2(E+F)}{4EF}\right]\frac{[F(F^2+2FI+D^2)^{1/2}]^{1/2}}{RDR} +$$

$$+ P_2^{(0)}(\iota_0)\frac{\alpha_2(EF)^{1/2}}{4}\left[\frac{IPA}{2RDR} - \frac{(F+E+2r)}{[(E+r)(F+r)]^{3/2}}\right] +$$

$$- P_2^{(0)}(\iota_0)\frac{\alpha_2^2-\beta_2^2}{4\alpha_2}\cdot\frac{(EF)^{1/2}}{RDR}(IPB + IPC - 2IPD + 2IPE + 4IPF)$$

where

$$RDR = \{(F+r)[(F+r)^2+2(F+r)I+D^2]^{1/2}\}^{1/2}$$

$$RER = [(F+r)^2+2(F+r)I+D^2]^{1/2}$$

$$IPA = \int \frac{(F+E+2r)}{[(E+r)(F+r)]^{3/2}}\cdot\frac{2(F+r)^2+3I(F+r)+D^2}{RDR\cdot RER}\,dr$$

$$IPB = \int \frac{(F+E+2r)}{[(E+r)(F+r)]^{3/2}}\cdot\frac{RDR}{F+r}\,dr$$

$$IPC = \int \frac{(F+E+2r)}{[(E+r)(F+r)]^{3/2}}\cdot\frac{(F+r+I)(F+r)^{1/2}}{RER^{3/2}}\,dr$$

$$IPD = \int \frac{1}{(E+r)^{1/2}}\cdot\frac{1}{(RER)^{3/2}}\,dr$$

$$IPE = \int \frac{1}{[(E+r)(F+r)]^{1/2}}\cdot\frac{(RER)^{1/2}}{(F+r)^{3/2}}\,dr$$

$$IPF = \int \frac{(F+r+I)^2}{(E+r)^{1/2}}\cdot\frac{1}{(RER)^{7/2}}\,dr$$

$$F = \frac{\alpha_1 \iota_0}{\alpha_2}$$

$$E = F \frac{\cos^2\theta_2}{\cos^2\theta_0}$$

$$I = D \sin\theta_4$$

and D given in (4.70).

Here $\gamma \equiv \iota_0+r$ denotes the total length of the transmitted PP ray from the source point to the receiver via the transmitted point, $P_2^{(1)}(\iota_0)$ the principal component of the first order transmitted PP wave at the transmitted point which will be determined by using the first order boundary conditions later.

When the incident P wave is perpendicular to the free surface, or equivalently when $\theta_0=\theta_2=0$, the principal component of the first order transmitted PP wave is given by:

$$(4.77) \quad P_2^{(1)}(\gamma) = P_2^{(1)}(\iota_0)\frac{F}{F+r} - P_2^{(0)}(\iota_0)\frac{2\beta_2^2-\alpha_2^2}{\alpha_2}\left[\frac{F}{(F+r)^2} - \frac{1}{F+r}\right]$$

The boundary values of the first order reflected and transmitted waves at incidence point on the interface boundary, $P_1^{(1)}(\iota_0)$, $S_3^{(1)}(\iota_0)$, $P_2^{(1)}(\iota_0)$ and $S_4^{(1)}(\iota_0)$, will be determined together by using the first order boundary conditions, which is given by substituting k=1 into the general expressions of the boundary conditions (4.18-1), (4.18-2), (4.18-2) and (4.18-4). That means we have to solve

the following first order boundary equations:

(4.78)

$$-\sin\theta_1 P_1^{(1)}(\iota_0)-\cos\theta_3 S_3^{(1)}(\iota_0)+\sin\theta_2 P_2^{(1)}(\iota_0)+\cos\theta_4 S_4^{(1)}(\iota_0) = \sin\theta_0 P_0^{(1)}(\iota_0)+\sin\theta_3 s_3^{(1)}(\iota_0)-\sin\theta_4 s_4^{(1)}(\iota_0)$$

$$\cos\theta_1 P_1^{(1)}(\iota_0)-\sin\theta_3 S_3^{(1)}(\iota_0)+\cos\theta_2 P_2^{(1)}(\iota_0)-\sin\theta_4 S_4^{(1)}(\iota_0) = \cos\theta_0 P_0^{(1)}(\iota_0)-\cos\theta_3 s_3^{(1)}(\iota_0)-\cos\theta_4 s_4^{(1)}(\iota_0)$$

$$\frac{\beta_1^2}{\alpha_1}\sin 2\theta_1 P_1^{(1)}(\iota_0) + \beta_1\cos 2\theta_3 S_3^{(1)}(\iota_0) + \frac{\beta_2^2}{\alpha_2}\sin 2\theta_2 P_2^{(1)}(\iota_0) + \beta_2\cos 2\theta_4 S_4^{(1)}(\iota_0) = \Phi_1^{(1)}(\iota_0)$$

$$-\frac{\alpha_1^2-2\beta_1^2\sin^2\theta_1}{\alpha_1}P_1^{(1)}(\iota_0) + \beta_1\sin 2\theta_3 S_3^{(1)}(\iota_0) + \frac{\alpha_2^2-2\beta_2^2\sin^2\theta_2}{\alpha_2}P_2^{(1)}(\iota_0) - \beta_2\sin 2\theta_4 S_4^{(1)}(\iota_0) = \Phi_2^{(1)}(\iota_0)$$

where $\Phi_1^{(1)}$ and $\Phi_1^{(1)}$ are given by (4.19) and (4.20).

By solving the above set of equations we are able to evaluate the values of the principal components of the first order transmitted and reflected waves at the point of incidence on the interface boundary. Then substituting the boundary value $S_4^{(1)}(\iota_0)$ into (4.73), or $P_2^{(1)}(\iota_0)$ into (4.76) will finally give the principal components of the transmitted PS and PP waves along whole transmitted rays. The first order boundary values of the reflected waves, $P_1^{(1)}(\iota_0)$ and $S_3^{(1)}(\iota_0)$, will be employed later when we discuss the principal components of the first order terms

for reflected waves in Model #5.

Up until now the derivation of expressions for the zero order and the first order approximations to ART for transmitted waves in Model #5 have been done analytically. The numerical implementation of these formulae will be shown in Figures 4.30, 4.31 and 4.32.

Figures 4.30 and 4.31 compare the vertical synthetic seismograms computed using the first order approximation of ART and the Alekseev-Mikhailenko Method. The receivers are located 5 WL below the interface in medium 2, so as to remove any possibility of Stonely wave arrivals being detected in the Alekseev-Mi. .ilenko seismograms. The time dependence of the source pulse used is given by (4.57). To detect the nonzero vertical components of the transmitted PS wave at near vertical incidence, only those epicentral distances in the high-frequency case, for which all arrivals of S* do not appear at all, are presented. On viewing these two figures, it is obvious that a generally good fit was obtained. The zero order ray theory synthetic traces presented in Figure 4.32 should be helpful to understand the difference between the zero order and the first order approximations to ART.

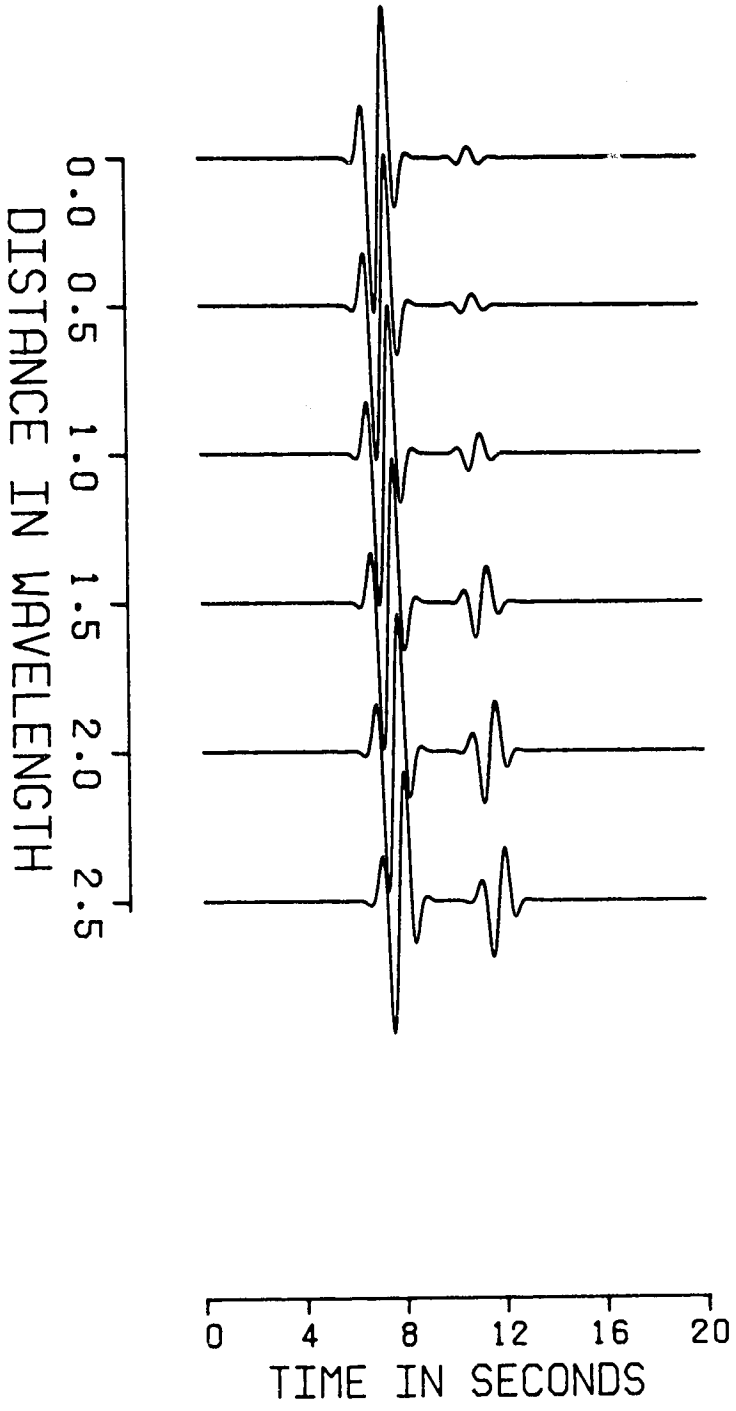

Figure 4.30 Vertical synthetic seismograms of the first order approximation of ART for the transmitted waves in Model #5. Source is at 0.25 WL into medium 1 while the receivers are located 5.0 WL into medium 2.

Figure 4.31 Vertical synthetic seismograms of the Alekseev-Mikhailenko method for the transmitted waves in Model #5. Again, source is at -0.25 WL and receivers at 5.0 WL.

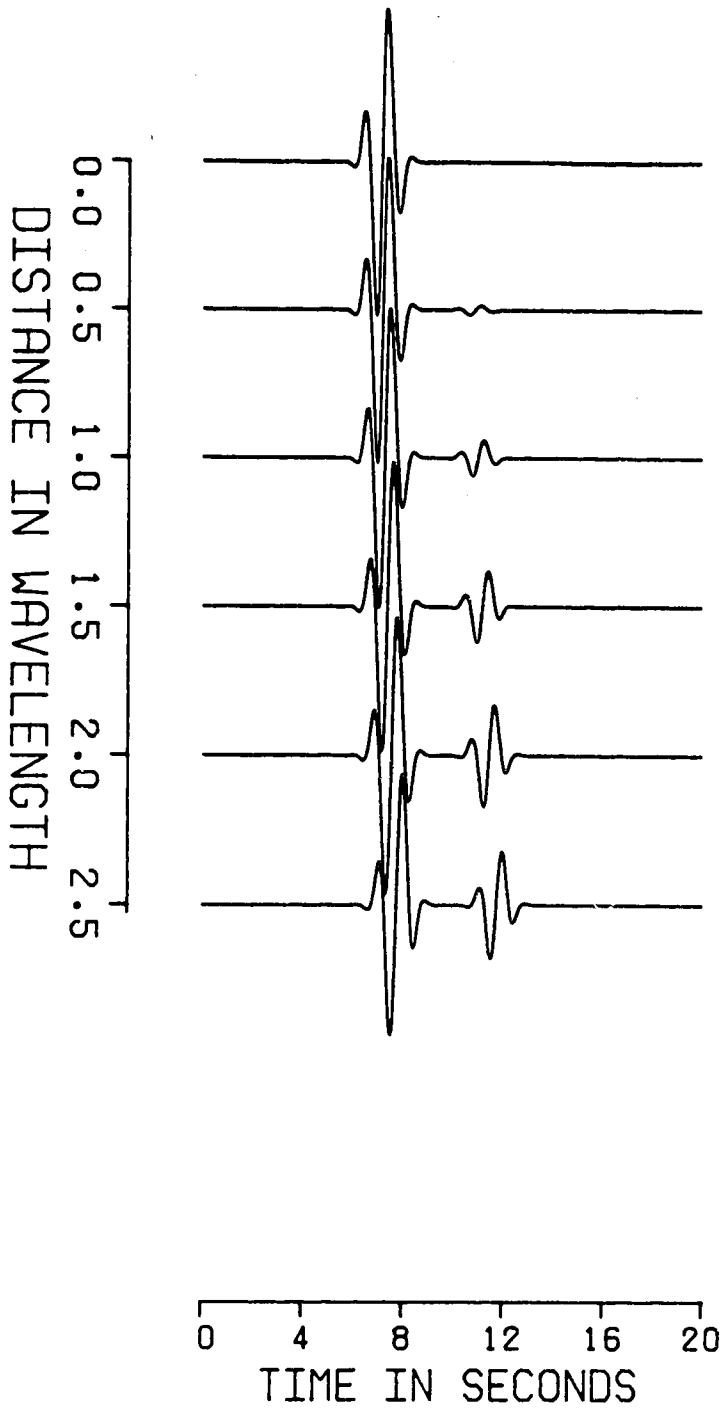

Figure 4.32 Vertical synthetic seismograms of the zero order approximation of ART for the transmitted waves in Model #5. The nonzero vertical components of PS wave disappear. Again, source is at -0.25 WL and receivers at 5.0 WL.

4.6 Model #5 and Related Seismograms for the Reflected Waves

In this section an investigation of the higher order effects of ART for reflected waves in Model #5 will be undertaken. The converted waves reflected from a free surface in Model #1 have been discussed in great detail in earlier sections, and as a result all formulae employed in studying Model #1 can be used directly for Model #5 except the boundary conditions which require different expressions. The boundary conditions of the reflected waves have been evaluated together with those of the transmitted waves in the previous section for the zero order and the first order terms. The total wave field, including the direct P and reflected PP and PS waves at the receiver location, $R=(r,0,-h_2)$, in the upper half-space (medium 1) in Model #5 may now be evaluated without any mathematical difficulties. We will restrict ourself to the discussion of results produced in our numerical experiments.

In Figure 4.33 the vertical components of displacements computed using the first order approximation of ART for the receiver depth h_2=3 WL at 6 epicentral distances are shown. The solution of the zero order approximation of ART is given in Figure 4.34. To clearly show the first order effects only, a set of synthetic seismograms are shown in Figure 4.35. It is evident from viewing these Figures that the first order terms of ART should be included in the expressions for the wave field at near vertical incidence in order to produce more accurate results.

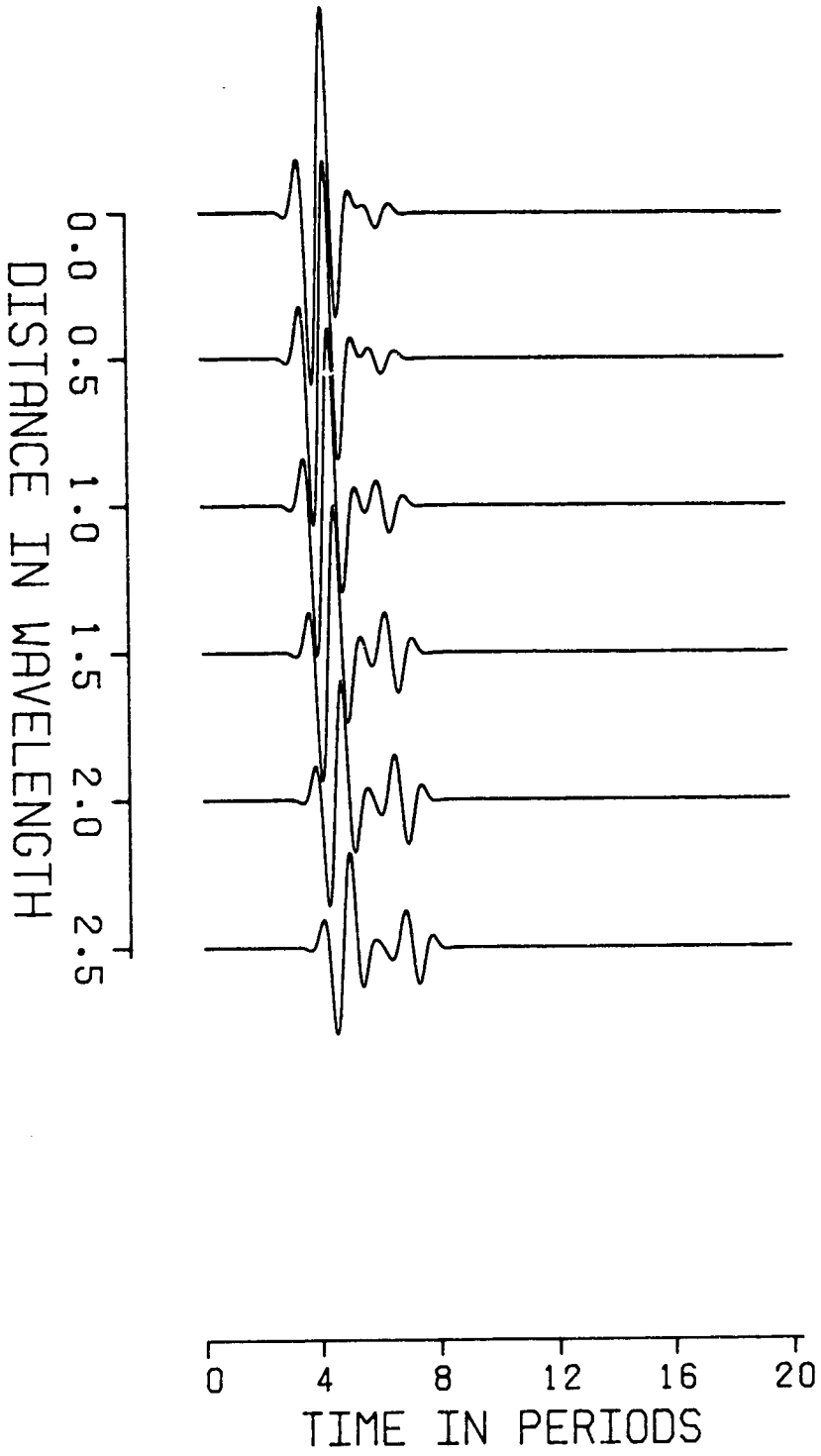

Figure 4.33 Vertical synthetic seismograms of the first order approximation of ART for the reflected waves in Model #5. Source is at h_1=0.25 WL and receiver is at h_2=3.0 WL into medium 1. α_1=1.3355 WL/T, β_1=0.771 WL/T, α_2=0.5 WL/T, β_2=0.2885 WL/T and $\rho_1=\rho_2$=1.0 gm/cc.

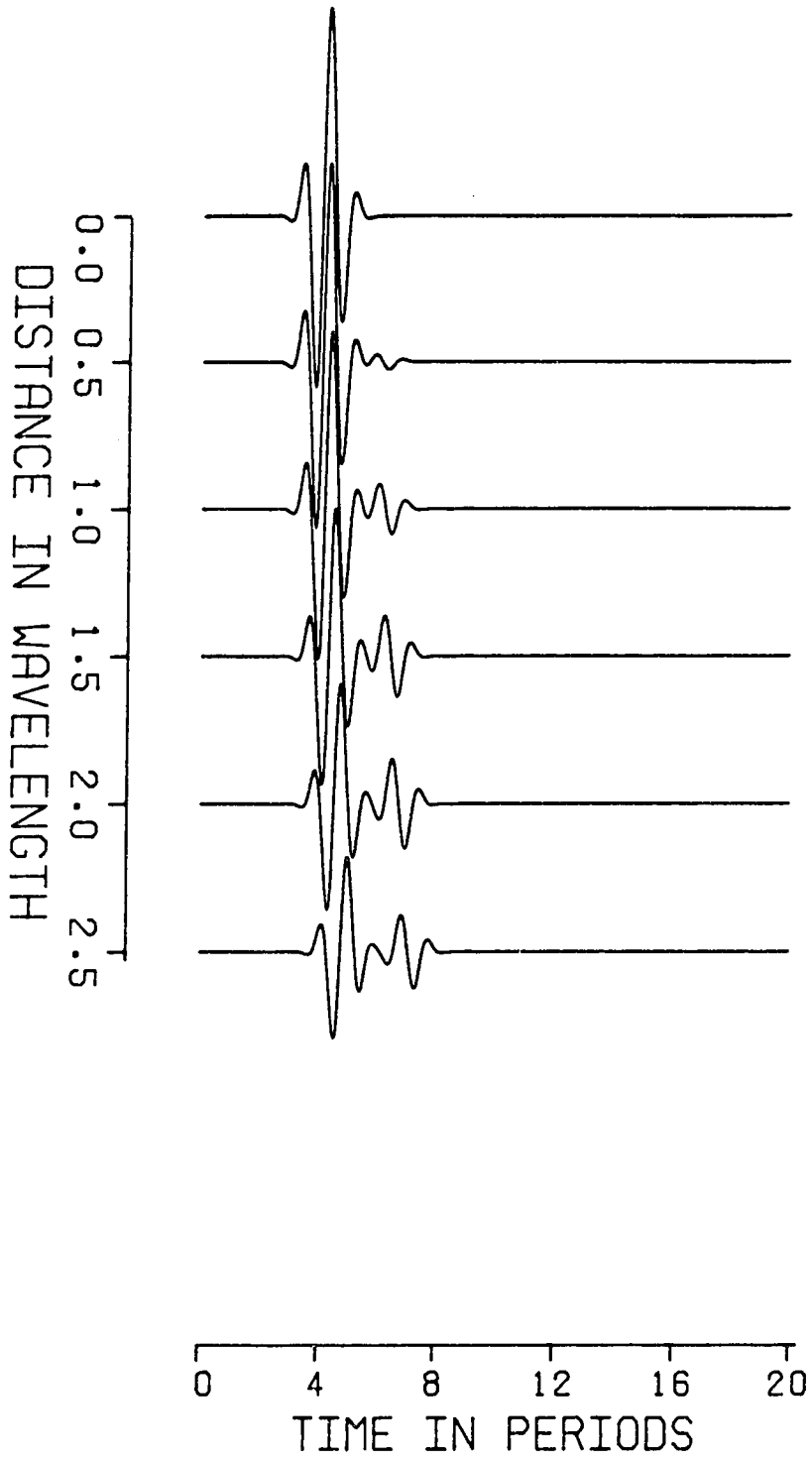

Figure 4.34 Vertical synthetic seismograms of the zero order approximation of ART for the reflected waves in Model #5. Source is at h_1=0.25 WL and receiver is at h_2=3.0 WL into medium 1. α_1=1.3355 WL/T, β_1=0.771 WL/T, α_2=0.5 WL/T, β_2=0.2885 WL/T and $\rho_1=\rho_2$=1.0 gm/cc.

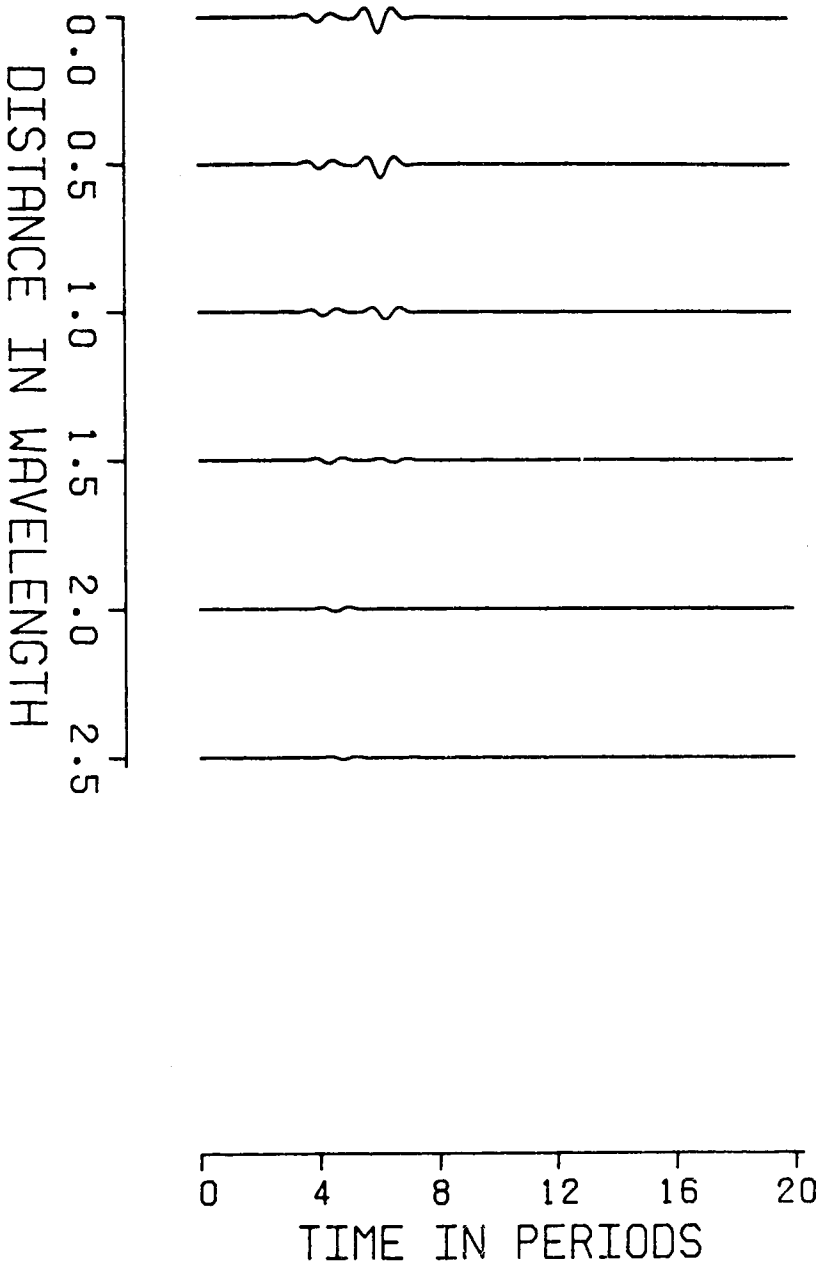

Figure 4.35 Vertical synthetic seismograms including the effect of the first order terms only in ART for the reflected waves in Model #5. Source is at h_1=0.25 WL and receiver is at h_2=3.0 WL into medium 1. α_1=1.3355 WL/T, β_1=0.771 WL/T, α_2=0.5 WL/T, β_2=0.2885 WL/T and $\rho_1=\rho_2$=1.0 gm/cc.

5. Conclusions

A more systematic and detailed treatment of the so called higher order approximations of Asymptotic Ray Theory was discussed. Due to the rather unwieldy character of the general expansions for higher order terms, a rigorous mathematical analysis of the first order approximation of ART to some typical problems has been especially derived.

In addition to the presentation of basic theoretical formulae, many demonstrations were given on the importance of the first order terms in the ray series, suggesting that they should be used whenever Asymptotic Ray Theory is applied to inhomogeneous media.

The first order correction to the zero order approximation of the vertical component of the PS and PP arrivals due to a P wave incidence on a free interface at near vertical incidence was computed. Basic properties of the nonzero vertical component of PS wave at vertical incidence, such as its linear polarization and strong dependence on the source depth and on the velocity ratio β/α, were shown in a series of computed synthetic seismograms. The accuracy of our formulae has been compared against the synthetic seismograms produced by the Alekseev-Mikhailenko Method. Numerical results show that our first order approximation was quite appropriate as it preserves the appearance of a nonzero vertical component of PS displacement at vertical incidence which is not predicted

by the zero order approximation of ART or Cagniard's method where no more than the zero order term is taken to approximate the disturbance.

The problem of a spherical wave incident on a boundary between two elastic media displaying many of the same properties observed in the fairly simple case was also considered in this thesis. Only the complexity of the derivations differs. The simplification of the problem may be made by dividing the range of incident angles into regions and focussing attention on the variables which most affect the solution in each of the regions. This is due to the fact that, from the mathematical point of view, transmitted and reflected wave fields are analogous as both are carrying energy away from the interface on which the incident wave impinged.

The first order approximation of ART expresses a significant contribution to the understanding of the nature of spherical waves, since it confirms the basic predictions of the Asymptotic Ray Theory on the polarization of higher order terms in the ray series.

REFERENCES

Alekseev, A. S., V. M. Babich, and B. Y. Gel'chinskiy (1958) Monograph on seismic waves - mathematical aspects, 40-42 (in Russian).

Alekseev, A. S., V. M. Babich, and B. Y. Gel'chinskiy (1961) Ray method for the computation of wavefronts, in Problems in the Dynamic Theory of Seismic Waves, vol. 5, G. I. Petrashen, Editor, Leningrad University Press, Leningrad, 3-24(in Russian).

Alekseev, A. S. and B. G. Mikhailenko (1976). Solution of Lamb's problem for a vertically inhomogeneous half-space, Izv. Akad. Nauk SSSR, Fizika Zemli 12, 11-25 (in Russian).

Alekseev, A. S. and B. G. Mikhailenko (1977). Numerical modelling of seismic waves propagating in a radially inhomogeneous Earth's model, Dokl. Akad. Nauk SSSR 235, 46-49 (in Russian).

Alekseev, A. S. and B. G. Mikhailenko (1978). Method of calculation of theoretical seismograms for complex models of media, Dokl. Akad. Nauk SSSR 240, 1062-1065 (in Russian).

Alekseev, A. S. and B. G. Mikhailenko (1979a).

Numerical modelling of transient wave fields in seismology and seismic prespecting (vertically-inhomogeneous half-space and radially-inhomogeneous sphere), The Siberian Branch of the Academy of Sciences of the USSR, Novosibirsk.

Alekseev, A. S. and B. G. Mikhailenko (1979b). Numerical modelling of trasient wave fields in seismology and seismic prospecting (some diffraction problem), The Siberian Branch of the Academy of Sciences of the USSR, Novosibirsk.

Alekseev, A. S. and B. G. Mikhailenko (1980). Solution of dynamic problems of elastic wave propagation in inhomogeneous media by a combination of partial separation of variables and finite difference methods, J.Geophys. 48, 161-172.

Alford, R. M., K. Kelly, and D. M. Broore (1974). Accuracy of finite difference modelling of the acoustic wave equation, Geophysics 39, 834-842.

Alterman, Z. and D. Loewenthal (1972). Computer generated seismograms, in Methods in Computational Physics, vol. 12, B. A. Bolt, B. Alder, and M. Rotenberg, Editors, Academic Press, New York.

Babich, V. and A. S. Alekseev (1958).
A ray method of computing wave front intensities, Izvestiya, Academy of Scences, USSR, Geophysics series, vol. 1, 9-15.

Bjorck, A. and V. Pereyra (1970).
Solution of Vandermode systems of equations, Mathematics of Computation, V.24, No.112, 893-903.

Boore, D. M. (1972).
Finite difference methods for seismic wave propagation in heterogeneous materials, in Methods in Computational Physics. vol. 11, B. A. Bolt, B. Alder, and M. Rotenberg, Editors, Academic Press, New York.

Cerveny, V. and R. Ravindra (1971).
Theory of seismic head waves, University of Toronto Press, Toronto.

Cerveny, V. and and J. Zahradnik (1972).
Amplitude-distance curves of seismic body waves in the neighborhood of critical points and caustics - a comparison, Zeitschrift fur Geophysik, v. 38, 499-516.

Cerveny, V. and F. Hron (1980).
The ray series method dynamic ray tracing system for three-dimensional inhomogeneous media, Bull. Seism. Soc.

Am. 70, 47-77.

Cerveny, V., I. A. Molotkov, and I. Psencik (1977).
Ray Method in Seismology, Charles University Press, Prague.

Daley, P. F. and F. Hron (1983a).
A high frequency approximation to the nongeometrical S* arrival, Bull. Seism. Soc. Am. 73, 109-123.

Daley, P. F. and F. Hron (1983b).
Nongeometrical arrivals due to highly concentrated sources adjacent to plane interfaces, Bull. Seism. Soc. Am. 73, 1655-1671.

Daley P. F. and F. Hron (1985).
Wave methods for shear waves in elastic media, Seismic Shear Waves, vol. 15, Geophysical Press, Amsterdam, 125-190.

Daley P. F. and F. Hron (1987).
Reflection of an incident spherical P wave on a free surface (near-vertical incidence), Bull. Seism. Soc. Am. 77, 1057-1070.

Gardner, G., L. Gardner, and A. Gregory (1974).
Formation velocity and density: The diagnostic basis for

stratigraphic traps, Geophysics, v. 39, 770-780.

Hron, F. and E. R. Kanasewich (1971).
Synthetic seismograms for deep sounding studies using asymptotic ray theory, Bull. Seism. Soc. Am. 61, 1169-1200.

Hron, F. (1984).
Introduction to Asymptotic Ray Theory in seismology, Institute of Earth and Planetary Physics and Department of Physics, University of Alberta, Edmonton, Alberta, Canada.

Hron, F. and B. G. Mikhailenko (1981).
Numerical modelling of nongeometrical effects by the Alekseev-Mikhailenko method, Bull. Seism. Soc. Am. vol. 71, 1011-1029.

Karal, F. and J. Keller (1959).
Elastic wave propagation in homogeneous and inhomogeneous media, J. Acoust. Soc. Am. v. 31, 694-705.

Keller, H. B. (1969).
Accurate difference methods for linear ordinary differential systems subject to linear constraints, SIAM J. Numer. Anal., V.6, pp.8-30. MR 40 #6776.

Keller, H. B. (1974).

Accurate difference methods for nonlinear two point boundary value problems, SIAM J. Numer. Anal. 11, 305-320.

Keller, H. B. (1968).

Numerical methods for two point boundary value problems, Blaisdell, London, 184 pp.

Kelly, K. R., R. W. Ward, S. Treitel, and R. M. Alford (1976).

Synthetic seismograms: a finite difference approach, Geophysics 41, 2-27.

Kline, M. (1951).

An asymptotic solution of maxwell's equations, Commun. Pure Appl. Math. 4, 225-263.

Lentini, M. and V. Pereyra (1977).

An adaptive finite difference solver for nonlinear two point boundary problems with mild boundary layers, SIAM J. Numer. Anal. 14, 91-111.

Lentini, M. and V. Pereyra (1975).

An adaptive finite difference solver for non-linear two point boundary problems with mild boundary layers, Comp. Sc. Dept. Stanford University Rept. STAN-CS-75-530, 40

pp.

Lentini, M. and V. Pereyra (1974).
A variable order finite difference method for nonlinear multipoint boundary value problems, Math. Comp. 28, 981-1004.

Mikhailenko, B. G. (1973).
Numerical solution of Lamb's problem for inhomogeneous half-space, in Mathematical Problems in Geophysics, vol. 4, Numerical Center of the Siberian Branch of the Soviet Academy of Sciences, Novosibirsk, 273-297 (in Russian).

Nettleton, L. (1940).
Geophysical prospecting for oil, New York, McGraw-Hill.

Pereyra, V., W. H. K. Lee and H. B. Keller (1980).
Solving two-point seismic-ray tracing problems in a heterogeneous medium, Bull. Seism. Soc. Am. 70, 79-99.

Pereyra, V. (1973).
High order finite difference solution of differential equations, Comp. Sci. Dept. Stanford University Rept. STAN-CS-73-348.

Pereyra, V. (1968).
Iterated deferred corrections for nonlinear boundary

value problems, Numer. Math. 11, 111-125.

Pereyra, V. (1967).
Iterated deferred corrections for nonlinear oprator equations, Numer. Math. 10, 316-323.

Pereyra, V. and C. Sewell (1975).
Mesh selection for discrete solution of boundary problems in ordinary differential equations, Numer. Math. 23, 261-268.

Zheng, B. (1985).
Some problems involving the ray approximation of the wave equation, M. Sc. Thesis, Department of Physics, University of Alberta, Edmonton, Canada.